Politecnico di Torino

ScuDo
Scuola di Dottorato ~ Doctoral School
WHAT YOU ARE, TAKES YOU FAR

Doctoral Dissertation
Doctoral Program in Energy Engineering (36^{th}cycle)

Multi-Vector Energy Integrated Networks for Local Energy Systems

By

Ilaria Abbà

******

Supervisor(s):
Prof. Stefano Paolo Corgnati, Supervisor
Prof. Ettore Francesco Bompard, Co-Supervisor
Dott. Edoardo Corsetti, Co-Supervisor
Ing. Vincenzo Casamassima, Co-Supervisor

Doctoral Examination Committee:
Prof. M. Beccali, Referee, Università degli Studi di Palermo
Prof. J. Kurnitski, Referee, Tallin University of Technology
Prof. E. Fabrizio, Politecnico di Torino
Prof. E. Guelpa, Politecnico di Torino
Prof. A. Angelotti, Politecnico di Milano

Politecnico di Torino
2025

Declaration

The work of the Ph.D. Candidate treated in this Thesis has been financed by the Research Fund for the Italian Electrical System under the Contract Agreement between RSE S.p.A. and the Ministry of Economic Development - General Directorate for the Electricity Market, Renewable Energy and Energy Efficiency, Nuclear Energy in compliance with the Decree of April 16th, 2018.

Throughout each year of the Ph.D. program, the Ph.D. Candidate has prepared RdS (Ricerca di sistema) Deliverables, referencing the studies and analyses conducted within the research activities framework. While some figures, tables, and content remain consistent, each instance is individually developed and written by the Ph.D. candidate, showcasing the ongoing and cumulative nature of their work.
The deliverables are the followings:

Report 2021 E. Corsetti, V. Casamassima, A. La Bella, I. Abbà. *Valutazione della flessibilità di sistemi multienergetici.* Ricerca sul Sistema Energetico (RSE). RdS Report n. 21010810, 2021 [1].

Report 2022 F. Bianchi, E. Corsetti, I. Abbà. *Analisi preliminare del potenziale di flessibilità dei carichi elettrici e approcci per l'aggregazione*. Ricerca sul Sistema Energetico (RSE). Rds Report n. 22013969, 2022 [2].

Report 2023 I. Abbà, C. Andreis, E. Corsetti, R. Lazzari, M.A. Muro Alvarad. *Sistemi multienergetici: sviluppo di modelli, architetture di controllo e impianti sperimentali per la validazione per reti calore.* Ricerca sul Sistema Energetico (RSE), RdS Report n. 23013281, 2023 [3].

I hereby declare that the contents and organization of this dissertation constitute my own original work and do not compromise in any way the rights of third parties, including those relating to the security of personal data.
Parts of the topics reported in this Ph.D. dissertation were also previously published in journals, conference proceedings and books, as mentioned in the following chapters.

Ilaria Abbà
2025

* This dissertation is presented in partial fulfillment of the requirements for **Ph.D. degree** in the Graduate School of Politecnico di Torino (ScuDo).

I would like to dedicate this thesis to my loving parents

Acknowledgements

***

Abstract

To limit the effects of climate change and move towards a post-carbon society, the ongoing energy transition must accelerate. The global and European objectives regarding enhancements in energy efficiency, greenhouse gas emissions reduction and increased adoption of renewable sources are ambitious and imminent. Therefore, it is necessary to speed up the process. Heating and cooling of buildings plays a key role in this transition. Interventions must take place on the demand side by reducing consumption, and on the supply side by modifying energy mix and production technologies, resulting in more efficient and less polluting configurations.

My Ph.D. research tackles this challenge, exploring the district heating field, recognized as a promising driver for decarbonizing the thermal sector. Given the different available technologies for present and future district heating, it can be considered as a multi-vector energy system (MVES) for local energy networks, thanks to the synergy of different energy carriers in satisfying thermal demand. As the European legislation will require an increasingly higher percentage of renewables to define the efficient district heating, having a flexible system has become a prerequisite for each network. The overall objective of the Thesis is therefore the assessment and quantification of the flexibility potential in multi-vector energy integrated networks.
A review conducted on the methods currently used in literature led to the identification of the gaps and the definition of a simulation-based methodology for the assessment of flexibility in MVES. In fact, one of the shortcomings of the methods analyzed was the lack of analysis of impacts of the networks on the calculation of flexibility. Thanks to the energy simulation it was possible to consider the system in its entirety, from production technologies to the network and users. This general theme was then divided into four more specific research questions which deal with the necessity of: (i) identifying the flexible sources for the district heating "of today" and "of the future", (ii) finding which instruments can facilitate the flexibility

assessment in MVES, (iii) evaluating the effects of all the involved components (including the network) and finally (iv) analyzing how flexibility can be exploited in an all-electric district heating system with heat pumps. The research questions are described in detail in the dissertation, and led to the development of two main applications.

Specifically, the first Case Study was mostly devoted to the development of a dynamic simulation tool, capable of conducting quick but accurate simulations of a third-generation district heating network. This application was chosen as representative of the district heating currently under operation, with a centralized layout and fossil fuels in the main power plant. Indeed, the power station was composed of a gas combined heat plant and a gas boiler able to provide heat to a high temperature network (almost 90°C). The results of the simulation phase allowed to understand the dynamic behaviour of such a complex energy system and then they were used as input for flexibility computation. In this first application, flexibility was evaluated from the supply side; technical and physical limitations were explored for conversion technologies but also for the thermal network, while users were considered as passive. Through Application #1 it was demonstrated how the dynamic simulation of the district heating network is a fundamental instrument not only for calculating flexibility, but also for verifying the functioning of the network through the hourly visualization of some reference quantities (e.g., temperature, pressure and flow rate along the pipes).

On the other hand, the second application was developed to analyze the issue from another perspective. Indeed, the simulation tool was customized to model a fifth-generation district heating network, with an all-electric layout, composed of a ground-water source heat pump in the main power station and water-to-water heat pumps at district level. In this case study, without neglecting the modeling effort, the objective was to investigate how to make the system flexible, since, without any backup unit, it was not possible to modify the generation profiles of the heat pump while guaranteeing the heat provision to users. Thus, in Application #2, it was studied how Demand-Side Management can be exploited on users' thermal loads. By varying the consumption according to external forcing (i.e., advantageous prices on intra-day market or presence of renewables) while maintaining acceptable comfort temperatures, it was possible to modify the electrical absorption of the heat pumps to follow the load, providing upward or downward flexibility to the electric grid. In this application, also financial implications were evaluated.

To conclude, the development of the MVES models on the dynamic simulation tool, coupled with the elaboration of results for flexibility computation, is a valuable instrument for the grid operator to understand the behaviour and operation of the system but also to calculate flexibility KPIs (both energy and financial ones) useful for improving the system management.

Contents

List of Figures

List of Tables

Chapter 1

Framing the research context

1.1 Energy transition: opportunities and challenges of multi-vector energy integrated networks

Throughout its history, humanity has been repeatedly forced to change the energy resources on which it depended and the ways it used them, for reasons of survival or to improve its lifestyle [4]. Civilization has evolved, developing new production techniques, modifying the surrounding environment and the socio-economic structure. The technological and scientific evolution of the last centuries, from the industrial revolution onwards, has yielded many benefits to society, but at the same time it has brought out new critical issues that must be addressed [5, 6]. Nowadays a new challenge is threatening the well-being of humans and the planet they live on: the climate change [7]. The constant growth in average temperatures and the increasingly frequent occurrence of extreme climate events are having a significant, and in many cases worrying, impact on the Earth's ecosystem. As Fazey stated in [8], in the field of climate change studies the main issue is no longer identifying the problem itself or the causes, but understanding how to facilitate effective modifications to avoid catastrophic effects caused by climate change. In the attempt of outline a common strategy for decarbonization and set long-term objectives, in 2015 the United Nations Conference of the Parties (COP21) signed the Paris Agreement [9]. The agreement commits Member States to limit the rise in the global average temperature to +2°C compared to the pre-industrial levels, with the aim to stay below +1.5°C. At the COP24 in Katowice [10] the rules for the implementation of the Paris Agreement

were approved, resulting in a Rulebook, while in the following COP26 and COP28, respectively in Glasgow in 2021 [11] and Dubai in 2023 [12], the objectives in terms of containment of temperatures were confirmed and it was reiterated the need to achieve carbon-neutrality by 2050.

In the energy field, the growing attention on climate change is provoking a transition towards a post-carbon society that is radically transforming the energy system, aiming to modify the current energy paradigm to address the issue of carbon-neutrality. Within the energy sector, the term transition means the shift from current sources of energy production, mainly fossil (oil, coal and gas) to renewable and efficient energy sources [13]. Nowadays the majority of the generation systems are still governed by large, highly polluting fossil-fuel power plants. In order to complete the energy transition, the key points to be developed will be: (i) the improvement of the efficiency of existing technologies to allow the reduction of energy demand; (ii) the development of renewables with a consequent increase in the potential for electrification; (iii) the study and application of new energy production and distribution infrastructures; (iv) the coupling of production systems with digital technologies; (v) the role of the active consumer. It is clear that this transition will have to expand beyond the technological sphere demanding for profound changes also from the socio-economic point of view. As previously mentioned, today's energy system is still strongly based on a centralized structure, governed by large plants and fossil fuels [14]. Until now, renewable sources have not replaced the traditional energy paradigm, but have simply joined it. The technological maturity achieved in recent years, however, allows to begin a process of replacing the existing energy system, creating solutions with small, interconnected distributed production plants and networks.

The phaseout of fossil fuels and the increasing use of renewable energy sources is pushing towards the progressive electrification of final uses [15] (e.g., in transportation [16] and buildings [17]), having an impact on energy generation and conversion, as well as on the operation and management of transmission and distribution networks. Indeed, the shift from a centralized to a decentralized energy system, affects not only the network infrastructure layout, but also the management and balance of demand and supply. For this reason, in response to the uncertainty and volatility arising from the increasing share of renewable sources, much more flexibility is required for the energy system, to continuously ensure the power balance between generation and demand [17–20].

In this context, the concept of Multi-Vector Energy System (MVES), or simply Multi-Energy Systems (MES), fits perfectly, representing an effective means to move toward a decentralized low-carbon system, thanks to the exploitation of the synergies between different energy vectors (e.g., electricity, heating, gas, as well as hydrogen and cooling) to satisfy users' needs [21, 22]. An example of a multi-vector integrated system could be an electricity grid coupled to a thermal network, or a building in which electricity, heat and gas utilities are jointly regulated to improve overall energy efficiency [23]. Among the numerous advantages of these configuration there is the fact that managing different energy vectors as a whole and exploiting their combined effect is more convenient than running traditionally separate energy systems. In fact, better performance is estimated at a technical, financial and environmental level and MVES can promote new commercial and market opportunities [23]. As an example, looking at the environmental sphere, the reduction of greenhouse gases (GHG) and pollutants emissions can be optimally valorised by MVES through their ability in exploiting the suitable conversion efficiencies of technologies and thanks to the harnessing of local RES [24]. Also, these configurations can lead to a reduction in the system operational costs. In [19], Turk et al., through the adoption of a two-stage stochastic scheduling scheme, demonstrated on a small-case test system that a wind farm coupled with an integrated multi-energy system with the ability to switch from one energy vector to the other, results in a reduction of the total cost of the system, in a better usage of reserves and in a more flexible system [23]. Similar result was obtained by Onen et al. [25] who demonstrated, applying the energy hubs technique, a reduction in the planning cost in the case of integrated planning with other energy carriers with respect to independent planning.

Moving to the technological sphere, conversion technologies certainly play a key role in enabling interactions between energy carriers. Indeed, there exist several solutions for multi-vector applications [26], already available on the market, each characterized by different efficiency, technical performances, emissions and costs. In line with the growing electrification of end uses [27], the so-called *Power-to-X* solutions are increasing their relevance and diffusion, being able to exploit also electricity from local renewable sources. However, gas technologies are still the most widespread and established on the market and are improving their efficiency in order to reduce their environmental impact. In this regard, Guelpa et al. [26] produced a comprehensive review of conversion technologies suitable for MVES applications, classifying them into: (i) *Gas-to-Heat, Cooling and Electricity* (e.g. gas condensing

boilers, chillers or trigeneration systems), (ii) *Power-to-Gas* (e.g. electrolysers), (iii) *Power-to-Heat* (e.g. electric boilers, heat pumps or polivalent heat pumps [28]) and (iv) *Power-to-Commodities* (e.g. mobility or desalination), with particular attention to storage systems, considered fundamental for separating the supply and demand phases. Witkowski et al. [29], using a similar classification, added information on the technical characteristics of the technologies (e.g., operating temperature level, efficiencies, part load conditions, etc.), as well as on the financial and flexibility data of the different alternative solutions.

However, if on the one hand the synergetic operation of different energy vectors domains may lead to the aforemetioned benefits and opportunities, on the other hand it implies an increased complexity from the modeling, simulation and control standpoints [30], and it introduces additional physical and regulatory constraints in the way energy is transmitted through the interfaced networks and converted between the different energy vectors. In [31] Arteconi proposed an overview of the criticalities to face when modeling multi-sector and multi-energy systems and has identified four main critical aspects to consider: scalability, uncertainties, robustness and optimal control. For the above reasons, assessing the opportunities and challenges of multi-vector energy systems is a current and trending research field, with significant interest both from the academic and in the industrial sector, in order to foster their integration in the energy sector [14, 21, 23, 25, 26, 32]. In this context, there are also European projects that are addressing this topic. As an example, the H2020 MAGNITUDE project (funded by Horizon 2020 program) has been recently carried out, with the objective of developing market mechanisms and tools to enhance MESs providing flexibility to the European power system, exploiting and optimizing the synergies among different energy vectors (i.e., electricity, heating and gas) [33]. Moreover, as an extension of the previous one, the SENERGY NETS project, funded by Horizon Europe program, is currently trying to showcase the technical and economic potential of MES in decarbonising the heating and cooling, electricity, and gas sectors. The project plans to create a set of tools to optimize, through sector coupling, the planning of district heating and cooling as well as distribution grids. These tools will also facilitate the provision of flexibility services [34].

1.2 The role of District Heating in the energy transition

One of the best existing example of multi-vector energy network is the district heating (DH), which represent the focus of this disseration.
The European programmes "FitFor55" [35] and "European Green Deal" [36] have set ambitious targets for the decarbonization of European countries. Among the sectors, one of the most affected is the one of heating and cooling, which in 2019 still used 75% of fossil fuels [37]. In this context, district heating is seen as one of the possible drivers towards decarbonization of the sector, thanks to the ability to diversify energy sources and integrate renewable plants [38].
Over the years, district heating has undergone changes that have gradually increased its compatibility with renewable technologies. Five generations have been identified and categorized by Lund [39], who was the first to also graphically represent the main characteristics of each generation, correlating the temperature of the heat transfer fluid and production technologies. The main objective of these developments has been to reduce the operating temperature of the grid in order to reduce thermal losses and promote integration with heat waste and renewable sources. In detail, the first-generation DH (1GDH) was commonly used until the 1930s, using steam as a heat transfer fluid, and had a centralized layout, with the main thermal plant operated by coal systems. Then, in 1930 the second-generation of DH gained ground and remained the preferred choice until the 1970s. 2GDH uses superheated water at a temperature above 100°C as a fluid. For this generation the network layout is also centralized, with cogeneration of coal and oil as the main technologies used in the thermal plants. Third-generation DH (3GDH) lowers the temperature below 100°C, usually around 90°C, using more efficient cogeneration units, also fed by biomass or waste fuels. The network has also been integrated with solar and geothermal systems in more advanced plants. Currently, most of the existing networks are still in the third generation [40, 41]. The fourth-generation (4GDH) has a supply water temperature range between 50-80°C and allows integration with renewable sources such as solar thermal and thermal waste [38, 42–44]. Starting from the 4GDH, also the role of building users become fundamental. Indeed, as stated by Lund, "the 4^{th} Generation District Heating and cooling technology implies coordinating the performance of the buildings and the district heating system in order to improve the energy efficiency of the total system [39]". Finally, the fifth-generation, in addition to further lowering

the temperature of the heat transfer fluid (<45°C) to be compatible with geothermal heat sources, also changes the structure of the district heating network. The layout goes from a centralized scheme powered by fossil fuels to a decentralized one, integrated with renewable sources and intermediate heating substations with heat pumps, also potentially powered by renewable electricity sources. This configuration allows, through the use of reversible heat pumps, to operate also in cooling mode, for summer air conditioning of buildings. For this reason, the fifth-generation is usually referred to as 5GDHC (5^{th} Generation District Heating and Cooling) [43].
In order to present a summary of the evolution of district heating thermal grids, Table 1.1 compiles information on the main features for each generation.

Generation	**Layout**	**Heat Carrier**	**Supply Temperature Range**	**Technologies**
First-Generation (1GDH)	Centralized	Steam	> 150°C	Coal-fired systems
Second-Generation (2GDH)	Centralized	Pressurized hot water	> 100°C	Coal and oil CHP plants
Third-Generation (3GDH)	Centralized	Pressurized hot water	< 100°C	High-efficient CHP plants, biomass, waste or fossil fuel boilers
Fourth-Generation (4GDH)	Mixed according to users	Low temperature water	50°C-80°C	Renewables and heat waste integration, geothermal plants
Fifth-Generation (5GDHC)	Decentralized	Ultra-low temperature water	<45°C	Reversible heat pumps, geothermal energy, renewables

Table 1.1 District Heating Generations, adapted from [39].

Alongside technological developments, the European regulatory framework has played a leading role in driving the deployment of district heating systems. However, the DH potential has not been fully exploited in Europe. In 2018, district heating and

district cooling covered about the 10% of heat demand in the European Union [45]. Nonetheless, in the Renewable Energy Directive (REDII) of 2018, the Committee on heating and cooling recognized potential for decarbonization of district heating by increasing energy efficiency and renewable energy deployment. In line with that, the recast of the European Energy Efficiency Directive (EED) of 2023, stated that: "All the district heating and cooling systems should aim for improved ability to interact with other parts of the energy system in order to optimize the use of energy and prevent energy waste by using the full potential of buildings to store heat or cold, including the excess heat from service facilities and nearby data centres. For that reason, efficient district heating and cooling systems should ensure the increase of primary energy efficiency and a progressive integration of renewable energy and waste heat and cold [46]". But what does efficient district heating and cooling mean? It is a system that uses heat produced at least 50% from renewable sources, or 50% waste heat (WH), or that it is produced at least 75% from cogeneration plants (CHP) or that at least 50% of the total heat is generated by a combination of renewables, waste heat and cogeneration. This definition and these minimum requirements will be valid until 2027. In fact, as for the other energy sectors at the European level, also for district heating targets of efficiency and decarbonization to be achieved within certain time milestones have been set. The steps are gradual and, starting from the mix of sources defined above, the goal is to have a completely green district heating sector in 2050, whose heat is produced 100% from renewable plants, waste heat, or a combination of the two. In detail, the future efficient district heating should meet the following criteria [46]:

1. From 2028, the system should use at least 50% RES energy, or 50% WH, or 50% WH + RES energy, or 80% of high-efficiency CHP or a combination of RES + WH + high-efficiency CHP, that covers at least the 50% of the produced heat and the renewable energy is at least 5%.

2. From 2035, the system should use at least 50% RES energy, or 50% WH or 50% WH + RES energy, or a combination of RES + WH + high-efficiency CHP, that covers at least the 80% of the produced heat and the quota of renewable energy or waste heat is at least 35%.

3. From 2040, the system should use at least 75% RES energy, or 75% WH or 75% WH + RES energy, or a combination of RES + WH + high-efficiency

CHP, that covers at least the 95% of the produced heat and the amount of renewable energy or waste heat is at least 35%.

4. From 2045 the system should use at least 75% RES energy, or 75% WH or 75% WH + RES energy. The use of CHP is not allowed anymore.

5. From 2050, the system should have heat produced 100% from RES, or WH or a combination of the two.

To better visualize the minimal requirements that district heating must meet in order to be defined as efficient, a graphical schematization is shown in Figure 1.1, with the details of technologies and penetration rates in the heat generation mix. Each column represents an alternative feasible solution.

	Renewables	Waste Heat	CHP	High-efficiency CHP	Renewables + Waste Heat	Overall Mix
Until 2027	50%	50%	75%	-	-	50%
From 2028	50%	50%	-	80%	50%	50% RES + WH + CHP (at least 5% RES)
From 2035	50%	50%	-	-	50%	80% RES + WH + CHP (at least 35% RES or WH)
From 2040	75%	75%	-	-	75%	95% RES + WH + CHP (at least 35% RES or WH)
From 2045	75%	75%	-	-	75%	-
After 2050	100%	100%	-	-	100%	-

Fig. 1.1 Graphical schematization of efficient district heating minimum requirements.

To conclude, district heating (and cooling) is recognized as a key technology for the success of the European energy transition [47]. As previously stated, the predominant district heating networks currently in operation belong to the 3GDH [40, 41]. Nevertheless, to align with European directives for decarbonization and to improve the efficiency of the district heating sector, the integration of renewable energy sources and waste heat is necessary and the configurations using fossil fuels will no longer be allowed from 2045. In line also with the technological development, this will shift the paradigm to distributed generation, sector coupling, electrification

and will lead to an active role for the user. The overarching trend is thus evolving from the third-generation towards the forth-/fifth-generation.

1.3 Flexibility in multi-energy systems

Another key pillar for the success of the energy transition is represented by the interconnection between gas, heat and electricity systems, known as sector coupling. Considering the heating sector, this can be achieved for example by linking district heating with electricity systems through conversion technologies as cogeneration plants, as well as through power-to-heat production in large-scale heat pumps. In a well-integrated multi vector energy system, the district heating provider can respond to fluctuations in electricity market prices, contributing to the balancing of the network by adjusting the production or consumption of electricity. As the electricity production is increasingly based on variable renewable energy sources, the importance of the flexibility offered by sector coupling become increasingly valuable [48]. Indeed, due to the growing share of renewable sources in today's energy systems, flexibility has become a new demand for energy networks. Flexibility in the energy sector can be defined as the capability of a system, such as a power plant, a building or an industrial process, to adapt its energy consumption or generation profile in response to requests, market signals or changing conditions. The ability to adapt in this way is crucial to mitigate fluctuations and uncertainties associated with supply and demand on various time scales and ensure a reliable and efficient electricity grid. In the current era of decarbonization powered by renewable sources, the concept of flexibility is of fundamental importance in the development of sustainable, efficient and resilient energy systems [49–51]. Although flexibility is often associated with the adaptability of the electricity carrier, multi-vector energy systems offer new opportunities beyond individual technologies and energy carriers [21, 52]. Therefore, in the perspective of increasing electrification of end uses and having networks of different energy carriers more interconnected, there is the emerging need to make flexible even systems not purely electrical [14].

Thanks to its wide arrangement, multi-vector energy systems can unlock new flexibility opportunities with respect to single technologies applications, and, through the exploitation of flexibility, they can open to new business and market opportunities [32, 52]. As suggested in [53] and [54], a MVES can enhance several sources of

flexibility, including: (i) the ability to switch between different energy carriers; (ii) the capability to use the same input vector to produce different outputs, depending on the conversion technologies installed; and (iii) the use of storage systems (for example, electric, thermal or gas) to decouple supply and demand over time, as well as to access to energy markets. In this respect, Kleinschmidt et al. [55] have classified flexibility resources into three main categories: Conversion, Storage and Demand-Side Management, being those encompassing the majority of the MVES flexibility potential. In addition, in [56] Lund et al. have enlarged the concept of flexibility from a pure technological- and energy-related matter to regulation and market considerations. Considering Conversion, [26] and [29] have provided information on the technical characteristics of some suitable conversion technologies (e.g., efficiencies, full load and partial load conditions, etc.), investment and maintenance costs, as well as information related to the assessment of flexibility, such as power ramps and responsiveness of each solution. "In this regard, Makarov et al. [57] have defined the flexibility of a conversion system not only in terms of available power, but through a triplet of necessary physical variables: power provision capacity [MW], power ramp-rate [MW/min] and energy provision capacity [MWh] [14]". Moving to the demand side, the building sector represents one of the main final users of multi-vector integrated networks. The possibility of enhancing the flexibility of the energy demand of individual buildings, clusters of buildings or energy communities through demand-side management actions has become a trending topic in recent years [58–63]. This arises from the need for networks to be more flexible, but is made possible by the growing awareness of users on energy matters and their desire to be protagonists of the ecological transition [14]. In [64], the flexibility triplet proposed by Makarov has been extended in order to make it suitable for the assessment of flexibility actions in buildings, also accounting for the thermal comfort of the occupants. Indeed, two metrics have been added: the comfort capacity [min], meaning how long the flexibility action can be maintained before the comfort limits are reached (i.e., upper or lower bounds) and the comfort recovery [min], which is the time that the building needs to restore nominal comfort level and can be ready to be subjected to a new flexibility action.

Various approaches have been proposed in the literature for calculating the aggregate flexibility of multi-vector energy systems, however, most of them only consider the installed conversion, generation and end-users' technologies, without taking into account the presence of multi-energy networks [31, 51, 65, 66]. A stochastic

smart district optimization model for demand- response in a multi-energy community has been proposed by Good and Mancarella [67], with the main focus on electric flexibility. Chicco et al. [53] have enlarged the MES framework to distributed MES (DMES) and a comprehensive overview of DMES modeling and key flexibility-related features have been provided. In detail, the authors extend the concept of power node (usually used in the electricity field) to multi-energy nodes for MES applications. Starting from the energy hub model, the authors represent the MES as input-output matrices, considering the constraints on conversion and storage devices, and underlining implications on the constraints of the electricity grid. A new multi-energy lattice framework has been developed to model and compute flexibility from multi-energy systems in [54], with the final aim to optimize the participation of the MES in the control frequency ancillary services. Specifically, the system is represented as a lattice of energy layers connected via conversion nodes. In contrast to the multi-energy nodes approach employed in [53], the multi-energy lattice methodology have been designed to facilitate and assess the system's engagement in multiple markets, rather than examining the physical functioning of the system. Furthermore, the concept of lattice means to arrange the relationships among the energy carriers with respect to dynamic needs (sometimes may be preveling the power on gas and heat, sometimes the gas poses stronger requirements on electricity and heating production) [54].

1.4 Objectives and Research Questions

Due to the aforementioned considerations, the research pathway is defined by the overall objective of assessing and computing the potential flexibility in a multi-vector energy integrated network. As discussed in preceding sections, district heating and cooling stands out as the perfect example of a multi-vector system, gaining growing significance in achieving European and global decarbonization goals. Therefore, the Ph.D. research delves into two applications related to DHC, enabling a comprehensive assessment of various aspects such as generation, layout, conversion technologies, and user types.
In this context, the Thesis attempts to answer to two cross-cutting research questions across the case studies, that are:

RQ 1 *Which flexible sources can be exploited in the network of 'TODAY' and 'TOMORROW'?*

RQ 2 *Which instruments can facilitate the flexibility assessment in Multi-Vector Energy Systems?*

To answer these general questions two case studies have been developed as follows:

Application #1: it is a third-generation, centralized district heating system that uses fossil fuels to provide heat to final users using a hot water network as a heat transfer fluid. The layout is centralized, with a main thermal plant composed of a CHP and an integrative gas boiler.

Application #2: it is a fifth-generation district heating and cooling network, employing heat pumps both centrally and in district-level substations to heat water for distribution to end-users. This results in an all-electric configuration with a distributed layout and a low-temperature distribution network. In line with the purpose of the analysis only the delivery of heat was investigated.

Moving the lens from the current situation to a probable one for the future, comparing the current versus a future paradigm, several aspects are investigated from different perspectives. In detail, Application #1 helps to address an additional question, in line with one of the identified research gap.

RQ 3 *How can the evaluation of flexibility in a district heating integrated system consider the influence of all the involved components, including the network?*

Instead, considering the Application #2, the new layout and the use of the heat pump as conversion technology has raised an additional research question.

RQ 4 *How can flexibility be introduced into an all-electric district heating system incorporating heat pumps?*

By 2050, there is the imperative of achieving 100% of heat production from renewable sources to obtain the efficient district heating certificate. Therefore, one solution can be a DHC configurations comprised solely of heat pumps powered by electricity generated from RES. Unlike previous applications that included gas boilers for

integration, this all-electric system lacks flexibility in its production mechanism. In this context is of interest to explore other flexibility strategies that can be used in the district heating of the future.

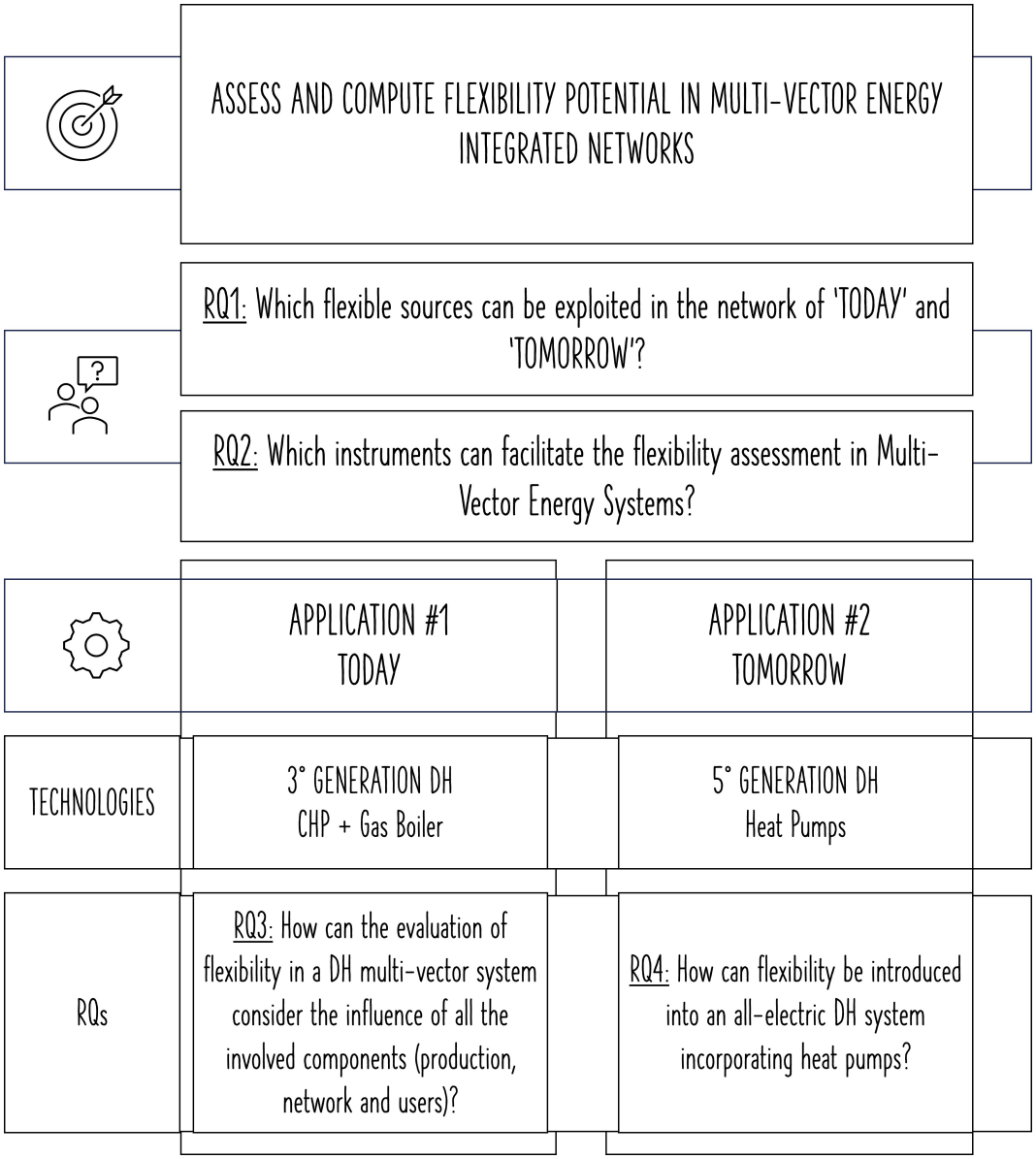

Fig. 1.2 Graphical representation of Ph.D. objectives, research questions and applications.

Figure 1.2 provides a visual synthesis encompassing the principal elements addressed across various applications. The graphical representation summarizes objectives, research questions and some features of the two applications. All of

these elements, including also instruments and tools used to attaining the research objectives, are explored in greater detail in the subsequent chapters of the dissertation.

1.5 Structure of the Ph.D. Thesis

Figure 1.3 schematically represents the structure of the Thesis. The tiles of a puzzle have been chosen to represent each chapter, because metaphorically the path that led to the definition and realization of the research discussed in this dissertation was like the creation of a puzzle. Each chapter fits into the previous and the next ones, but investigating a specific topic, just as the puzzle pieces differ in shape or color. The integration of tiles helps in the visualization of a broader and more complete framework.

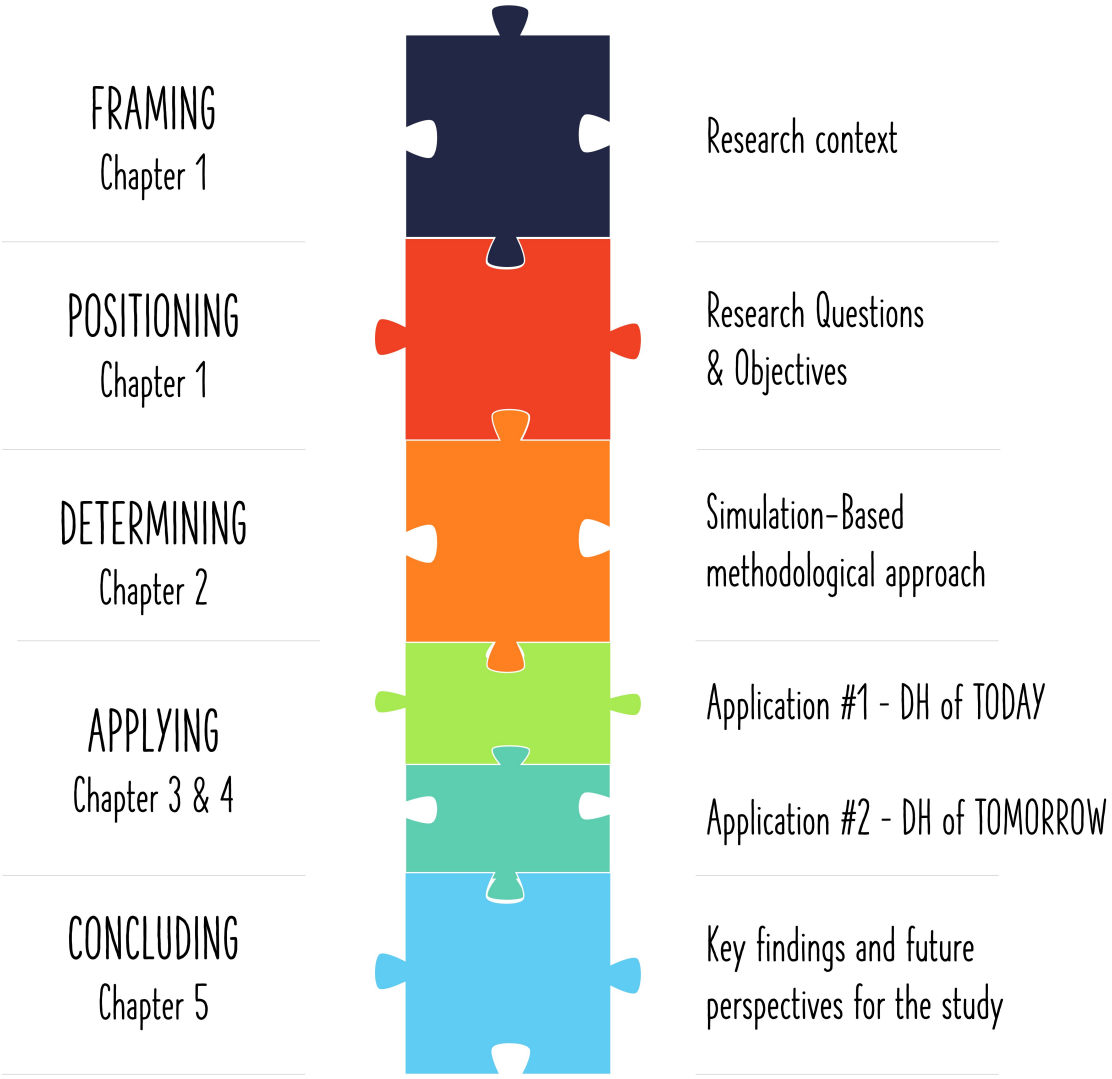

Fig. 1.3 Structure of the Ph.D. Thesis.

Out of metaphor, Chapter 1 serves to set the research context and define the key concepts for the development of the study. Moreover, the research questions that will be the leitmotif of the narrative are also defined. In Chapter 2, starting from a global perspective on the calculation of flexibility in multi-vector energy systems, an overall methodological approach is proposed. It is emphasized that the methodology is simulation-based and all steps of the procedure are discussed more in detail. Then the phases are retraced through the application on two Case Studies in Chapter 3 and 4. Specifically, Application #1 refers to a present-day district heating system (*DH of TODAY* in Figure 1.3), hence the 3^{rd} generation, centralized, and fossil fuel-based network, while Application #2 explores a future district heating scenario (*DH of*

TOMORROW), the 5^{th} generation, with a decentralized and all-electric layout. The Case Study chapters also present the results of each individual application in terms of the simulation outputs and flexibility assessment.
Finally, Chapter 5 summaries the main outcomes of the current research, answering to the research questions of the study and highlighting the potentialities and limitations of the proposed methodological approach and also suggesting potential future expansions for the work.

Chapter 2

Simulation-based approach for flexibility evaluation

This section delineates the methodological framework developed for the estimation of the potential flexibility that a multi-vector energy system can offer. The main characteristic of this methodology is the simulation-based method, therefore the simulation aspect becomes fundamental for the implementation and successful realization of the methodological approach. Indeed, thanks to the dynamic simulation of each component of the energy chain, it is possible to take into account not only the individual technologies installed within the multi-vector system, but also the network effect. The results of the simulation phase are then used as input for the computation of the selected flexibility indicators.

Keywords *Multi-vector Energy System; Simulation-based Methodology; Physical Flexibility; Operational Flexibility; Cross-carrier Flexibility*.

Declaration The topics described in Chapter 2 were previously published in the following publications:

- **Abbà, I.**, La Bella, A., Corgnati, S. P. and Corsetti, E. (2024). Assessing flexibility in networked multi-energy systems: A modelling and simulation-based approach. Energy Reports, 11, 384-393 [14].

- **Abbà, I.**, Andreis, C., Corsetti, E., Lazzari, R., Muro Alvarad, M.A. (2023). Sistemi multienergetici: sviluppo di modelli, architetture di controllo e impianti sperimentali per la validazione per reti calore. Ricerca sul Sistema Energetico (RSE), RdS Report n. 23013281, 2023 [3].

- **Abbà, I.** and La Bella, A. (2022). Multi-energy systems as enablers of the flexible energy transition. REHVA JOURNAL, 59(1), 10-14 [23].

2.1 Overview and objectives

The literature review on the flexibility of multi-energy systems reveals a predominant emphasis on installed technologies throughout all the energy chain (i.e., conversion, generation, and final users' technologies), often omitting the existence of multi-energy networks and their associated physical constraints. However, due to the varying dynamics of energy networks across different carriers, which impact overall flexibility, it is not sufficient to model multi-vector energy systems exclusively in terms of generation and load nodes, as commonly done in the energy hub concept [14]. Accounting for networks can be an advantage that leads to unlock new forms of flexibility, as some of them are inherent storages (e.g., thermal and gas networks), but at the same time it introduces additional limitations due to their physical constraints [53]. In fact, energy networks of different carriers can be characterized by different dynamics affecting the overall MVES flexibility; for instance, thermal grids have much slower dynamical transients compared to electric networks. In detail, these aspects increase the difficulty and complexity of modeling and simulating a MVES, since different energy vectors imply diverse spatial and temporal scales, as well as different temporal resolutions and approaches [30–32]. However, there is a lack of studies in literature regarding the impact of energy networks on the availability of flexibility in a complex system. Therefore, finding a method and a tool able to account also for the presence and the dynamic of the networks is essential for two reasons: to understand network's implications on the analysed system and to determine the flexibility effectively available [14].

2.2 Simulation-based overarching methodology

Considering the above-mentioned context and literature gaps, the current dissertation proposes a simulation-based methodology to evaluate flexibility in a multi-vector energy system, taking into account not only the individual installed devices but also the network effect. The overall methodology is presented in Figure 2.1 and it is composed of five main pillars, which need to be investigated through specifically focused methods.

Step 1 Establish the goals and relevant stakeholders, taking into account their scopes and interests related to flexibility (e.g., delineate flexibility profiles for market participation).

Step 2 Model and simulate the selected multi-vector energy system in accordance with the specified objectives.

Step 3 Quantify and calculate flexibility based on the results derived from previous steps. As outlined before, there exist diverse methods for quantifying and assessing the flexibility of a multi-vector energy system, encompassing various types of flexibility.

Step 4 Investigate cross-domain flexibility implications aligned with stakeholders' requirements. This stage aims to assess flexibility beyond the energy domain, considering its impacts in other sectors, such as conducting financial or environmental evaluations.

Step 5 Evaluate and discuss the findings of the study regarding simulation. If stakeholders require, this phase should also involve the provision of graphical tools or other user-friendly representations to ensure clarity of the analysis outcomes, especially for non-expert audiences (e.g., end-users).

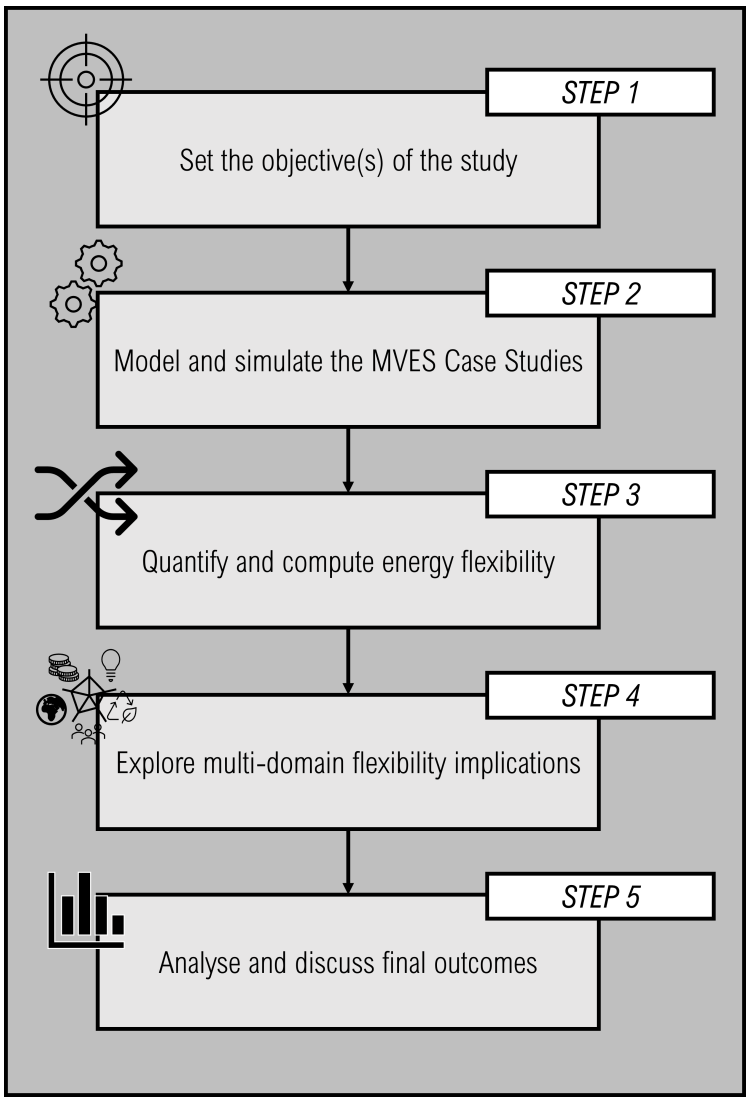

Fig. 2.1 Overall methodology.

Each step of the overarching methodology requires a separate in-depth examination. Starting from Step 2, the focus is on modelling and simulating multi-energy systems and it is further divided into several methodological sub-steps, as highlighted in Figure 2.2.

Step 2 is the core of the entire methodology and has dual purpose, functioning both as a means to assess system flexibility and as a standalone procedure for the examination and evaluation of the Case Studies operation and dynamics. In the current dissertation, on the one hand, the case study of Application #1 aims to represent the majority of district heating systems currently in use. It is a 3^{rd},

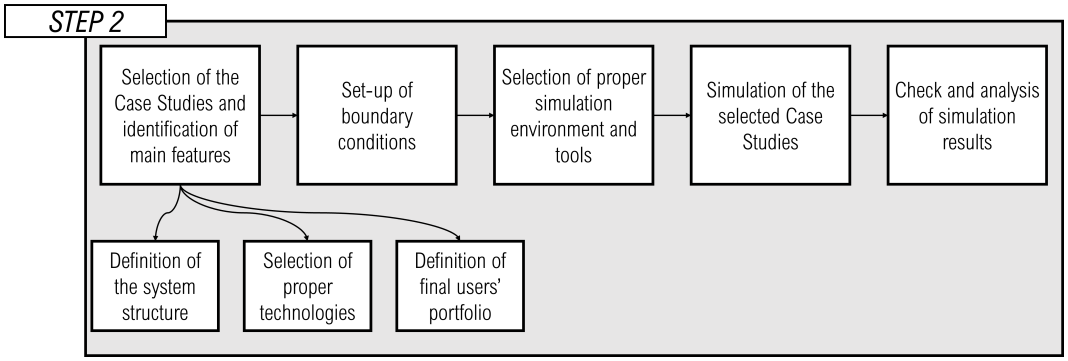

Fig. 2.2 Step2 - Development procedure.

centralized system that uses fossil fuels to provide heat to final users using a hot water network as a heat transfer fluid. For this application, the concept of flexibility is to be intended as supply-side flexibility. On the other hand, in line with future trends regarding the development of the district heating sector towards decarbonization and electrification of thermal uses [37, 38, 42, 43, 56], Application #2 focuses on a case study involving a 5^{th} generation district heating network. In broad terms, the network operates at lower temperatures, employing heat pumps both centrally and in district substations to heat water for distribution to end-users. This results in an all-electric configuration. As outlined in Chapter 1, given the inherent inflexibility of a system composed of only heat pumps, there is the need to understand how to make this configuration flexible.

While these steps will be revisited in Chapter 3 and 4, which present the two examples of application, it is pertinent to provide a concise overview of the simulation tool. As previously mentioned, the selection of an appropriate simulator is fundamental for obtaining coherent results. Various tools are available for simulating energy systems, including those supporting the Modelica language, such as OpenModelica, DYMOLA, and SimulationX. Tools facilitating simplified simulation of energy networks encompass TRNSYS or TERMIS, along with MATPOWER, NEPLAN, or PowerWorld specifically tailored for the electricity and renewable sources domain [52]. In this case, to provide accurate but quick results of the simulation of different energy vectors in a unified environment, the chosen software is Simscape [14, 23], a MATLAB tool developed within the Simulink environment [68]. It enables the construction of object-oriented models grounded in physical links between components. This choice is based on its versatility, with numerous libraries covering all pertinent physical domains involved in MES analysis—namely, electri-

cal, thermal, fluid, and gas. Specifically, within each domain, energy flows are linked to two (or more) variables, denoted as *Through* and *Across* variables, characterized by their intensity and sign. *Through* variables relate to the flow through simulation components (such as electrical currents, liquid and gas flows, etc.), while *Across* variables are measurements taken across components (such as voltages, pressure differences, etc.).
From the various Simscape libraries, the Thermal Liquid library was selected to model the AROMA district heating network. Unlike most domains characterized by two variables, the thermal liquid domain is defined by four variables: mass flow rate [kg/s] and energy flow rate [kW] serve as the *Through* variables, while temperature [K] and pressure [Pa] are the *Across* variables. Specifically, within this domain, the dynamic changes in pressure and temperature are governed by the principles of mass conservation and energy conservation, respectively. In relation to the *Through* variables, the mass flow rate is determined by the principle of momentum conservation, while the energy flow rate is computed using the thermal energy conservation equation. The equations corresponding to these principles are integrated into the blocks of the Simscape library and should be consistently defined for blocks manually created by the user. Each block includes at least one inlet port/node (A) and one outlet port (B) associated with the aforementioned variables [68].
This tool aligns with the requirements for simulating the third- and fifth-generation district heating network utilized as the Case Studies in this research. However, it is essential to note that the proposed simulation-based methodology can also be implemented using other simulation environments, such as Modelica.

Moving to Step 3, concerning the flexibility calculation, firstly, it is necessary to identify which key performance indicators (KPIs) are suitable for the purposes of the research and are compatible with the data available. Limiting the analysis to the energy and technological level, three types of flexibility with their respective indicators have been identified from the study proposed by Corsetti et al. [54]. Therefore, using the outputs of the simulation phase, physical, operational and cross-carrier flexibility are computed (see Figure 2.3).

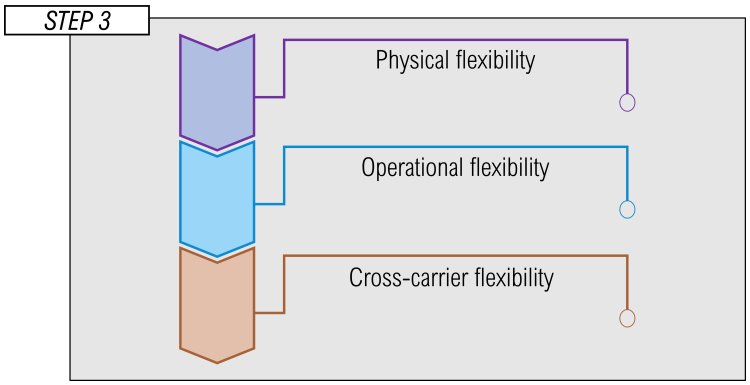

Fig. 2.3 Step3 - Types of flexibilities

In detail, the physical flexibility of an energy vector is related to the characteristic of the installed devices. Focusing on the single technology, it is the maximum allowed modulation for the energy carrier according to the physical limits of the device. The KPI is computed according to Eq. 2.1.

$$F_{ph,d_i} = P_{max,d_i} - P_{min,d_i} \tag{2.1}$$

Where:
d_i: i-th installed device;
F_{ph,d_i}: Physical flexibility indicator of the i-th device [kW];
$P_{max,d_i}/P_{min,d_i}$: maximum and minimum allowed power modulation of the i-th device [kW].
The physical flexibility indicator for the j-th energy vector F_{ph,v_j} of the overall system is the sum of the contributions of all the devices related to that vector, as in Eq. 2.2.

$$F_{ph,v_j} = \sum_{i=1}^{N} F_{ph,d_i} \tag{2.2}$$

The operational flexibility of an energy vector is the ability of the energy carrier to modulate its capacity with respect to a given baseline operation point. Therefore it results in upward (UP-flex) and downward (DOWN-flex) flexibility indicators, meaning the positive and negative displacement to the baseline. Eqs. 2.3 and 2.4 are used to compute UP- and DOWN-flex KPIs for the i-th installed device, after

defining the baseline profile.

$$F_{op,UP,d_i} = P_{max,d_i} - P_{base,d_i} \tag{2.3}$$

$$F_{op,DOWN,d_i} = P_{min,d_i} - P_{base,d_i} \tag{2.4}$$

Where:
$F_{op,UP,d_i}/F_{op,DOWN,d_i}$: UP-flex and DOWN-flex indicators [kW];
P_{base,d_i}: baseline operation point for the i-th device [kW].
In depth, UP-flex relates to the device's ability to increase its power output with respect to a base operating point, vice versa for DOWN-flex. Also in this case, the operational flexibility (UP/DOWN) pertaining to the specific j-th energy carrier can be computed as the sum of the individual operational flexibility of all devices involving that energy vector (Eq. 2.5, 2.6).

$$F_{op,UP,v_j} = \sum_{i=1}^{N} F_{op,UP,d_i} \tag{2.5}$$

$$F_{op,DOWN,v_j} = \sum_{i=1}^{N} F_{op,DOWN,d_i} \tag{2.6}$$

In line with these definitions, it is also possible to define the physical and operational flexibility of the energy demand. Considering the load as if it is a consumer-side device associated to an energy vector, it is possible, using the Eqs. 2.1-2.6, to define profiles and margins. These are not tethered to the installed technology's characteristics but rather to physical constraints and user acceptability regarding altering their consumption patterns. For instance, a constraint might involve permitting adjustments to room set-point temperatures within certain user-acceptable bands of variation; or on the electrical side, it could entail the option to advance or delay the usage of certain household appliances based on external forcing.

Finally, it is necessary to calculate the cross-carrier flexibility, since in a multi-vector energy system, the possibility of offering flexibility through an energy carrier is influenced not only by the devices that involve that carrier, but also by the limits imposed by the other devices that contribute to the production/absorption of power

for the system. Therefore, the Eqs. 2.7 and 2.8 represent the two constraints, F_{UP_CC} and F_{DOWN_CC}, for cross-carrier flexibility.

$$\{F_{UP\_CC}\}_{v2} \leq \{F_{op,UP,v1}\}_{v1} * \sigma_d^{v1,v2} \tag{2.7}$$

$$\{F_{DOWN\_CC}\}_{v2} \leq \{F_{op,DOWN,v1}\}_{v1} * \sigma_d^{v1,v2} \tag{2.8}$$

Where v1 and v2 are the two energy vectors under examination (e.g., thermal and electric carriers), and $\sigma_d^{v1,v2}$ is the conversion factor that transform one vector in the other.

Regarding the Step 4, the non-energy implications of calculating flexibility in a multi-vector system can be different, including environmental and economic ones. They can be both a cause and a consequence of flexible actions. Starting from the environmental theme, typically one of the objectives of a profile modification intervention is to reduce energy consumption, with a consequent reduction in emissions of pollutants into the environment. Another driving factor can be the desire to exploit the availability of renewable sources, which requires the system to absorb or produce more or less electrical power during the day, depending on the moments of maximum production from renewables.
From a financial perspective, flexible intervention can be motivated by external forces, such as changes in price signals on the market, with the ultimate goal of achieving savings or revenues compared to the *Baseline* case.
These multi-energy flexibility implications are addressed in Chapter 4.

All the methodological steps proposed in this Chapter are applied below in Chapters 3 and 4, allowing to demonstrate the consistency and versatility of the procedure.

Chapter 3

Application #1

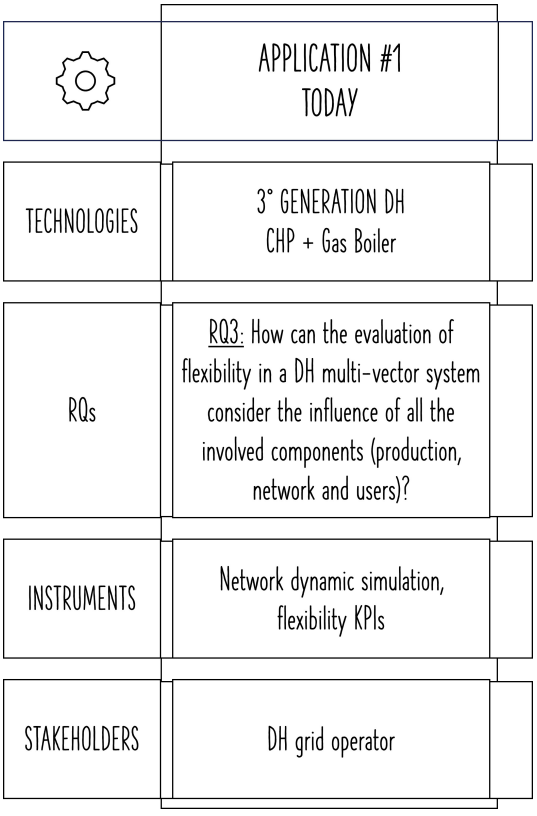

In this Chapter Case Study #1 is comprehensively outlined, trying to address the following research question (RQ 3): *How can the evaluation of flexibility in a district heating integrated system consider the influence of all the involved components, including the network?*

Firstly, the context and objectives of the application are defined. Subsequently, considerable attention is devoted to characterizing the case study, covering simulation processes and flexibility strategies, following the methodological steps detailed in Chapter 2. More in detail, the reference system of this application is a third generation district heating system, which uses as its main fuel the gas to produce heat for a district heating network of high temperature (supply temperature of 90°C) serving five residential users. Finally, the simulation results and flexibility assessment findings are reported and discussed.

Keywords *Multi-vector Energy System; Third-Generation District Heating; Dynamic Energy Modeling; Physical Flexibility; Operational Flexibility; Cross-carrier Flexibility.*

Declaration The topics and application described in Chapter 3 were previously published in the following publications:

- **Abbà, I.**, La Bella, A., Corgnati, S. P. and Corsetti, E. (2024). Assessing flexibility in networked multi-energy systems: A modelling and simulation-based approach. Energy Reports, 11, 384-393 [14].
- **Abbà, I.** and La Bella, A. (2022). Multi-energy systems as enablers of the flexible energy transition. REHVA JOURNAL, 59(1), 10-14 [23].
- Corsetti, E., Casamassima, V., La Bella, A., and **Abbà, I.** (2021). Valutazione della flessibilità di sistemi multienergetici. Ricerca sul Sistema Energetico (RSE). RdS Report n. 21010810 [1].

3.1 Overview and objectives

This Chapter presents a proposal for a novel tool tailored for the efficient simulation of MESs, taking into account network dynamics. Figure 3.1 summarizes the two main objectives, subdivided into: Simulation/Modeling and Flexibility. Indeed, the primary objective of this proposed tool is to deliver prompt insights into the performance of a multi-vector energy system, an essential attribute when dealing with energy optimization and control algorithms [23]. To achieve this, the simulator is intentionally designed as a lightweight tool, capable of conducting accurate but also quick simulations. It simplifies the modeling of certain components compared to their actual operations. This deliberate simplification is justified by the broader scope of this research, which extends beyond the functioning of individual components to encompass the entire energy system, form generation, to the distribution network, and end-users. The results from the simulation phase are subsequently utilized to achieve the ultimate objective of the Case Study, which is to show the behavior of the system while meeting the thermal demand and consequently to illustrates the flexibility margins of the system from a supply-side perspective. In fact, in this application, flexibility is analyzed from the point of view of the power plant and its ability to modify its generation profiles. Technical and physical limitations are imposed not only on conversion technologies but also on the thermal network to explore the limits of potentially exploitable flexibility. In this Application #1 users are considered as passive.

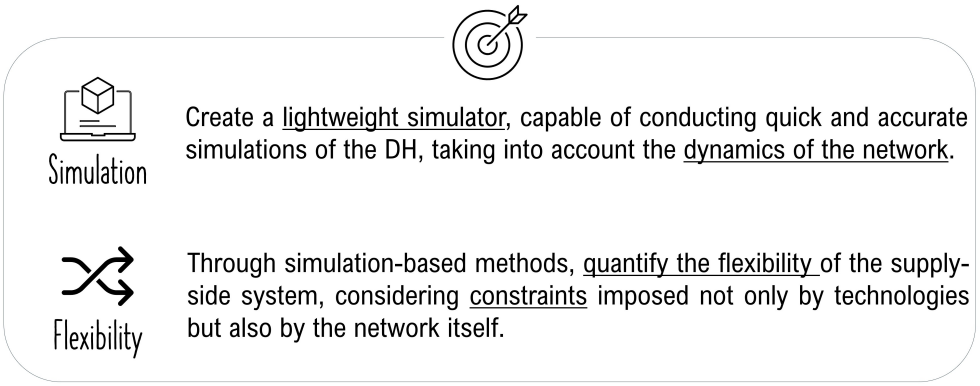

Fig. 3.1 Objectives of Application #1.

3.2 Modeling and simulation of Case Study #1

In this section, the main features of the case study and the assumptions made in the creation of the application are examined in detail.

3.2.1 Identification of main features of the Case Study

Given that the MVES concept involves the coexistence and synergy of various energy vectors, a local district heating network was chosen as the benchmark system for this application. Indeed, this network has the capability to integrate multiple heating sources and technologies to serve diverse user needs and can interface with the electrical through devices such as cogeneration and heat pumps. To delve into the specifics, the analysis started with the creation of a simulator for the thermal vector, and the AROMA network, selected from the literature [69], was adapted to be used as the Case Study for the current investigations. A scheme of the system layout is presented in Figure 3.2.

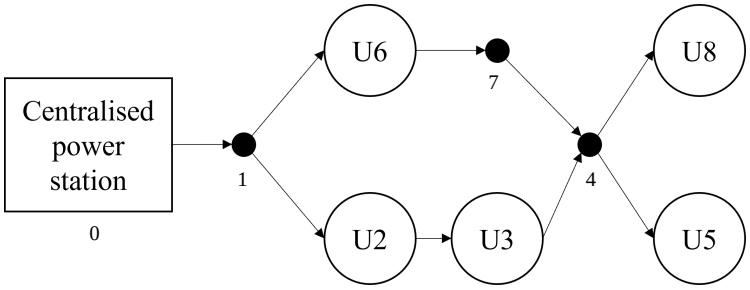

Fig. 3.2 Scheme of the supply network of the AROMA network. (Ui-th = final user). Adapted from [69] and [14].

The district heating network comprises two supply branches and incorporates a loop. The system adopts a centralized architecture, featuring a central thermal plant responsible for supplying the necessary thermal power to heat the water flow rate in the supply pipes. This ensures that the thermal demand of the end-users connected to the network is met consistently throughout the day. Specifically, the central power station comprises (i) a cogeneration plant (CHP), which serves as the technology connecting thermal and electric vectors (taking into account the outputs of the CHP) and the gas vector (also considering the utilized fuel); and (ii) a gas boiler (GB), connected in series to the CHP. Given these characteristics, the district heating system

falls under the classification of third-generation district heating [42, 56]. As shown in Figure 3.2, addressing the thermal energy demand involved distributing loads among five end-users (depicted as Ui-th in the schematic), following the weighted allocation outlined in [69]. The varying shapes and peak powers observed in the load profiles were derived from the analysis of monitoring data collected from an actual district heating system in the north of Italy. Figure 3.3 presents the hourly thermal demand for each user.

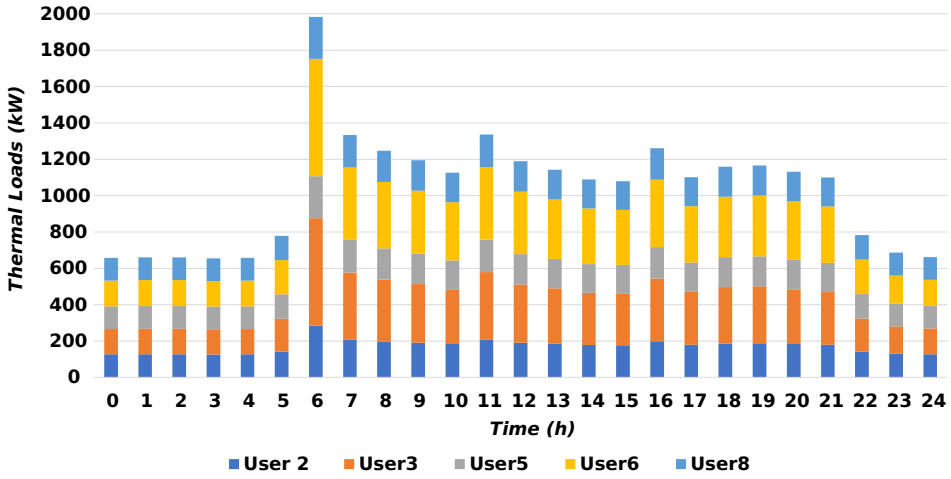

Fig. 3.3 Users' thermal profiles, from [14].

Moving to the distribution network, the structure and geometric attributes (including lengths and diameters) of both the supply and return pipes were sourced from [69]. Table 3.1 details the parameters for the supply network, and these same values were applied to the return line.

Pipe section	Length [m]	Diameter [m]
P01	500	0.107
P12	282.8	0.107
P23	500	0.083
P34	282.8	0.083
P45	400	0.070
P47	282.8	0.083
P16	282.8	0.107
P67	500	0.083
P78	600	0.070

Table 3.1 Network's geometrical features [14].

3.2.2 Set-up and boundary conditions

The performance of the district heating changes according to the location in which it is placed. In this Application, the assumption was that the district heating system was situated in a northern region of Italy, specifically in Turin. The ground temperature was considered constant throughout the year, maintaining a value of 12°C. Hot water, treated as an incompressible fluid, served as the heat transfer fluid in the DH network. Boundary conditions for temperatures within the thermal network included setting a supply temperature of 90°C at the central power station's exit and a return temperature of 65°C downstream of the users' substation [14, 23, 69]. Ad-hoc controllers are implemented to monitor and maintain the desired reference temperatures throughout the simulation, ensuring a reliable supply of thermal needs.

3.2.3 Simulation: tools and description of component blocks

As mentioned in Section 2, the Simscape simulator was used to simulate the Case Studies. The subsequent section provides a concise overview of the key components of the system, emphasizing the ad-hoc created blocks and their associated conservation equations. In contrast, only the overall functionality of pre-existing blocks is outlined, as comprehensive explanations of the equations can be found in Simscape

guides [68].

Central power station The centralized thermal power station is a subsystem designed to deliver the thermal power at the desired temperature to meet the requirements of users. It is constructed by assembling various blocks, with some sourced from reference libraries and others crafted manually. The power station encompasses not only blocks directly associated with power generation but also includes blocks dedicated to overseeing flows, temperatures, and pressure, as depicted in 3.4.

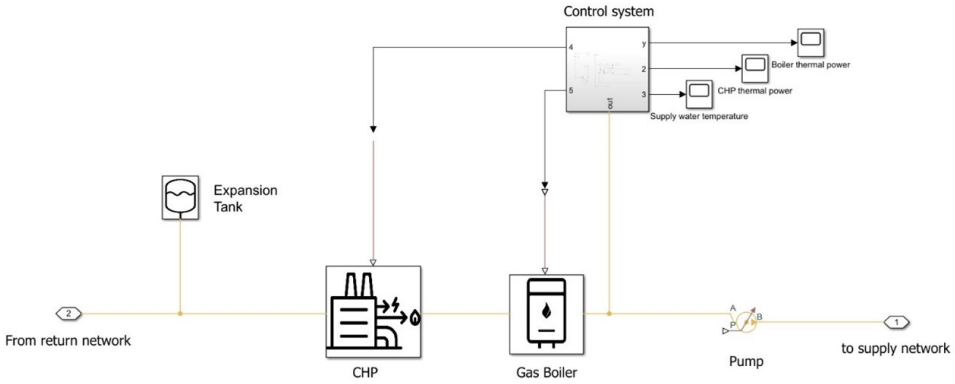

Fig. 3.4 Scheme of the centralized thermal power station [14].

Focusing on the temperatures of supply and return from the plant, in supply the thermal station guarantees a temperature of at least 90°C, while on the return it settles on 65°C. The 90°C was chosen to ensure that even the most disadvantaged user of the network receives the needed heat, while the 65°C are the result of heat delivery and temperature losses along pipes [14, 23, 69]. Delving into the operational complexity of the station, the cogeneration plant and the gas boiler arranged in series are independently activated and regulated by a dedicated control system. In specific terms, the CHP is controlled to follow a reference power profile. A CHP with a maximum thermal capacity of 2 MW was chosen, with a unitary power-to-heat ratio and having the ability to modulate its output power hourly within a range of $30-100\%$ of the nominal power. For flexibility assessment, a reference thermal power profile for the CHP was defined as the *Baseline* for calculations. If the tracked CHP thermal production is not sufficient to deliver the required heat to the network, the water flowrate proceeds through the GB stage for further heating. A proportional

control system ensures that the boiler's output temperature aligns closely with the desired reference temperature of 90°C. If not, it dispatches a power regulation signal to the boiler, modulating its thermal power output, up to a maximum of 1 MW.

Table 3.2 summarized the main features of the production technologies of the thermal station.

Technology	**Maximum power**	**Controlled variable**
CHP	2 MW	Thermal power profile
Gas Boiler	1 MW	Supply temperature (90°C)

Table 3.2 Thermal power plant characteristics [14].

CHP and GB blocks were represented in Simscape by the associated heat exchangers, using the equations (Eqs. 3.1, 3.2, 3.3 and 3.4) based on the chosen simulation detail level [70].

$$Q_u = \dot{m}_A * c_p * (T_A - T_B) \tag{3.1}$$

$$\dot{m}_A + \dot{m}_B = 0 \tag{3.2}$$

$$\phi_A + \phi_B + Q_u = 0 \tag{3.3}$$

$$p_A + p_B + k_{HX} * \dot{m}_A^2 = 0 \tag{3.4}$$

Where:
A: inlet port;
B: outlet port;
Q_u : thermal power provided to the final user [kW];
c_p: water specific heat (assumed constant and equal to 4.186 kJ/(kgK));
T: water temperatures [K];
ϕ: energy flow rates, entering the A port and exiting the B port [kW];
$\dot{m}$: water mass flow rate [kg/s];
p: water pressures [Pa];
k_{HX}: pressure loss coefficient for heat exchangers.

Lastly, the central station plant is furnished with both an expansion tank and a pump designed for the oversight and regulation of network pressure values. Specifically, the expansion tank compensates for alterations in pressure and volume within the district heating network resulting from temperature fluctuations along the pipes. The expansion vessel's reference pressure is set at $5 * 10^5$ Pa, and the block is manually created to simulate the expansion vessel as a closed chamber capable of adjusting its volume to guarantee that the flow entering the chamber exits with the intended pressure. Conversely, the circulation pump block is derived from Simscape libraries and is tasked with enforcing a pressure increase of $5.5 * 10^5$ Pa [69] on the flow rate passing through it. This mandated pressure differential ensures the delivery of the required water volume with the desired thermal characteristics, even to users situated farthest from the power plant. To impose the pressure differential, an isentropic compression power Q_p is applied to the fluid following Eq. 3.5, where ρ_{avg} is the mean density of the fluid obtained as the average between input (A) and output(B) values.

$$Q_p = \frac{\dot{m}_A * (p_B - p_A)}{\rho_{avg}} \tag{3.5}$$

Substation at users' side Similarly to the central power station, the substations utilized by users are composed of a combination of pre-existing and manually generated blocks and they represent the interface between the DH network and the building distribution system. The primary objective of these substations is to convey the designated amount of thermal power from the supply network to the end user, while adhering to specific boundary conditions. As previously mentioned, one condition pertains to the return temperature, which must match the specified reference temperature of 65°C. To address this requirement, each user's substation incorporates a heat exchanger and a dedicated control system. This control system, utilizing a valve, manages the flow rate of water entering the heat exchanger. In a more detailed explanation, the control system takes various inputs into account, including the reference temperature for the return network (set at 65°C) and the user's load profile. Subsequently, it compares the reference temperature with the temperature of the water flow rates exiting the heat exchanger. If disparities are identified between these temperature values, the Proportional-Integral (PI) controller transmits a signal to the regulating valve. The valve, through adjustments to its

section, either increases or decreases the water flow rate accordingly. In this scenario, the modeling of the heat exchanger follows a simplified approach, utilizing Eqs. 3.1-3.4, as outlined in [23] and [69].

Pipelines Pipelines constitute the dedicated network for conveying the heat transfer fluid within enclosed ducts. The Simscape library already includes modeled pipe blocks. In the simulation environment, every connection between distinct blocks, such as between the central station and the initial user's substation, is established using a pipe block. This component enables the simulation of water flow dynamics over time and along the pipes for both the supply and return networks. The simulation accounts for factors like temperature and pressure drops, as well as thermal losses occurring between the pipes and the ground. The model used to describe this phenomenon is that of finite volumes, which involves discretizing the liquid into multiple control volumes that interact with each other through interfaces. The "pipeline" block represents a segment of the network containing a fixed volume of liquid. Within the pipe, the liquid experiences pressure drops due to friction and heat losses due to convection between the fluid and the tube wall (if it is at a different temperature than the liquid). To be more faithful to reality, the Simscape block also allows for the consideration of dynamic compressibility and fluid inertia, at the expense of increased complexity of equations and consequently computational time. In the specific case under consideration, hot water is considered as an incompressible fluid, and consequently, by the principle of conservation of mass, the inlet flow rate is equal to the outlet flow rate. To elaborate, viscous frictions are represented through the Darcy-Weisbach equation, while the heat transfer is governed by correlations that incorporate the calculation of Nusselt numbers, contingent upon whether the flow is laminar or turbulent. The detailed listing and explanation of the equations employed can be found in [68], and as such, they will not be reiterated in this section. Here, are just presented the energy balances in Eqs. 3.6 and 3.7 (which regulates the heat exchanged between the external layer of the pipe and the environment, the ground in this case).

$$V\frac{\partial(\rho u)}{\partial t} = \phi_A + \phi_B + Q_H = 0 \tag{3.6}$$

$$Q_H = Q_{conv} + \frac{k * S_H}{D} * (T_H - T) \tag{3.7}$$

Where:
A: inlet port of the block;
B: outlet port of the block;
V: volume of the water in the pipe [m^3];
ρ: water density [kg/m^3];
u: water velocity along the pipe [m/s];
ϕ: energy flow rates, entering the A port and exiting the B port [kW];
Q_H: power exchanged between the pipe outside layer and the environment [kW];
Q_{conv}: convective power associated to a non-zero water flow [kW];
k: thermal conductivity of the fluid [W/mK];
D: pipe diameter [m];
S_H: tube lateral surface, obtained by multipling the tube diameter by the length [m^2];
T_H: tube temperature [K];
T: water temperature in the pipe [K].

Case Study simulation After defining the boundary conditions, selecting blocks from the library, and incorporating new components based on their constitutive equations, the simulator was constructed, culminating in the final AROMA network layout depicted in Figure 3.5. The image represents the schematic layout of the supply network as implemented in Simscape, the return network follows the same path therefore it is not represented in the figure.

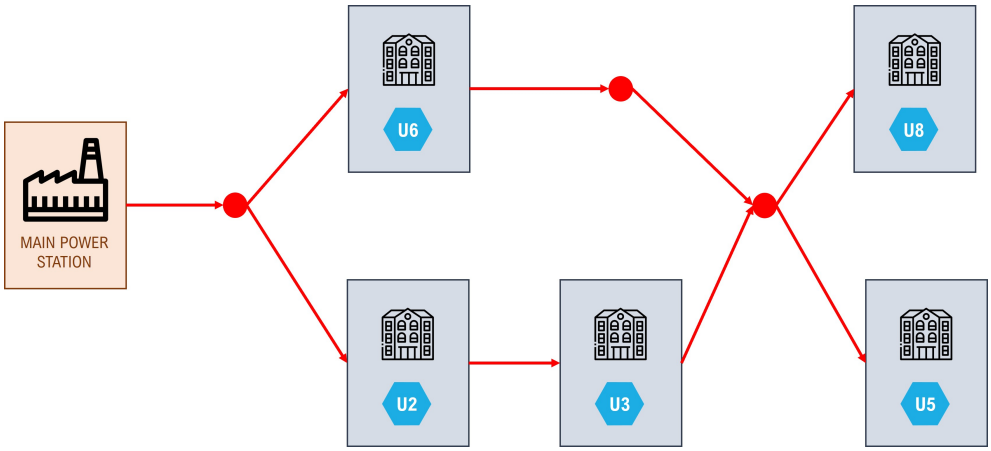

Fig. 3.5 Schematic layout of the third-generation district heating network as implemented on Simscape [14].

The simulation of the supply side and distribution network was directly carried out using Simscape. The load profiles of users, derived from the analysis of actual monitoring data (see Section 3.3), were integrated into the simulator as signals entering the control systems of the substations. The chosen time frame for the simulation spans 24 hours, with the aim of assessing the system's performance over a complete day and overcoming any initial stabilization transients. Given that the monitoring campaign provides thermal load data on an hourly basis, it was assumed that consumption remains constant throughout each hour.

3.2.4 Assumption for flexibility calculation

Moving to the evaluation of system flexibility, the aim in this context is not to introduce novel metrics or quantification methods but rather to demonstrate the utility of the previously described simulator for such assessments. The specific emphasis in this application is on power flexibility from the central station. Starting with the examination of physical flexibility in the current case study, it is important to note that electricity production is solely attributed to the CHP. However, given that the CHP is not the exclusive conversion technology in the central power station, a mere assessment of its power limits is inadequate. In reality, boiler production must also be taken into account, as users must consistently receive the required amount of heat within an acceptable range of supply temperatures at each time step. In addition, the analysis does not limit to consider the constraints arising from the two conversion technologies, as traditionally done by considering multi-vector systems as energy hubs, but thanks to the exploitation of dynamic simulation, can also take into account the effect of the thermal network. Consequently, to ascertain the maximum and minimum operating limits for the main power plant, the following constraints were imposed:

$$90^{\circ}\text{C} \leq T_{out,PS} < 100^{\circ}\text{C} \tag{3.8}$$

Eq. 3.8 implies that the temperature $T_{out,PS}$ of the water leaving the power station must not exceed 100°C to ensure the fluid remains in a liquid phase.

$$85^{\circ}\text{C} \leq T_{in,U5} < 90^{\circ}\text{C} \tag{3.9}$$

Through Eq. 3.9, the user facing the greatest disadvantage, identified as User5 (U5) in this scenario and situated farthest from the centralized station, should receive hot water in the substation at a temperature $T_{in,U5}$ of at least 85°C to guarantee the correct amount of heat delivery. This second constraint considers the thermal losses experienced along the district heating network.

The flexibility calculations were performed utilizing the formulas outlined in Section 2 (Eqs. 2.1-2.8), which are integrated into MATLAB to analyze the results obtained from the Simscape simulations within the same simulation environment.

3.3 Analysis and discussion of final outcomes

This section is dedicated to the analysis of the outcomes of Application #1 to verify that the developed simulator performs as expected and to evaluate the dynamics of the reference case study. Additionally, the results in terms of flexibility are presented to highlight how the proposed simulator can be suitable to identify upper and lower flexibility bounds and evaluate the effect of these bounds on the network. Indeed, it has to be said that the strength of the modelling step of the simulation-based methodology lies in the fact that results can be used a stand-alone outputs to make some consideration on MVESs behaviour, as well as inputs for the evaluation of the operational flexibility that complex systems can offer.

First of all, it is interesting to analyse the power outputs of the centralized station in order to use these values for the assessment of the flexibility of the Case Study. Given the technological composition, the power station is where the different energy vectors interact with each other through conversion technologies such as the CHP and GB. Both machines use gas as input fuel, while their outputs differ when considering the different technologies involved. In detail, the gas boiler is a *gas-to-heat* configuration, therefore its output is the sole thermal power, while the CHP contributes to the production of thermal power to feed the DH network and electricity to be injected into the power grid (*gas-to-power & heat* configuration). Starting from the *Baseline* definition, Figure 3.6 shows CHP (in orange) and GB (in green) thermal power output profiles, while the dotted black line represents the hourly sum of thermal demand from the five users. The design and sizing of the central station started with the definition of the CHP hourly profile, indeed the CHP is the leading technology of the system. It is assumed that the CHP unit is used to meet the minimum hourly load and can adjust its power output only twice a day; the decision behind this choice is influenced by the dynamics of the electricity market [14]. In the *Baseline* scenario, the generation profile of the CHP is designed to minimize energy generation during nighttime when there is lower demand for thermal energy. In contrast, it maximizes power production during the day, starting from 06:00-07:00 time slot, aligning with the peak demand from users. This thermal production pattern for the CHP closely resembles the typical operational behavior of CHP plants in district heating networks, consistent with [71]. Once the CHP's operation is defined, the gas boiler is employed to integrate thermal power and ensure

the total required thermal power is met. Following this basic operation, all users are satisfied, and the reference supply temperature (90°C) is maintained across all substations.

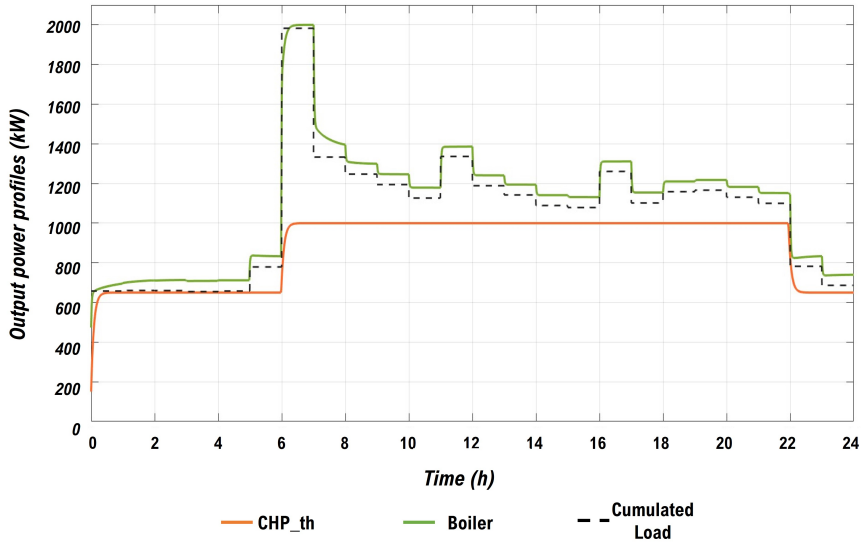

Fig. 3.6 Baseline thermal power hourly profiles of the central station. From [14].

As can be seen in Figure 3.6, the CHP serves the majority of total heating demand, reaching almost 84%, while the GB is mostly used to help the CHP in presence of peaks, resulting in a more variable shape. In terms of the pure simulation aspects, the simulation takes approximately two minutes, with the initial transient phase lasting one hour (3600 seconds) within the overall simulation time span of 24 hours. By setting the limitation on network's temperatures exposed in Section 3.2.4, through the use of the simulator it is possible to obtain various CHP power profiles (both thermal and electric) and to identify those that aligns with the constraints, thus establishing the maximum range of physical flexibility. The upper margin of flexibility was obtained by verifying that the supply temperature exiting the central power station ($T_{out,PS}$) does not exceed 100°C. The sole CHP, without the GB integraition, is able to achieve this condition if it can adjust its production profile every hour.
On the contrary, to establish the lower flexibility bound, the first try was made by switching the CHP off, in order to identify the system's extent. Nevertheless, it was not possible to switch the CHP off for the entire runtime because sole boiler's thermal power is not sufficient to meet all the thermal demand of the users, maintaining at

least 85°C throughout the entire supply network. This because of the design size of the boiler [14].

Once the upper and lower boundaries of physical flexibility are established, the operational flexibility of the system can be computed using Eqs. 2.1-2.6. This involves comparing the flexibility limits with the *Baseline* power profile. The focus is here on the electricity energy vector. Operational flexibility, defined as the system's ability to adjust its power relative to a given baseline. However, since the objective of the DH system is to ensure the needs of the load, once the physical and operational limits of the installed devices plus the contribution of the network have been identified, it is necessary to combine the effects of the different generation units to verify that the thermal power produced is sufficient to satisfy the users [2]. This analysis, through the application of the Eqs. 2.7 and 2.8 led to the identification of the regions of feasible flexibility points in Figure 3.7. Recalling definitions, UP-flex represents the positive deviation from the baseline, calculated by subtracting the baseline from the upper bound (depicted in the blue area in the figure). Conversely, DOWN-flex represents the negative deviation from the baseline, illustrated in the red area. These areas signify the system's ability to increase or decrease electrical power production compared to the basic profile, as needed.

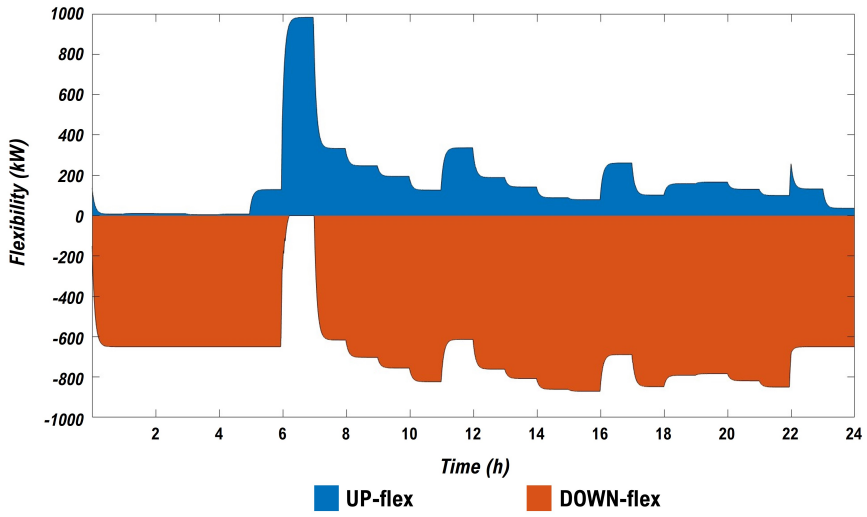

Fig. 3.7 UP- and DOWN-flex electric flexibility profiles. From [14].

The cross-carrier flexibility margins for the electricity vector for one day for the Application #1 are displayed in Figure 3.7 in which the colored regions depict the

entirety of feasible points for offering flexibility. The UP-flex is illustrated along the positive y-axis while the DOWN-flex is represented by negative y-values. With the *Baseline* profile proposed in Figure 3.6, the shape of upward and downward flexibility is non-symmetrical and they are not balanced in terms of energy available in the 24 hours. For instance, in the first hours of the day, the CHP can increase its electric production a little until the load is covered, while in the same time span, it can drop the electric production a lot because the GB compensates for the lack of heat production.

Looking at the situation from the grid standpoint, the blue area is a surplus of electric energy at the disposal of the grid coming from the plant with respect to the predicted quantity, while the red area means a deficit of electricity. Up to this point, the simulator has been employed to identify flexibility boundaries. However, the issue can also be examined from a different perspective. In situations where there is a requirement of an amount of flexibility from the grid operator within a defined time frame, the tool can be used to verify if complying with the requested flexibility aligns with the physical constraints of the network, such as temperature limitations. As an example, during the morning peak demand between 06:00 and 07:00, the system is unable to provide downward flexibility (see Figure 3.7); the system can at most match the *Baseline*. Consequently, if the operator asks for a decrease in electricity production from the CHP during that hour, the system cannot meet the grid's request. "Otherwise, the temperature of the supply water flowrate reaching the most disadvantaged users will be lower than 85°C, resulting in user dissatisfaction. Using the simulator, the energy manager of the plant can easily answer positively or negatively to the grid operator with a reasonable response time. To check these boundaries, one of the outputs of the simulation tool is the temperature trend at the inlet (in) and outlet (out) nodes of each component [14]". In relation to this, Figure 3.8, Figure 3.9 and Figure 3.10 illustrate the two main physical quantities involved in the three flexibility scenarios. Specifically, for each Scenario two graphs are presented, the first one is the representation of the temperature evolution throughout the day in two relevant nodes (i.e., the outlet for the thermal station $T_{out,PS}$ and the inlet of the most disadvantaged user $T_{in,U5}$); while in the second one the CHP thermal power output profiles are portrayed.

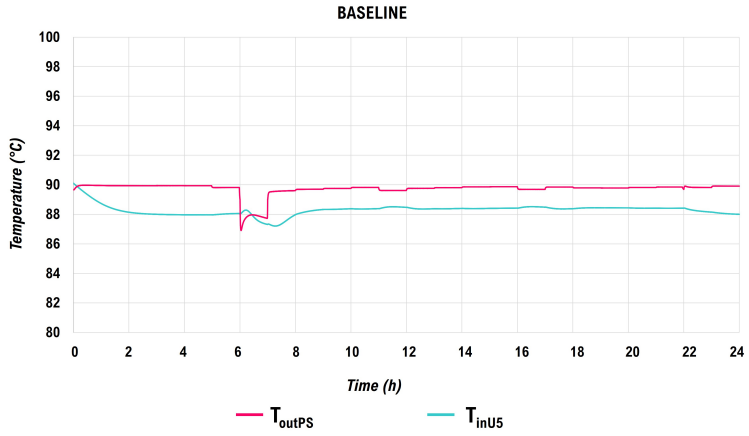

(a) Temperatures.

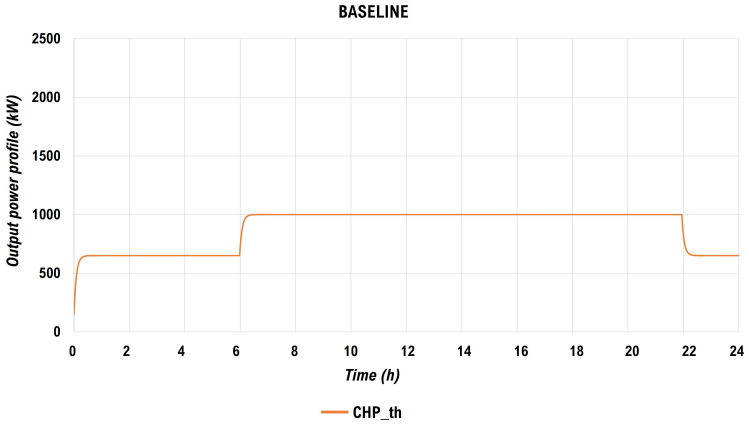

(b) CHP thermal production profile.

Fig. 3.8 *Baseline* scenario. Left: Trend of temperatures (inlet of User5 and outlet of the central station); Right: CHP thermal output power profiles. From [14].

Analyzing the *Baseline* scenario (Figure 3.8(b)), the thermal power profile of the CHP reflects the standard operation of the device and serves as the benchmark for calculating operational flexibility. Concerning temperatures, except from peak periods, the supply temperature remains relatively constant at the desired 90°C, with water delivered at almost 88°C to User5, due to thermal losses throughout the thermal network. Furthermore, it is interesting to note the time delay between the response to the peak request on the supply temperature at the central station and the propagation of the event until User5. This is caused by the slow dynamic of the thermal grid [14].

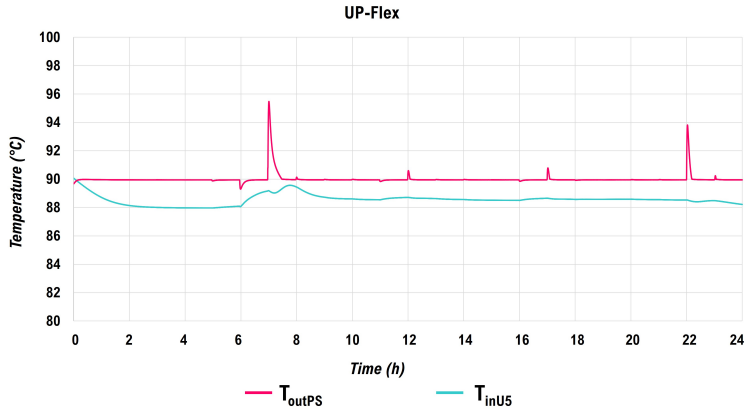

(a) Temperatures.

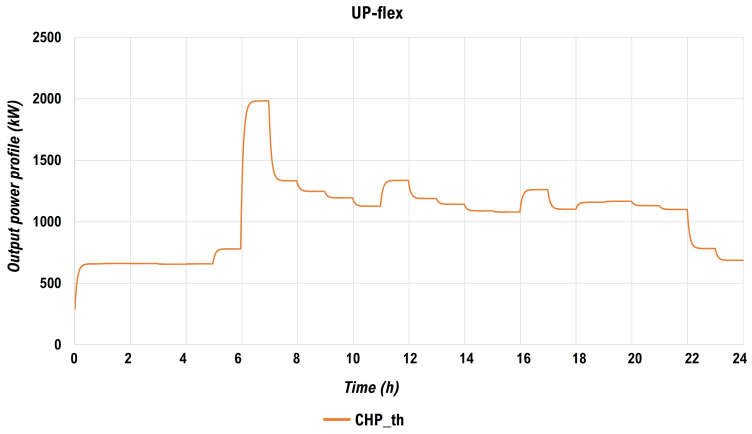

(b) CHP thermal production profile.

Fig. 3.9 *UP-felx*scenario. Left: Trend of temperatures (inlet of User5 and outlet of the central station); Right: CHP thermal output power profiles. From [14].

The results for the *UP-flex* scenario are portrayed in Figure 3.9. With respect to the *Baseline* scenario, the temperature $T_{out,PS}$ oscillates more around the set-point of 90°C, this is caused by the influence of the proportional controller used to manage the central station operation and its convergence, but the limit temperature of 100°C is never reached. Comparing the thermal profile of the *UP-flex* scenario Figure 3.9(b) with that of the *Baseline* in Figure 3.8(b), it is evident that the thermal power values are elevated due to the CHP's capability to heat water to a higher temperature, forcing it to operate to meet the peak demand. In this scenario, the CHP fulfills the 98% share of demand, while the gas boiler covers to the remaining percentage.

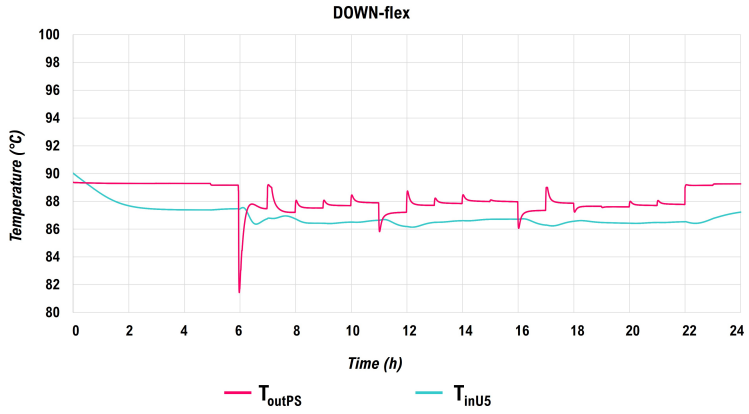

(a) Temperatures.

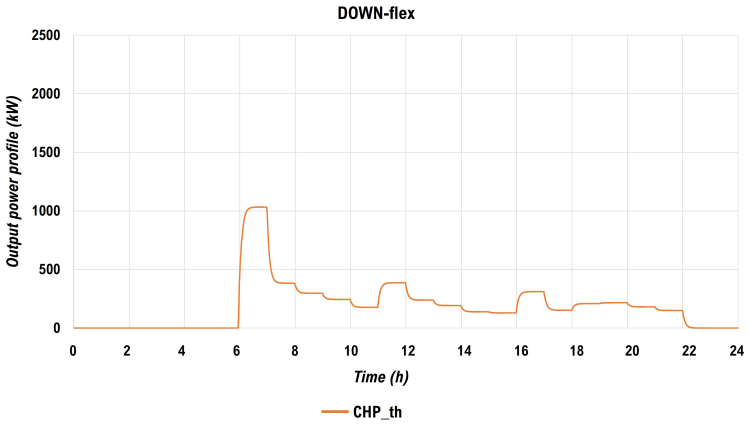

(b) CHP thermal production profile.

Fig. 3.10 *DOWN-flex* scenario. Left: Trend of temperatures (inlet of User5 and outlet of the central station); Right: CHP thermal output power profiles. From [14].

Finally, Figure 3.10 shows temperature profiles and thermal profiles in *DOWN-flex* Scenario. In this case, it is imposed that the CHP produces the minimum possible thermal power, while ensuring that the User5 is satisfied, and then the combination of CHP + GB guarantees at least a water temperature of 85°C in input to User5's substation [14]. The $T_{out,PS}$ is lower than the set-point temperature of 90°C, as can be observed with the pink curve. As a consequence, accounting for the heat losses along the network, also the the $T_{in,U5}$ is lower than 88°C of the two previous scenarios, but is, in any case, higher than 85°C, value set as boundary condition. The minimum temperature value reached by the pink curve (82°C at 06:00) is due to oscillations caused by the convergence of the PI controller, it is not a value really experienced by

the fluid in the pipe. This is also evident from the fact that at the input of the User5 the temperature value is > 82°C.
In this scenario, the CHP accomplishes a daily share of 18% of total thermal request.

3.4 Conclusions

With the intention of answering the research question (RQ 3): *How can the evaluation of flexibility in a district heating integrated system consider the influence of all the involved components, including the network?*, Case Study #1 was developed to test the proposed simulation-based methodological framework. In detail, the application provided a deep spotlight on the system modelling and simulation tool, as well as on flexibility assessment. In line with this, a lightweight simulator was developed to simulate the operation of the multi-vector energy system, consisting of a small district heating network powered by a central power station, with promising results in capturing the dynamics of the system. In the application, the simulator was used not only to explore the behaviour of the system while meeting the thermal demand, but also to find the physical, operational and cross-carrier flexibility bounds of the multi-carrier system, concerning the electricity vector. In fact, it was demonstrated that, through the use of the simulator, it is possible to calculate the margins of flexibility both upwards and downwards, respecting the constraints of the thermal network and users (i.e., temperatures and delivered heat). The results showed that, once the *Baseline* is defined, the processing of simulation outputs allowed to determine and graphically represent the cross-carrier flexibility border for the electrical vector. Indeed, two areas were identified representing all the feasible points for available flexibility (UP- and DOWN-flex). "Thus, it was demonstrated that the simulator can be used both to find flexibility margins to define a flexibility profile to offer for ancillary services, and also to verify if the flexibility required from grid operators is consistent with network physical restrictions [14]". However, the importance of choosing the appropriate base operating points for the plant is due to the fact that different baselines can lead to different operational flexibility profiles. In this regard, one of the main limitations of this application is the lack of optimization for managing the combined operation of CHP and GB in the central power plant. However, this should be done to obtain a more realistic baseline for calculations. Therefore, future research will try to resolve this issue.

To address the strengths of the proposed methodology, the developed simulator can be used to assess the potential flexibility obtained from complex systems, as well as provide some considerations regarding the behavior of multi-vector system when used as a standalone model. In fact, the simulator allowed to observe the hourly variations of two fundamental variables within the system, namely temperature and cogeneration power, over the three different flexibility scenarios: *Baseline* (no flexibility), upward and downward flexibility. Additionally, other variables such as pressure and flow rate can be obtained at any point within the multi-vector system if desired. In summary, to answer the RQ 3, the dynamic simulation and in particular the developed simulation tool allows to assess the flexibility of a multi-vector energy integrated system considering the different characteristics and dynamics of all the involved components, from the conversion technologies installed in the main thermal station, to the distribution network of the district heating. Moreover, the simulator is suitable for different types of customization including different types of assets, networks, and end users.

3.4.1 Potential expansions of the work

Future research could aim to address potential weaknesses of Case Study #1 and expand its concept and application. As for future prospects, it is conceivable to first compare the operation and results of the simulator with actual cases together with actual measurement data. This analysis provides an opportunity to validate the simulator and adjust the *Baseline* against real data if necessary. The work conducted with this Case Study focused mainly on technical/energy issues because it arose from the need to find a way to simulate complex systems and evaluate their flexibility taking into account different dynamics and physical limits of the elements involved. Potential future expansion of the work could also enlarge the analysis to not purely energetic fields. It would be important for forthcoming tasks to also examine the financial sphere of the problem, analysing the interaction and combination of the electricity/heat and gas markets and participation in ancillary services markets. It would be significant to understand how the willingness to offer flexibility and flexibility itself are economically enhanced.
Finally, the potentiality of Application #1 is linked to the chosen Case Study, so to a medium temperature district heating network with passive users. To further explore all possible fields and types of flexibility, Application #2 has been selected and

described in Chapter 4. This allows observing the issue from a different perspective and achieving new goals. Indeed, Case Study #2 represents the natural evolution of Application #1 from the point of view of technological generation and layout for the district heating of the future. Returning to the initial metaphor of the puzzle, Application #2 represents an essential piece of the puzzle that allows for a better definition of the overall framework.

Chapter 4

Application #2

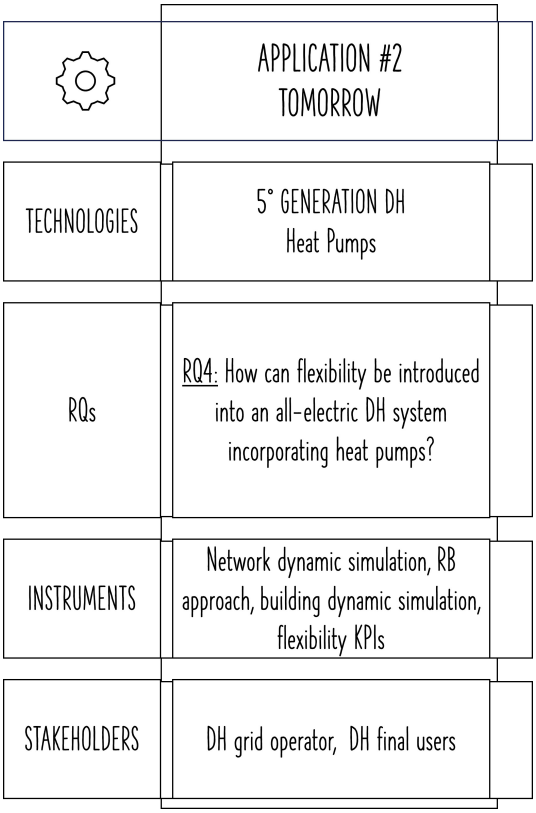

In this chapter, Case Study #2 is thoroughly elucidated, following the methodological steps outlined in Chapter 2. Initially, the context and objectives of the application are clearly defined. Subsequently, significant focus is dedicated to characterizing the case study, encompassing simulation processes and flexibility strategies. Lastly,

the Chapter presents and discusses the simulation results and findings from the flexibility assessment. More in detail, this chapter presents the activity related to the implementation of a simulator for an innovative low-temperature district heating network that feeds a set of districts in a big city. This consists of a main station and six distributed substations, all powered by heat pumps. If in Application #1 the building consumption data derived from monitoring campaigns, in this Case Study they are the results of the dynamic simulation of buildings, defined using the Reference Buildings approach. Therefore, a significant part of the Chapter is also dedicated to the characterization and modeling of the Reference Buildings. Then, since the system composed only of heat pumps, without integration boilers, is inherently un-flexible, this Application allows to answer to the research question (RQ 4) "*How can flexibility be introduced into an all-electric district heating system incorporating heat pumps?*"

Keywords *Multi-vector Energy System; Fifth-Generation District Heating; Ultra-Low Temperature District Heating; Decentralization; Heat Pumps; Dynamic Energy Modeling; Reference Buildings; Flexible Districts; Demand-Side Management; Physical Flexibility; Operational Flexibility*.

Declaration The topics and application described in Chapter 4 were previously published in the following publications:

- **Abbà, I.**; Crespi, G.; Vergerio, G.; Becchio, C.; Corgnati, S.P. (2024). Key Performance Indicators for Decision Support in Building Retrofit Planning: An Italian Case Study. Energies, vol. 17(3), n. 559 [72].
- Corsetti, E. and **Abbà, I.** (2023). Interazione dei mercati dell'energia e dei servizi di dispacciamento elettrico per sistemi di Generazione Distribuita con molteplici vettori energetici. Ricerca sul Sistema Energetico (RSE). Rds Report n. 23013281 [3].
- CEF TELECOM 2018, «DYnamic Data Analytics Services (DYDAS). Project Number: 2018-IT-IA-0101».Technical Report, 2023 [73].
- Bianchi, F., Corsetti, E. and **Abbà, I.** (2022). Analisi preliminare del potenziale di flessibilità dei carichi elettrici e approcci per l'aggregazione. Ricerca sul Sistema Energetico (RSE). Rds Report n. 22013969 [2].

4.1 Overview and objectives

The European programs, particularly the "European Green Deal" and "FitFor55", aim to achieve ambitious decarbonization targets for European countries [35, 36]. District heating is considered a key driver for reaching a post-carbon society due to its capacity to incorporate diverse energy sources, including renewables and waste heat [38]. As mentioned in Chapter 1, the evolution of district heating passes through five generations, reflecting advancements that enhance compatibility with renewable technologies [56]. These developments primarily aim to lower grid temperatures, thereby reducing thermal losses. The aim of this Application aligns with the context. Based on the results of the multi-vector energy simulation of a district heating system, coupled with the calculation of thermal flexibility transformed into electrical flexibility, the specific methodology has been applied. The Case Study #2 is a decentralized, all-electric fifth-generation district heating system with intermediate heating substations equipped with heat pumps, designed to serve six building districts to meet their heating needs. The layout of the proposed system actually makes it a hybrid between the fourth- and fifth- generations, defined as ultra-low-temperature district heating (ULTDH) in [37]. The classification in this category arises from the fact that fifth-generation systems are not directly compatible with serving buildings requiring temperatures around 60/70°C for optimal operation. In general, such buildings were mostly constructed before the '80s and have emission systems (radiators and fan coil units) that require high temperatures to perform properly. Therefore, it can be asserted that the goal of gradually lowering the supply temperature of district heating has encountered a limiting factor in buildings of 'old design'. These buildings constitute the vast majority in Italy and require significant adaptations due to the thermophysical characteristics of the building envelope and emission systems. Therefore, Application #2 aims to provide insights into combining the need to lower the supply temperature with the constraints imposed by buildings with 'traditional' high-temperature systems. Additionally, the system includes an "innovative" residential district, comprising only buildings constructed after 2001, equipped with radiant panel emission systems compatible with low temperatures. These buildings, with their low-temperature heating systems, represent a future trend and are increasingly adopted as retrofit technologies. Finally, since the examined district heating system is all-electric, composed of only heat pumps both in the central unit and in the intermediate heating substations, the system's flexibility is

studied concerning the modification of users' thermal loads. Through a demand management mechanism, it is assumed that users consent to the variation in heat supply in their buildings, while still respecting comfort constraints (which will be discussed in detail in the followings). For this reason, the role of the demand-side and occupants become crucial for this application, aligning with the increasing importance of users.

Figure 4.1 summarizes, the objective of this Case Study subdivided by themes: Simulation/Modeling and Flexibility. Indeed, the simulation objective is to adapt the simulator used in Application #1 to establish a low-temperature district heating network served by heat pumps. Furthermore, by examining flexibility on the demand side, allowing for adjustments to the thermal load profiles of users, it becomes possible to observe how these modifications impact the network and, consequently, influence the flexibility of the heat pumps in both the central plant and substations.

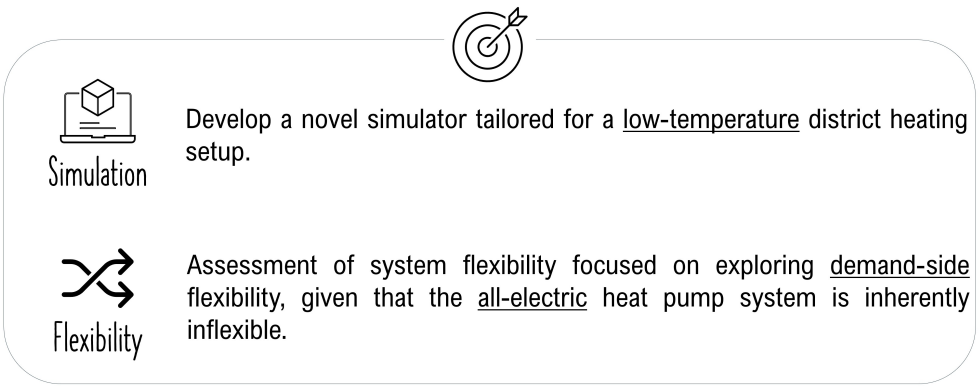

Fig. 4.1 Objectives of Application #2.

4.2 Modeling and simulation of Case Study #2

In this section, the main features of the case study and the assumptions made in the creation of the application are examined in detail.

4.2.1 Identification of main features of the Case Study - Demand side

Definition of final users' portfolio

To perform energy analyses and forecasts regarding the flexibility of buildings, the knowledge of the buildings under examination and their key characteristics is essential, and having only monitored data is not enough. Since simulating the energy behavior of each building within a stock is challenging due to a lack of complete and homogeneous data and the excessive computational time required, the decision was made to leverage the Reference Buildings (RB) approach. The concept of Reference Buildings was first introduced in the European Directive 2010/31/EU [74], better known as the EPBD recast of 2010, where Member States are required to create RBs to establish a benchmark for buildings that are representative of a portion of the national building stock, to be compared with real buildings in terms of optimal energy performance levels. By definition, "Reference Buildings are buildings characterized by their functionality and geographical location, including internal and external climatic conditions, and are representative of these characteristic [74, 75]". In other words, Reference Buildings are benchmark buildings or prototype buildings, whose characteristics and performances are considered representative of a certain portion of the building stock in the region/nation under consideration. At the European level, the definition and characterization of RBs had its greatest expression in the TABULA Project [76], continued in EPISCOPE [77], whose results are still used today as reliable references for constructing RBs. Internationally, the U.S. Department of Energy (DOE) has also created a benchmark for building models, still used in some dynamic simulation software [78]. Starting from these projects, it is possible to define the types of Reference Buildings and highlight their main characteristics. According to the DOE, the information needed to build a reference building model can be classified into four subcategories, which are:

- Function: including "how" the building is used, with information about location and climatic conditions, use designation, occupancy schedules, and use of building equipment;
- Shape: defining the type and geometric parameters of the building (dimensions, orientation, percentage of opaque and transparent surfaces);
- Building envelope: containing information about materials and stratigraphies (layers of materials that make up the building envelope);
- Building systems: referring to all systems installed in the building, from heating, ventilation, and air conditioning (HVAC) to controls on lights and equipment.

Finally, depending on how data for each of these categories of information are obtained (e.g., statistical analyses, manuals, regulations and standards, expert experience), the TABULA classification recognizes different modeling approaches for reference buildings [76]: (i) Real Example Building when reliable statistical data is lacking, and the building is modeled based on expert experience; (ii) Real Average Building when a real existing building is chosen that has geometric and construction characteristics matching the statistical averages of the analyzed building sample and (iii) Synthetical Average Building or Theoretical Building is a virtual, non-real building characterized by properties identified through statistical analysis within a sample of buildings. Each of these approaches can be used to define the building as a whole or applied separately to each subcategory of information. Hybrid models can be created, for example, featuring geometric characteristics based on real experience and building systems derived from statistical analysis, or vice versa.

In the current research, the aim was to obtain reference building models that are easily adaptable and provide energy results with varying levels of aggregation within a reasonable computational time. Therefore, the Reference Building approach was applied concerning the Italian building stock, specifically focusing on residential and office buildings. These types are the most extensively addressed in the literature and offer the greatest availability of geometric and thermophysical data. The selection and characterization of these RBs were carried out in alignment with the activities undertaken by the Ph.D. candidate during the execution of the European project DYDAS [73]. Additionally, to extend the exploration into the services sector, a Reference Building for a mall was also developed and analyzed.

Residential Buildings In the context of the residential sector, a preliminary analysis was conducted to classify buildings based on their construction periods and primary typologies. The objective was to assess the current state of the Italian building stock by integrating information from the 2011 ISTAT census on population and housing [79] with the data provided by the TABULA project [76]. The residential building portfolio was categorized into three classes: Single Family House (SFH), Multi-Family House (MFH), and Terrace House (TH), across three construction periods: pre-1980, 1981-2000, and post-2001 [72, 80, 81].

From the TABULA database, key information such as building geometry, efficiencies of emission and distribution subsystems, and wall stratifications were extracted. Additionally, the thermal properties of the components were further refined based on the climatic zone. It is noteworthy that the TABULA buildings primarily pertain to the Piemonte region, with a specific focus on the city of Turin, situated in the Italian climatic zone E. This aspect aligns well with the imposed boundary condition that the case study is located in Northern Italy, specifically in the climatic zone E [82]. In detail, concerning SFHs, the models represent buildings exposed on all four sides to the external environment and arranged over two floors, with each floor representing a different thermal zone. THs exhibit the same geometry as SFHs but are considered to be adjacent to other buildings on two sides, following the guidelines in [76]. In this case as well, the thermal zone covers the entire floor. In SFH and TH built during the second and third construction periods, there is also an unconditioned basement located 2.4 meters below ground level. As an exemplification, Figure 4.2 shows the 3D model of SFH and TH RBs of the construction period post-2001.

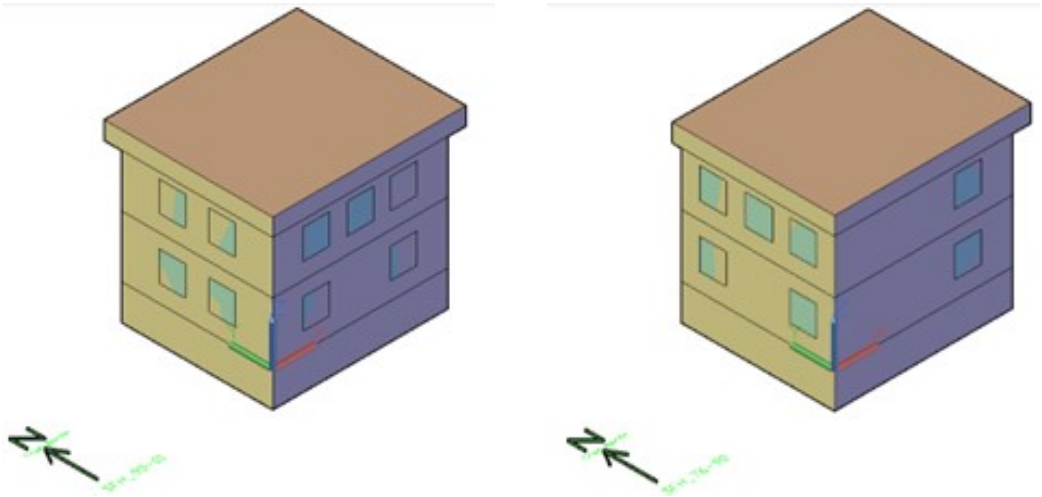

(a) 3D view of a Single Family House RB, post-2001.

(b) 3D view of a Terrace House RB, post-2001.

Fig. 4.2 Example of 3D representation of SFH and TH, post-2001 [73].

Multi-family houses, or condominiums, feature two different geometries depending on the construction period they refer to. For buildings constructed before 1980, the structure is spread over 5 floors and includes an unheated basement. For the second and third construction periods, the geometry was assumed to be the same, comprising a three-story building with pilotis on the ground floor (see Figure 4.3). The models of MFHs also include unconditioned spaces, encompassing staircases, basements, and attics.

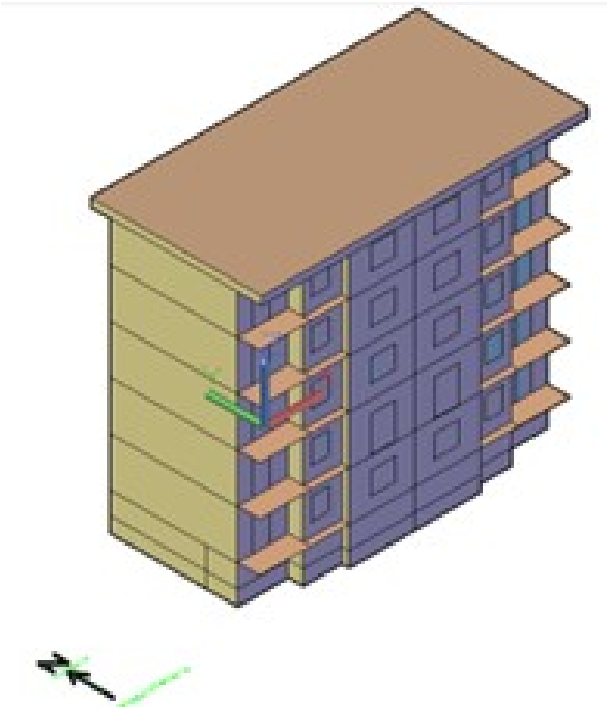

(a) 3D view of a Multi Family House RB, pre-1980.

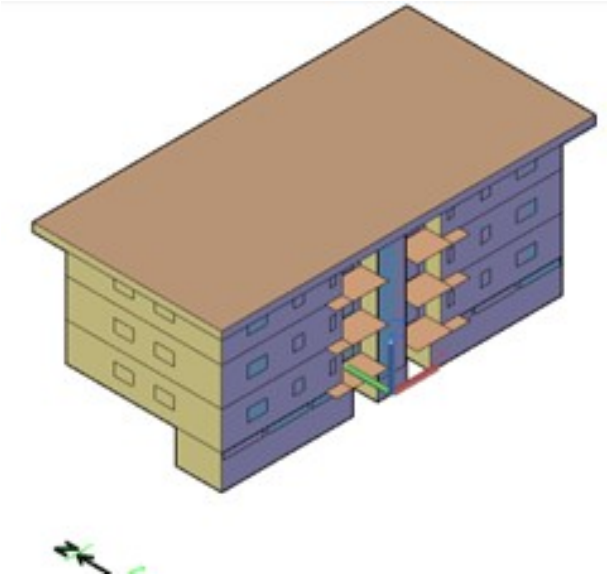

(b) 3D view of a Multi Family House RB, post-1980.

Fig. 4.3 Example of 3D representation of MFHs for the three period of constructions [73].

A more detailed description of the geometric and thermophysical characteristics of the Reference Buildings is provided in the Appendix A.

Regarding internal gains, information on schedules were derived from European regulations. Specifically, diversification factors for occupancy, lighting, and appliances, as well as daily profiles, were obtained from the European standard EN 16798 - Part 1 [83]. In SFH and TH, the reserved floor area per person is 42.5 $m^2/person$, while in MFH, it is 28.3 $m^2/person$. Two distinct occupancy profiles were assumed for weekdays and holidays (see Figure 4.4), while diversification factors for lighting and appliances were considered valid for the entire week, following [83].

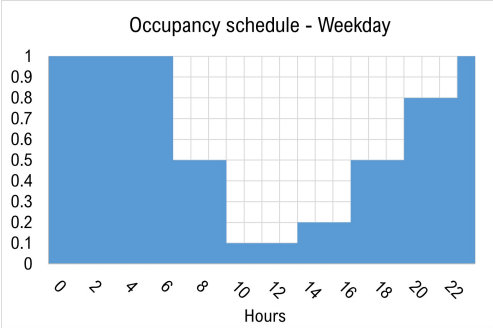

(a) Residential buildings occupancy profile during weekdays.

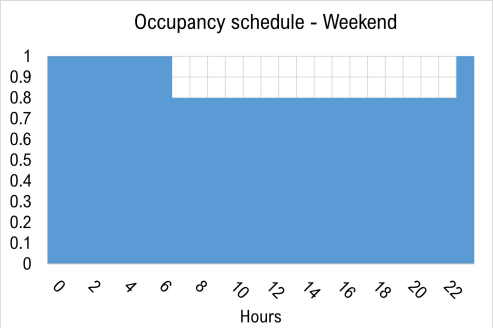

(b) Residential buildings occupancy profile during weekend.

Fig. 4.4 Occupancy profiles in residential buildings.

Values for the power density of electrical appliances, retrieved from EN 16798, are 3 W/m^2 in MFH and 2.4 W/m^2 in the other two construction types. Additionally, in MFH, the presence of an internal elevator was assumed (not required for SFH and TH since they consist of only two above-ground floors), and it was modeled following examples developed by the DOE for the EnergyPlus software [84], with a nominal power of 16.05 kW. Shifting attention to lighting, the power density is assumed to be 7 W/m^2, in accordance with the UNI/TS 11826 standard [85]. In Figure 4.5 the diversity factors used for appliances and lighting are summarized.

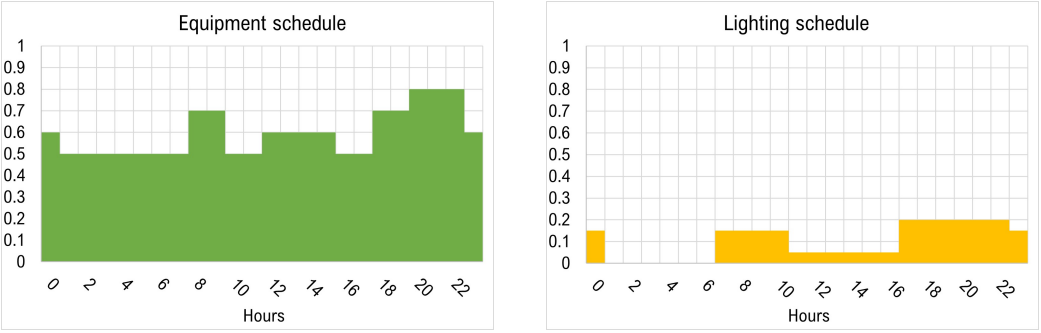

(a) Residential buildings equipment profile.

(b) Residential buildings lighting profile.

Fig. 4.5 Appliances and lighting schedule profiles for residential buildings.

Finally, the ultimate purpose of modeling the buildings was to utilize the simulation results within a multi-energy system simulator, consisting of a district heating system. The goal was to assess the system's flexibility, considering not only the electrical network but also the thermal network. For this reason, the heating system modeled in residential buildings has district heating as the heat source. Considering the HVAC emission systems installed in the building, two different scenarios were modeled: (i) radiators, which, according to [76], are the most commonly used technologies for each RB and (ii) radiant floors only for RB post-2001, in order to capture the trend where radiant systems are preferred in new buildings due to their ability to provide better comfort conditions for occupants. Concerning radiators, to adapt the system to the temperatures of next-generation district heating systems, the design temperature of the radiators was set to 63°C, while for radiant system the design temperature is 40°C. Additionally, for the summer season, a cooling system was envisaged, comprising an direct expansion system coupled with fan coil units for the emission of cool air. The HVAC system is used to guarantee the correct amount of heating or cooling at the desired temperature, according to the season. More precisely, the duration of the heating and cooling seasons varies based on distinct climatic zones in accordance with Italian Legislation (DPR 412/93 [82]). As the analyzed system is presumed to be situated in climate zone E, the heating season spans from October 15^{th} to April 15^{th}, allowing for a maximum of 14 hours of operation for centralized systems. During the heating period, a temperature set-point (SP) of 20°C was ensured in the intervals 06:00-10:00, 12:00-13:00 and 16:00-24:00 [86] while a set-back (SB) temperature of 18°C was maintained for the remaining hours. Conversely, for the cooling season, the temperature set-point was established

at 26°C while 28°C is the set-back, aligning with the guidelines outlined in EN 16798 [83]. The information regarding internal gains, as well as that pertaining to the HVAC system, were assumed to be valid for all residential RB models, regardless of the typology and construction period under consideration.

Offices For the design of office building archetypes, the primary resources employed were the collaborative research conducted by Cresme with ENEA and the subsequent ENEA report focusing on the characterization of typical office buildings [87]. This report served as a valuable reference for collecting data related to the geometric aspects, construction periods, building stratifications, and other essential features of the office archetypes. Additionally, it provided insights into the prevalent HVAC configurations. Similar to the approach followed for residential buildings, the initial step involved classifying offices based on their size categories—small, medium, or large. Given the widespread occurrence of medium-sized office buildings in Italy, this dissertation concentrates on this category [87]. Figure 4.6 illustrates the floor plan and spatial arrangement and the 3D view of typical medium-sized offices.

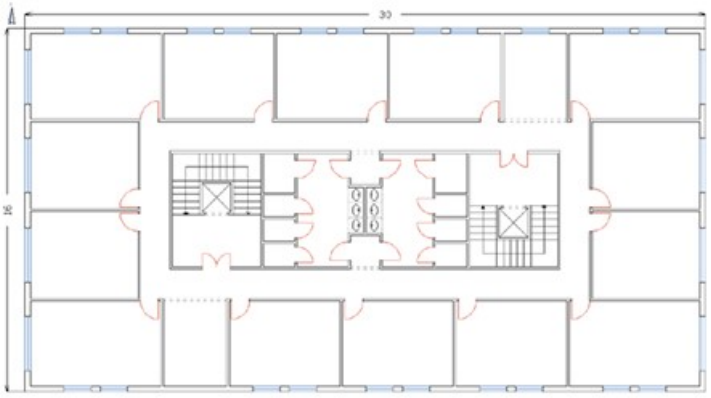

(a) Typical floor plant, from [87].

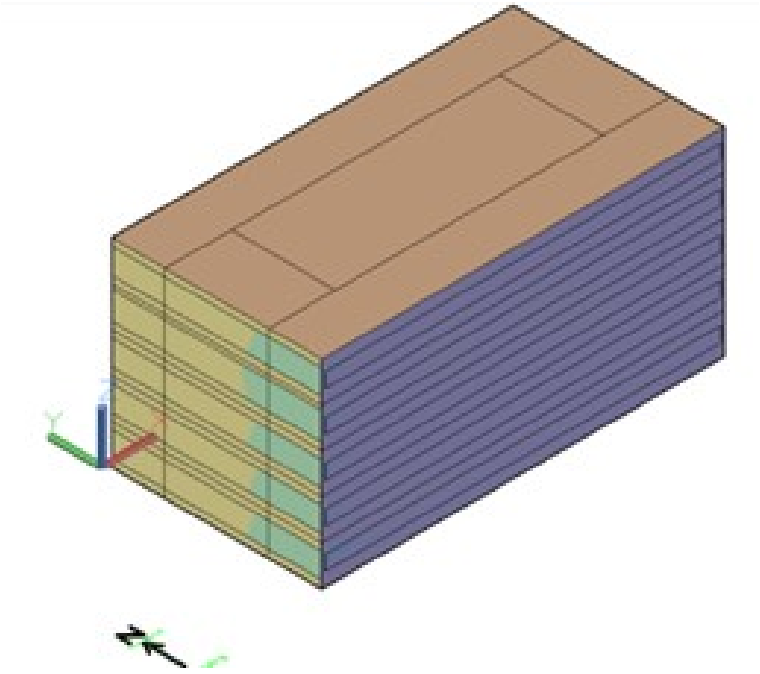

(b) 3D view.

Fig. 4.6 Geometrical representation of a medium dimension office.

Each simulation model comprises five floors, with each floor divided into five distinct thermal zones, one for each orientation. Additionally, a central distribution area is assumed to encompass corridors, reception spaces, elevator locations, and archives. For the sake of modeling simplicity regarding windows, a "strip window" approach was adopted, ensuring equal total window area on each orientation. Then, five distinct construction periods (two more than in the residential case) were consid-

ered as representative: pre-1991, 1992-2005, 2006-2010, 2011-2015, and post-2016 [73]. Characteristics such as geometric details, stratifications, and thermophysical properties for the period before 1991 were sourced from the ENEA report [87]. The geometric features were then assumed to remain unchanged in subsequent periods, while the thermal transmittance values for the other eras of construction were determined based on the minimum legal requirements for both opaque and transparent walls [82, 88, 89]. Details on materials and stratigraphies are summarized in Appendix A.

In the realm of internal gains, the layout of the office building delineates dedicated zones for work activities and distribution zones, such as corridors, each with distinct contributions. Specifically, as per the UNI 10339 standard [90], the occupation density was set as 0.06 $persons/m^2$ in offices and 0.03 $persons/m^2$ in corridors. The diversification factors, representing the presence of individuals in the office building, remain uniform across all thermal zones (following the European standard EN 15232 [91]), albeit with variations between weekdays and holidays. It was assumed that during weekends, the building remains unoccupied, resulting in a diversification factor of zero. Concerning electrical appliances, the power density was set at 12 W/m^2 for office zones and 2.9 W/m^2 for corridors, in accordance with the EN 16798 standard [83]. During weekends, all appliances were presumed to be either switched off or in standby mode, given the absence of occupants, resulting in a constant usage profile set at 0.5. Additionally, the presence of two internal elevators was postulated, modeled following the DOE model with a total power density of 32.10 kW. Figure 4.7 illustrate the hourly profiles for occupancy and equipment usage in office buildings during weekdays.

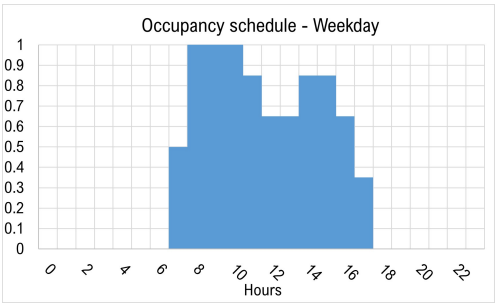

(a) Office occupancy profile during weekdays.

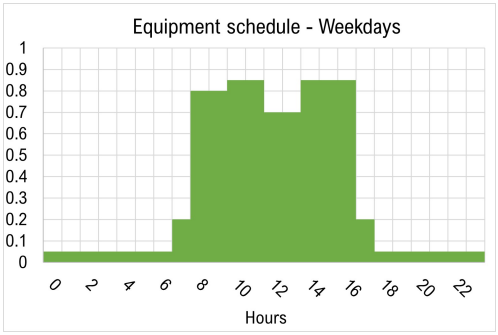

(b) Office equipment scheduling profiles during weekdays.

Fig. 4.7 Occupancy and appliances schedule profiles for offices during weekdays.

In terms of lighting of spaces, the luminous power density was assumed to be 15 W/m^2, a typical value associated with fluorescent light sources for offices constructed before 2015. For the more recent period (post-2016), a value of 5 W/m^2 was adopted, aligning with the prevalent use of LED sources. During weekends, the illumination rate in offices was considered zero, while that in the distribution area remains constant at 0.1, accounting for continuously active emergency lights. Diversification factors for offices were derived from literature, simulating the behavior of an average user, while those for corridors were extracted from [91] focusing on automation systems (see Figure 4.8 for schedule profiles).

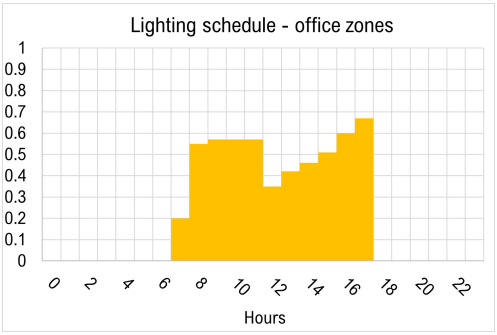

(a) Office lighting schedule profile during weekdays.

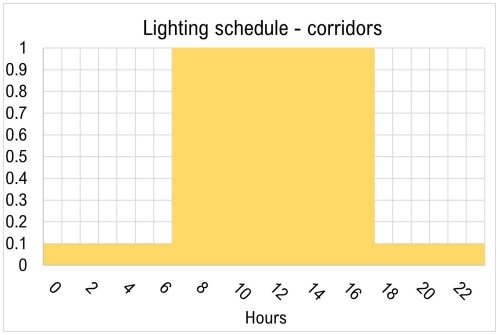

(b) Corridors lighting schedule profile during weekdays.

Fig. 4.8 Lighting schedule profiles for offices and corridors during weekdays.

Moving to the HVAC system, similarly to residential buildings, the assumption was to connect offices to a district heating network. Consequently, the heat source for the heating system was the hot water supplied by the district heating network. Fan coils were the predominant emission system in offices, employed both in the winter and summer seasons [87]. Fan coils have been modeled for all RBs, while for offices built post-2016 also a scenario with radiant ceiling was included in the analysis. Considering the cooling system, it involves a water refrigeration unit with evaporation tower. Concerning temperature set-points, it was crucial to maintain a temperature of 20°C during occupied working hours (from Monday to Friday) in the heating season and 26°C during the summer period. It is noteworthy that holidays were also taken into account, ensuring the required set-backs (16°C and 32°C, respectively) for non-occupied hours [83]. The data concerning internal gains and the HVAC system were assumed to be applicable to all office RB models.

Mall Concerning the shopping mall, the process of selecting and constructing the reference building model followed a different path compared to the previous ones. This deviation stems from the absence, at the Italian level, of databases or reference reports containing all the requisite information essential for developing a highly detailed building model, as mandated by this application. Consequently, the decision was made to turn to the mall model found within the U.S. Department of Energy (DOE) database [78]. This comprehensive database was created within a broader framework, aiming to establish benchmark models for buildings of diverse usage, subject to continuous updates in compliance with emerging laws and standards. The choice for this application was the "Stand-alone retail" building due to its geometric resemblance to a typical Italian supermarket, as depicted in Figure 4.9.

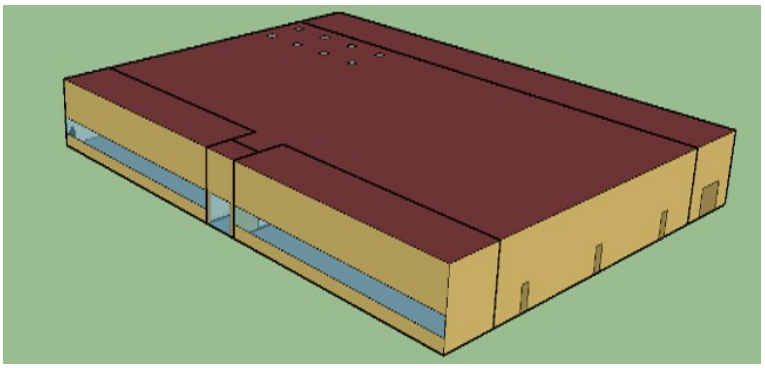

Fig. 4.9 3D view for the mall RB [78].

The building comprises five thermal zones: Back Space, Core Retail, Point of Sale, Front Retail, and Front Entry. Concerning the architectural features such as geometry, stratifications, and materials defining different walls and fenestration elements, the entire model developed by the DOE was utilized. Similarly, the diversity factors and power density related to internal lighting and appliances were incorporated following the specifications outlined by the DOE. In terms of space occupancy, each thermal zone adhered to the standard value of 17 $m^2/person$ as per EN16798 [83], while maintaining the occupancy profile sourced from the DOE. Regarding the HVAC system, adjustments were made compared to the reference RB. This modification aligns with the expectation that, similar to residential and office buildings, the mall is connected to the district heating network. Consequently, district heating serves as the heat source, complemented by an electric refrigeration unit for cooling purposes. The emission system comprises four-pipe fan coil units, one dedicated to each thermal zone. To better integrate the building into the Italian context, refinements were applied to the set-point and set-back temperatures within the structure. More precisely, throughout the entire operational hours of the commercial building (9:00-22:00) in the heating season, the set-point temperature was assumed to be 20°C, while it may decrease to 16°C during the remaining nighttime hours. Conversely, in the summer season, the set-point temperature during operational hours was set at 25°C, with a set-back of 32°C [83].

District composition As explained in 4.2.2, the layout of the fifth-generation network under consideration is decentralized. It consists of a central station powered by a groundwater heat pump, followed by district substations where low-temperature water is heated to a temperature compatible with the requirements of users' emission systems. Therefore, once all the RBs necessary for defining the portfolio of end-users were identified, a process of aggregating the RBs into characteristic districts was carried out. The goal was to obtain, as output, the profiles of thermal power demand to be associated with each district substation.
The decision was to use the San Salvario neighborhood, actually existing in the city of Turin, based on the availability of extensive data on the current state of the building stock through the Geoportale [92]. The Geoportale of the City of Turin serves as the infrastructure for territorial data in the city, and its data, geo-services, and cartography tables are openly shared with all the city's sectors, making them accessible to everyone. Therefore, following a similar approach as described in

[93, 94], data were extracted for each building, encompassing information such as end-use, construction period, surface area, building height, and the number of floors. Utilizing these details, and considering the occupied surfaces, a statistical distribution of the prevalence of different uses was conducted (refer to Figure 4.10). Furthermore, based on the occupied area, the frequency for each construction period corresponding to each intended use was distributed. Finally, using the information on the number of floors, residential buildings were classified into SFH, TH, MFH categories. By integrating the Geoportale data with that from Tabula [76], the various RBs described in Section 4.2 were distributed across the different districts.

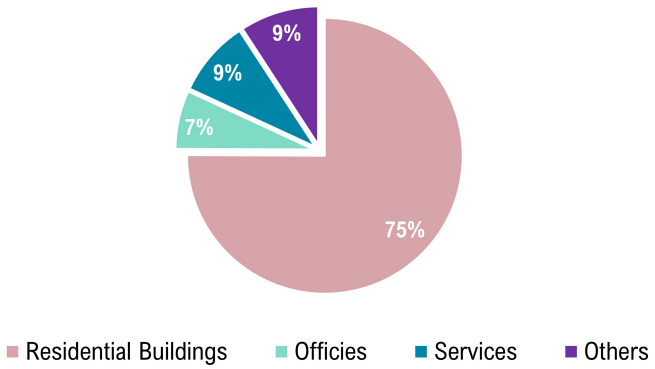

Fig. 4.10 San Salvario Building Distribution.

Below is the detailed composition of the districts.

District 1 - D1 Residential neighborhood comprising exclusively SFHs and THs. The distribution of building types and construction periods aligns with the statistical pattern observed in the reference neighborhood in Turin.

District 2 - D2 Exclusively residential neighborhood mirroring the overall statistical composition of the reference district in Turin. It encompasses a distribution of MFHs, SFHs, and THs across various construction periods. Apartment Blocks are included in the MFH category.

District 3 - D3 Mixed district, combining residential, office, and mall spaces. It reflects the actual distribution of the analyzed Turin neighborhood in terms of usage destinations, building types, and construction periods.

District 4 - D4 Mixed neighborhood with a blend of residential and office spaces, assuming a distribution of 65% residential buildings and 35% office buildings.

District 5 - D5 Entirely commercial district featuring a mall and the remaining buildings designated for office use, distributed across different construction periods as per statistical data.

District 6 - D6 "Innovative" district comprised solely of residential and office buildings built after 2001. What distinguishes it from other districts is that all buildings are equipped with radiant panels as their emission systems (i.e., radiant floors for residential and radiant ceilings for offices).

District 6 was included in the study for several reasons. Firstly, radiant systems represent a future trend in HVAC systems, providing greater occupant comfort and compatibility with low-temperature heat sources. This characteristic makes them intriguing for the study as it enables the analysis of the direct coupling between the low-temperature 5^{th} generation district heating network and the building without the need for an additional heating substation. Secondly, it aims to understand how this different heat emission technology, with a slower dynamic response and greater thermal inertia, influences the flexibility of the system under consideration. In Table 4.1, a detailed breakdown is provided for the number of buildings in each district, categorized by end-use, building type, and construction period.

Type of building	Era of construction	D1	D2	D3	D4	D5	D6
MFH	pre-1980	0	39	32	18	0	0
	1981-2000	0	4	3	2	0	0
	post-2001	0	1	1	0	0	25
TH	pre-1980	175	3	2	1	0	0
	1981-2000	7	0	0	0	0	0
	post-2001	2	0	0	0	0	10
SFH	pre-1980	46	1	1	0	0	0
	1981-2000	0	0	0	0	0	0
	post-2001	1	0	0	0	0	10
OFFICE	pre-1991	0	0	5	9	18	0
	1992-2005	0	0	0	1	1	0
	2006-2010	0	0	0	1	1	0
	2011-2015	0	0	0	1	1	0
	post-2016	0	0	0	1	1	10
MALL	post-1990	0	0	1	0	1	0

Table 4.1 Number of buildings for each District.

4.2.2 Identification of main features of the Case Study - Supply side

Moving to the supply side, Case Study #2 concerns a 5^{th} generation district heating network, operating at low temperatures, with a decentralized system architecture designed to serve six districts for heating services. In detail, the network features:

- a "centralized" main thermal power plant consisting of a groundwater source heat pump (GWHP);
- a primary distribution network;
- six district substations, of which five include a set of two heat pumps in series;
- a secondary distribution network reaching individual buildings within the various districts.

The network layout was established by hypothetically selecting a real neighborhood in Turin and measuring distances using Google Maps as a reference. In Figure 4.11 the district heating layout is represented, with some information on reference temperatures.

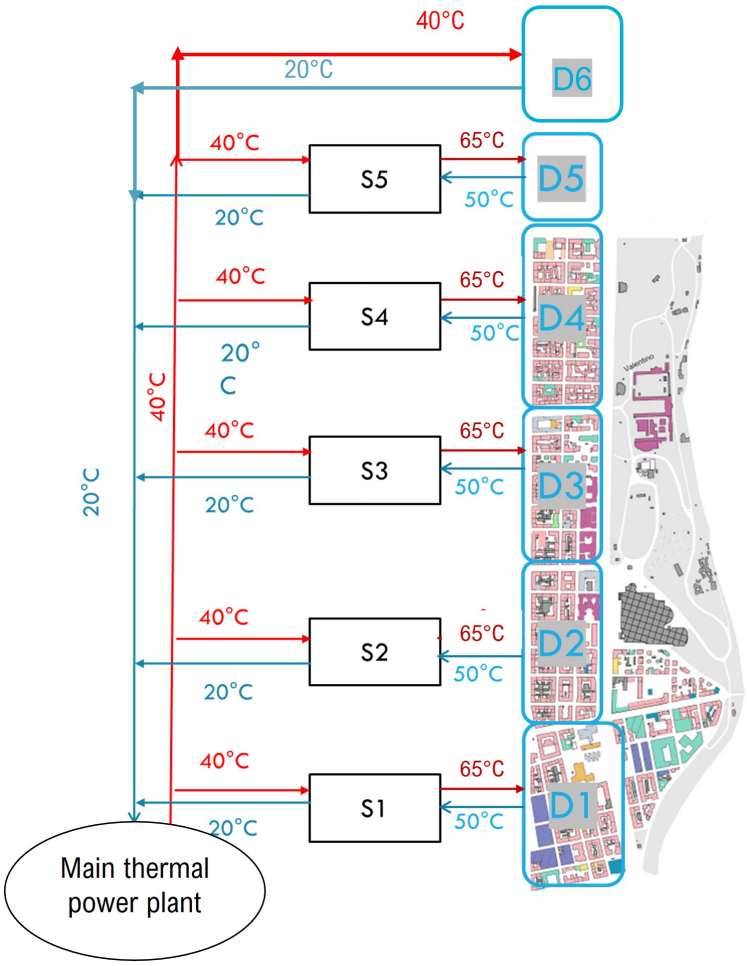

Fig. 4.11 Layout of the district heating network.

In the following each component of the system is described in detail.

Main thermal power station

In the thermal power plant, there is a 11 MW water-to-water geothermal heat pump that uses groundwater as a heat source. It was assumed to extract the warm water at 20°C and reintroduce it at a temperature of approximately 10°C [1]. For this

application, the issue of thermal interference between the supply and return aquifer was not been taken into account. It was supposed that the two wells are at a sufficient distance to avoid such interference. In Figure 4.12 the schematic layout of the main station is depicted, along with some reference temperatures.

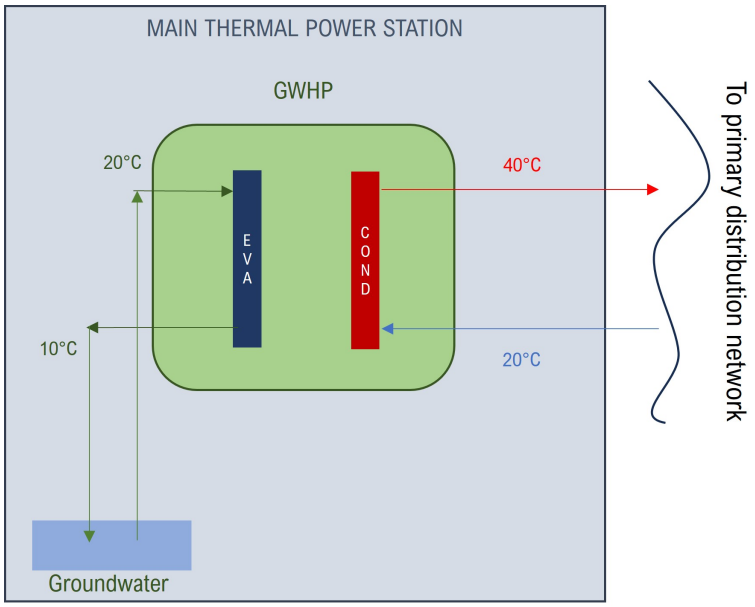

Fig. 4.12 Schematic layout of the groundwater heat pump in the main thermal station.

The heat pump was modeled on the simulation software as a manually crafted block, since it was not in the library of the tool. The block represents a simplification of the actual machinery, as the constituent components (condenser, valve, evaporator, and compressor) were not modeled separately. Instead, it was considered as a single block based on the conservation equations for mass, energy, and momentum. The physical cycle of the refrigerant fluid was not explicitly modeled; nevertheless, for the analysis outlined in this application, the adopted level of detail remains adequate for evaluating the heat pump's impact on network flexibility. The machine was modeled as reversible, since an expansion of the model can be the application also for cooling services during summer periods. To model the functioning of the heat pump, some boundary conditions were defined, including system operating temperatures. In winter operation, a condenser output temperature ($T_{o,cond,SP}$) of 40°C was set, representing the discharge temperature to the primary distribution network. The objective of the block is to evaluate the performance of the machine (it is of interest mainly the electrical power absorbed by the compressor, Q_e) to

ensure an output temperature equal to $T_{o,cond,SP}$, with varying inputs. To enhance clarity, it is important to specify which are the inputs to the heat pump block. From the evaporator side, there is an entering mass flowrate $\dot{m}_{eva}$ at a temperature $T_{i,eva}$, a pressure $P_{i,eva}$ and a thermal flux $\phi_{i,eva}$. From the condenser side, the entering flowrate is $\dot{m}_{cond}$ characterized by $T_{i,cond}$, $P_{i,cond}$ and $\phi_{i,cond}$. Concerning the model, a first check state if the machine is on or off. Then, since it was assumed that the heat pump is reversible, a second control checks if the unit is set on heating or cooling mode. Given that the focus of this Case Study is on heating, the operation of the heat pump is described in detail with formulas and operation logic only for the heating period. Once fixed the $T_{o,cond,SP}$ and knowing the $T_{i,cond}$, from the tables of fluid properties in the Simscape library, corresponding enthalpies are obtained ($H_{o,cond,SP}$ and $H_{i,cond}$). Then, through the Eq. 4.1 the thermal power ($Q_{h,cond}$) required to the condenser to guarantee the set-point temperature ($T_{o,cond,SP}$) is calculated.

$$Q_{h,cond} = \dot{m}_{cond} * (H_{o,cond,SP} - H_{i,cond}) \tag{4.1}$$

The performance of the heat pump varies with partial load, as well as with the temperatures of the water entering the condenser and evaporator. Being a water-to-water heat pump, the outside air temperature has no influence. Through the integration into the model of technical data provided by the manufacturers of an actual machine, it was possible to determine, through linear interpolation, the thermal power ($Q_{h,n}$) that the heat pump can produce, the corresponding coefficient of performance (COP_n) and consequently the electrical nominal power ($Q_{e,n}$), with $T_{i,eva}$ as inlet temperature. It is calculated using Eq. 4.2.

$$Q_{e,n} = \frac{Q_{h,n}}{COP_n} \tag{4.2}$$

At this point, it must be confirmed whether $Q_{h,cond}$ exceeds or falls short of the effectively deliverable power. If $Q_{h,n} > Q_{h,cond}$ the heat pump is working at partial loads, the thermal power provided at the condenser is $Q_{h,cond}$ and the electric power absorbed by the compressor is obtained by Eq. 4.3.

$$Q_e = \frac{Q_{h,cond}}{COP_n} \tag{4.3}$$

As a consequence of the principle of conservation of energy, the thermal power withdrawn at the evaporator is computed by using Eq. 4.4.

$$Q_{h,eva} = Q_{h,cond} - Q_e \tag{4.4}$$

If $Q_{h,n} < Q_{h,cond}$, the thermal power that can be effectively produced by the heat pump is lower than the required one. In this situation, the machine is working at full load at $Q_{h,n}$ and from Eq. 4.5 it is possible to obtain the entalphy at the exit of the condenser.

$$Q_{h,n} = \dot{m}_{cond} * (H_{o,cond} - H_{i,cond}) \tag{4.5}$$

Using the tables of fluid properties in the Simscape library the temperature at the outlet of the condenser is calculated, and it is lower than the desired set-point. Then also the electrical power absorbed and the evaporator thermal power are determined (4.2, 4.6).

$$Q_{h,eva,n} = Q_{h,n} - Q_{e,n} \tag{4.6}$$

The same operating principle applies during the summer operation, with the distinction of identifying a set-point temperature at the evaporator outlet ($T_{o,eva,SP}$).

Primary distribution network

The primary distribution network was modeled as a two-pipe circuit (one pipe for supply and the other for the return), from which branch off secondary pipelines, also in dual tubing, reaching the district substations. The sizing of the network was carried out by assuming the pipe lengths based on actual measurements of the distance between districts in the reference Turin neighborhood (*San Salvario*), depicted in Figure 4.11. Subsequently, a project sizing of the entire network, including the diameters of various pipelines and pressure losses, was performed. To conduct this sizing, the following project thermal loads were set for the different districts: D1 = 1.6 MW, D2 = 1.8 MW, D3 = 2.1 MW, D4 = 1.9 MW, D5 = 2.4 MW, D6 = 2.3 MW. Then, by using Eq. 4.7, the flowrate flowing in each pipelines section was determined, starting from the amount of water that should reach each substation ($\dot{V}_{Dx}$ in m^3/s).

$$\dot{V}_{Dx} = \frac{Q_{h,Dx}}{c_p * (T_{i,Dx} - T_{o,Dx})} \tag{4.7}$$

With $Q_{h,Dx}$ as the thermal loads of the D_x district substation, and T_i and T_o as input and outlet temperatures.

Finally, by setting v = 1.5 m/s as the velocity for the pumped fluid [95], the inner diameter d_i of each segment was calculated using Eq. 4.8.

$$d_i = \sqrt{\frac{4 * \dot{V}_{Dx}}{\pi * v}} \tag{4.8}$$

Subsequently, consulting technical sheets of actual pipelines, the commercial diameter that best suited the theoretical calculation was selected. The computation of pressure losses was then carried out using the commercial diameter. The lengths of the supply pipelines for the main distribution network are indicated in Table 4.2. Lengths and diameters are supposed to be equal for supply and return pipelines for the same branch.

Pipe section	**Length [m]**	**Diameter [m]**
MDS_{C-D1}	1000	0.31
MDS_{D1-D2}	550	0.26
MDS_{D2-D3}	530	0.26
MDS_{D3-D4}	590	0.21
MDS_{D4-D5}	550	0.16
MDS_{D5-D6}	550	0.16

Table 4.2 Network's geometrical features. MDS = Main Distribution Supply network.

Considering the tube section that from the distribution network deviates and reaches the substation, values of length and diameter are presented in Table 4.3.

Pipe section	**Length [m]**	**Diameter [m]**
DDS_{D1}	50	0.11
DDS_{D2}	50	0.12
DDS_{D3}	50	0.13
DDS_{D4}	50	0.12
DDS_{D5}	50	0.14
DDS_{D6}	50	0.15

Table 4.3 Deviation pipes, from distribution network to districts' substations, geometrical features. DDS = Deviation from Distribution Supply network.

In Simscape, the pipe element already exists, it is the same used for Application #1 and thus, it was used without adding or modifying equations. Descriptions of the constitutive equations can be found in paragraph 3.2.3, and more in detail in the online guide of the software [68].

Decentralized intermediate heating substations

The purpose of the district substation is to raise the temperature of the water flowrate to a level that is suitable for the building's emission systems to operate efficiently. The substation's composition varies depending on the type of district under consideration. For districts D1, D2, D3, D4 and D5, the substation includes (i) a System-Level Heat Exchanger (HX_{L-L}) from the software thermal liquid library, (ii) two in-series heat pumps (HP1 and HP2) that were manually crafted, (iii) an ideal heat exchanger (HX) that represents the heat exchange between the distribution network and buildings and which was manually modeled, (iv) blocks to regulate the pressure within the substation and (v) a control system that regulates the water flowrate to ensure the delivery of heat at the desired temperature. In these five districts, the temperature leaving the second heat pump is 65°C, which is compatible with the operating temperature for radiators and fan coils. In district D6, a temperature of 40°C is sufficient to ensure the proper functioning of the radiant panels. As a result, the district substation contains only the ideal heat exchanger and the flow control system, as the supply temperature from the central plant is 40°C.
Each component is described in detail in the following paragraphs.

System level heat exchanger The system level heat exchanger (HX_{L-L}) was used in this application as a connecting element between the primary and secondary distribution thermal network. The block is part of the Simscape library and is suitable for the application since it is able to model the heat exchanger "based on performance data between two thermal liquid networks" [68], rather than the geometrical information of the installed machine. This capability enables the modeling of the heat exchanger's operation in situation like the one under consideration, where the network does not exist and there are not actual technology installed, even in the absence of geometric data for the element. Descriptions of the constitutive equations and more information the block can be found in detail in the online guide of the software [68].

Heat pumps The scope of the heat pumps in the district substation is to raise the temperature of the water flowrate from 40°C (the primary network supply temperature) to 65°C (the typical operation temperature for a conventional radiator). In the substation two heat pumps were placed in series for this purpose. In Figure 4.13 the schematic layout of the heat pumps in the district substation is depicted, along with some reference temperatures. Specifically, hot water at 40°C from the primary network transfers heat to the substation through the liquid-liquid system heat exchanger HX_{L-L}. On the substation side, the water leaving HX_{L-L} enters the first heat pump (HP1) on the evaporator side. Through the heat pump cycle, the water on the evaporator side cools down, transferring heat to the refrigerant. The refrigerant, in turn, transfers the heat through thermodynamic processes to the water leaving the condenser. Downstream of HP1, the water temperature is 56°C. However, the substation aims to raise it to the set-point temperature of 65°C. Therefore, the water is directed to the second heat pump, located in series with the first one. Here, it is heated to the desired temperature before being routed to the ideal district heat exchanger (HX). On the evaporator side, the water leaving HP1 is directed to the evaporator of HP2, where it continues to cool down before being sent to the liquid-liquid system heat exchanger HX_{L-L}.

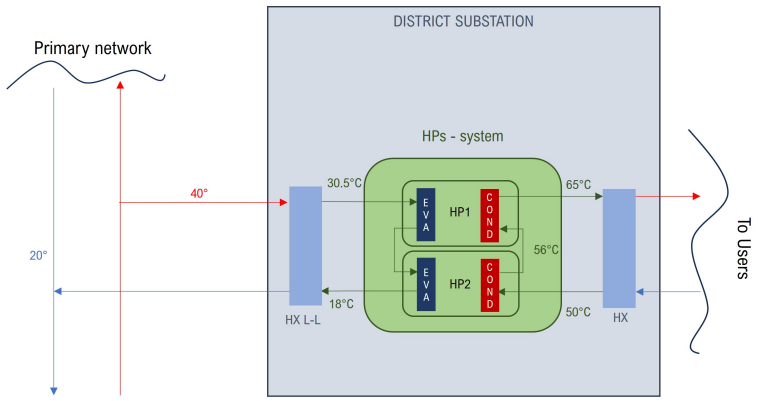

Fig. 4.13 Schematic layout of the heat pumps in the district substation.

The heat pump physical model is the same used for the machine in the central station. Also the substation's heat pumps are water-to-water units, governed by the equations described in Section 4.2.2 (Eqs. 4.1, 4.2, 4.3, 4.4, 4.5 and 4.6). What changes with respect to the main thermal power station are the sizes and the reference temperatures exiting from the condensers of the two heat pumps. In Table 4.4 the inlet and outlet temperatures for each component of the substation are listed. Concerning the sizing of the heat pumps, for districts from 1 to 5 (the traditional ones), it is assumed to install units with a nominal thermal power output of 2 MW. A detailed description of the HP functioning and technical data are reported in Appendix C.

Technology	Nomenclature	Value
Heat Pump 1	$T_{i,cond,HP1} = T_{o,HX}$	50°C
	$T_{o,cond,HP1} = T_{o,cond,HP1,SP}$	56°C
	$T_{i,eva,HP1} = T_{o,HX,L-L}$	almost 30.5°C
	$T_{o,eva,HP1} = T_{i,eva,HP2}$	variable, depends on the simulation
Heat Pump 2	$T_{i,eva,HP2} = T_{o,eva,HP1}$	variable, depends on the simulation
	$T_{o,eva,HP2} = T_{i,HX,L-L}$	variable, depends on the simulation
	$T_{i,cond,HP2} = T_{o,cond,HP1}$	56°C
	$T_{o,cond,HP2} = T_{o,cond,HP2,SP} = T_{i,HX}$	65°C

Table 4.4 Characteristic temperatures of heat pumps (i = input, o = output).

Symbols and names used in the table are listed and explained in the Nomenclature section (5).

Ideal heat exchanger and control system The rationale behind the model of the ideal heat exchanger is the same described in 3.2.3. The block is governed by energy, mass and momentum conservation equations (Eqs. 4.9, 4.10, 4.11 and 4.12).

$$Q_d = \dot{m}_A * c_p * (T_A - T_B) \tag{4.9}$$

$$\dot{m}_A + \dot{m}_B = 0 \tag{4.10}$$

$$\phi_A + \phi_B + Q_d = 0 \tag{4.11}$$

$$p_A + p_B + k_{HX} * \dot{m}_A^2 = 0 \tag{4.12}$$

Where:
A: inlet port;
B: outlet port;
d: district;
Q_d : thermal power provided to the district [kW];
c_p: water specific heat [kJ/(kgK)];
T_A: water temperatures of the inlet flowrate [K], corresponds to $T_{i,HX} = T_{o,cond,SP,HP2}$ in Table 4.4;
T_B: water temperatures of the inlet flowrate [K], corresponds to $T_{o,HX} = T_{i,cond,HP1}$ in Table 4.4;
ϕ: energy flow rates, entering the A port and exiting the B port [kW];
$\dot{m}$: water mass flow rate [kg/s];
p: water pressures [Pa];
k_{HX}: pressure loss coefficient for heat exchangers.

Moving to the control and regulation system, it elaborates the desired temperature exiting the HX (50°C) and the thermal profile required from the district. It compares the set-point temperature with the real one exiting the heat exchanger and, in case of discrepancies it sends a signal to the flowrate generation block. This regulation varies the water flowrate to guarantee the correct heat flux in accordance with the desired temperature. The flowrate thus identified is that circulating in the district substation through the HX and the condenser side of HP1 and HP2.

In the "innovative" district (D6) it is not necessary to heat further the water coming from the distribution network because it is already at a temperature compat-

ible with the operating temperature of the radiant panel (38°C in this application). Therefore, the substation of D6 is solely composed of the ideal heat exchanger, governed by the aforementioned equations, and of the control system. As for the users' heat exchanger described in section 3.2.3, the HX block receives as input the D6's thermal demand profile and through the control system it modulates the flowrate to ensure the temperature exiting HX is 20°C (the return temperature of the primary network).

4.2.3 Set-up and boundary conditions

Outlined below are the key boundary conditions applied to Application #2, with some of them recalling conditions previously mentioned in the preceding sections. The main assumption concerns the location of the Case Study, which is Turin. For this application and location, the ground temperature was considered constant throughout the year, maintaining a value of 12°C. Low-temperature water, treated as an incompressible fluid, serves as the heat transfer fluid in the DH network. Boundary conditions for temperatures within the thermal network include setting a supply temperature from the main thermal power plant of 40°C and a return temperature of 20°C downstream of the districts' substation [23]. Ad-hoc controllers were implemented to monitor and maintain the desired reference temperatures throughout the simulation, ensuring a reliable supply of thermal needs. Concerning the groundwater, it was assumed that the water temperature is 20°C [1] as in [1].

4.2.4 Simulation: tools and run details

As for the Application #1, the software used for the overall simulation of the system is Simscape. The variations in comparison to the previous application's model lie in the sizing of individual blocks and the system layout. However, the blocks utilized remain consistent, with the exception of those specifically created and detailed in section 4.2.2. Therefore, the constitutive equations remain the same.

Moving to the demand side, to simulate the diverse buildings involved in the analysis, the EnergyPlus (E+) simulation software [84], version 9.3, was selected. It

[1]The ground and groundwater temperature were considered constant throughout the simulation runtime. Since the simulations last one day, it is reasonable to assume that these temperatures remain unchanged.

is an open-source and modularly structured code, developed by the U.S. Department of Energy in 2001 and continuously updated. EnergyPlus integrates the capabilities and features of BLAST and DOE-2, relying on the thermal balance method to determine the loads of each thermal zone in the building. It has the capacity to model various HVAC systems comprehensively. Additionally, the software allows for the computation and logging of multiple model variables (e.g., temperature trends in different thermal zones, demand profiles - both electrical and non-electrical, etc.) for the desired time horizon and temporal resolution in both aggregated and disaggregated forms. As an example, with this tool, it is possible to calculate the annual electrical energy required for the building, discern the share required by each thermal zone, and break down electrical consumption into various services such as lighting, appliances, and HVAC systems. The software for dynamic simulation serves the analysis well by providing control and management capabilities for a multitude of variables. This enables a detailed examination of how these variables can alter building load profiles and, consequently, their impact on available flexibility.

Case Study simulation Once having defined and modeled all components on the supply and demand side, the simulations can start. The dynamic simulation of buildings evaluates the annual performance of the RBs, with an hourly timestep. Since the RBs operation depends also on the conditions of the surrounding environment, to run the simulation E+ requires a weather file as input. For this application the ITA_Turin_160660_IWEC file was chosen. The models of the residential and office RBs were validated in terms of thermal loads with the values indicated by TABULA [76] and STREPIN documents [96] respectively. As a clarification, when referring to building thermal load profiles, the focus is on the sole space heating need. In fact, in the city of Turin, used as a case study, it is common for users to be connected to the network for only one of the two services (space heating and domestic hot water), and the majority are connected only for the heating purpose. This means that the shape of the thermal profile of the DH network can almost entirely be attributed to the heating demand, which is why the contribution of the DHW was not specifically considered in this analysis.

On the other hand, the simulation of the supply side runs one day, with a variable timestamp in order to guarantee the simulation convergence. Therefore, to couple demand and supply side simulation, one day for each season was selected for the E+ weather files, as the reference day. For the winter season, the typical day is February

the 6^{th}. Also in reality, late January and early February are the coldest periods for Turin, during which the highest district heating demand is recorded. Therefore, by choosing the 6^{th} of February as representative for the winter period, a cautious approach was used. From the annual outcomes of buildings' performances, relevant data for the typical day were extrapolated (e.g., thermal demand, temperature profiles, etc.). To conclude, in Figure 4.14, the schematic layout of the 5^{th} generation district heating network implemented on Simscape is depicted.

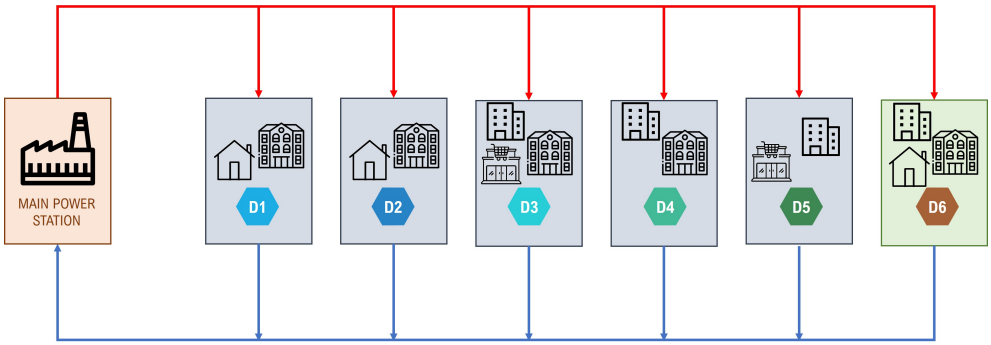

Fig. 4.14 Schematic representation of the network layout implemented on Simscape.

4.2.5 Assumption for flexibility calculation

Kleinschmidt classified flexibility sources of a MVES into three classes: conversion, storage and demand-side management [55]. Since this all-electric system, composed only of heat-pumps, lacks flexibility in its production mechanism, to evaluate the flexibility for Application #2, demand-side flexibility was studied. Indeed, as done in [97], it was assumed that buildings, through an ad hoc demand-side management system, can vary their thermal profiles in a certain time range, to provide electric flexibility to the power network, changing their expected demand (*Baseline*). Providing less or more thermal power to a building has an impact on the indoor temperature; therefore, limits should be set on the allowable deviation between the *Baseline* and *Flexible* profiles. It should be noted that the results are based on a significant assumption regarding the users. Specifically, it is assumed that all affected users have agreed to allow modifications to their load profiles and have accepted the network operator's proposals. Focusing on the *Baseline*, the HVAC building system is used to ensure that set-point and set-back temperatures defined in section 4.2.1 are maintained in each thermal zone. Based on this statement, in making load profiles flexible, the

choice was made to ensure the satisfaction of occupants' comfort, thus maintaining the sensation of thermal comfort.
Therefore, from the Standard UNI EN ISO 7730:2006 [98], three comfort categories were identified (i.e., A, B and C) in relation to the deviation from the set-point temperature. In detail:

- Category A: $\pm$ 1
- Category B: $\pm$ 2
- Category C: $\pm$ 3

In line with the procedure used in [97], Category B was selected to define the range of allowable temperatures in the building. The same temperature difference of plus or minus two degrees was used both during temperature set-point maintenance hours and during set-back hours. As an example, in residential buildings the set-point temperature was set at 20°C. In the hypothesis of modifying the supplied thermal power while maintaining the comfort Class B, a temperature modulation from 18°C to 22°C was allowed (20 $\pm$ 2°C). Figure 4.15 shows graphically this example; the blue curve is the *Baseline* temperature daily profile, so with an alternation between set-point and set-back temperatures. The other two curves - yellow and green - represent, instead, the maximum and minimum acceptable temperatures within the thermal zones of a residential building, allowing them to remain within the comfort Class B.

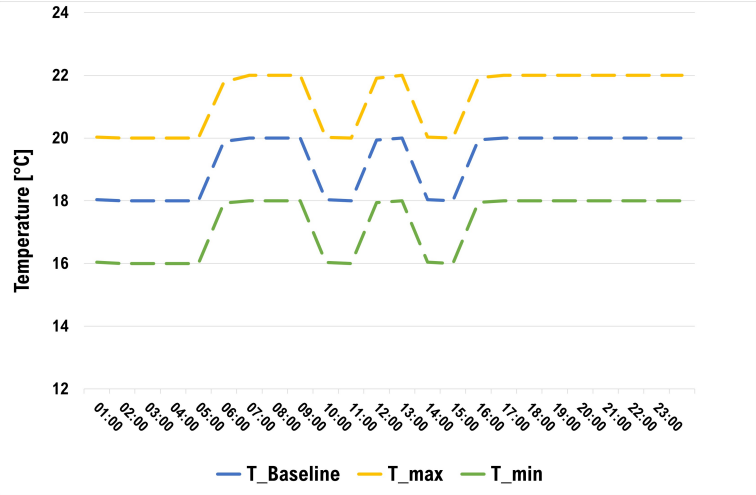

Fig. 4.15 Temperature profiles desired in thermal zones of residential buildings.

In Figure 4.16 the same example is presented for an office building during a working day. In this way, the boundaries for physical flexibility computation have been set.

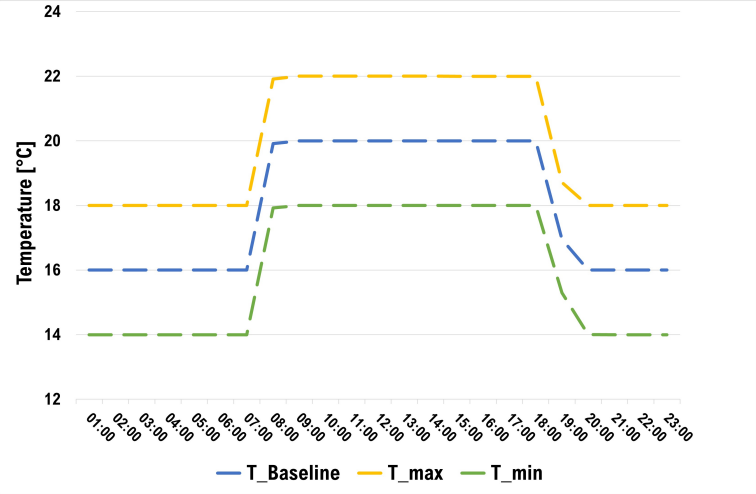

Fig. 4.16 Temperature profiles desired in thermal zones of offices during working days.

To a temperature set-point profile corresponds a thermal power profile (see Figure 4.17, in blue). Then to let the profile become flexible some demand-side management strategies should be implemented. So, in this application two strategies were developed:

Strategy #1 It was assumed to do peak shaving in the early morning, so to anticipate the heating provision with respect to the *Baseline* to follow convenient energy prices on the Intra-Day Market (IDM).

Strategy #2 It was hypothesized to integrate the district heating system with a photovoltaic plant, to serve the heat pumps with renewable electricity. Therefore it is assumed that the heat pumps absorption from the grid is modulated promoting the consumption of PV production.

Strategy #1 purpose was to achieve financial savings from the district heating operator standpoint. By knowing the hourly absorption profile of all the heat pumps for a given day D, the operator knows how much electricity needs to be purchased. By participating in the Italian Day-Ahead Market (DAM), the operator purchases the necessary energy at a specific price on day D-1. Then, if on day D the operator

realizes that energy prices on the Intraday Market (IDM) are more advantageous than those previously contracted on the DAM, he/she can chose to buy more energy in the time intervals in which prices are more convenient and resell the excess. By modifying the profiles of purchased electricity, the absorption of heat pumps is consequently altered, impacting the thermal energy supplied to the buildings. This modulation of heat supply, without compromising internal comfort conditions, is possible by exploiting the thermal inertia of the buildings.

As an exemplification, Figure 4.17 shows the temperature and thermal profiles modification in case of Strategy #1 application.

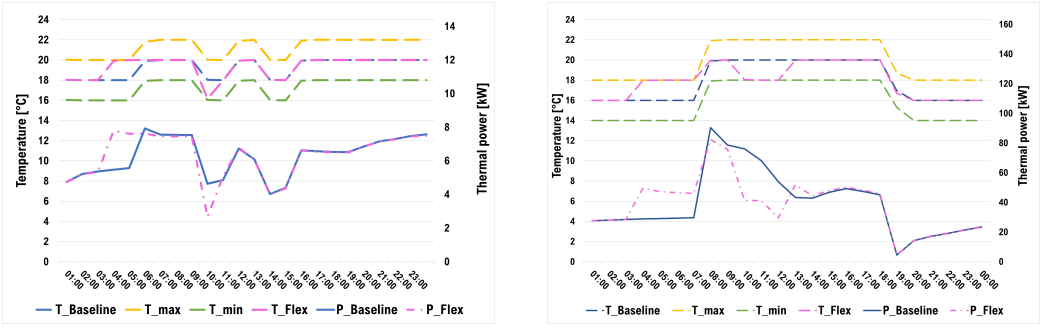

(a) Residential buildings.

(b) Offices during working days.

Fig. 4.17 Thermal power and temperature profiles in *Baseline* and *Flexible* scenarios for Strategy #1.

In line with future trends concerning the integration of renewables in district heating systems [37, 38, 42, 43, 56], Strategy #2 was proposed to evaluate the behaviour of the system in response to external signals, in this case the availability of electricity produced by a PV plant. The *Baseline* scenario is the same one of the Strategy #1, separated from the operating logic of external systems but driven by users' needs only. The *Flexible* scenario was created by allowing the modification of the thermal demand profiles of buildings to follow the electricity PV production curve in Figure 4.18, in order to bring also financial and environmental savings. The graph illustrates the production curve of a photovoltaic panel installed in Turin on February 6^{th}, representing the typical winter day. The simulation was performed using the online tool PVGIS, with a peak power installation of 1 kWp. The focus was not primarily on the overall energy yield of a hypothetical photovoltaic system

but rather on analyzing the production profile. The goal was to identify optimal times for drawing additional electricity from the grid, particularly when generated from renewable sources.

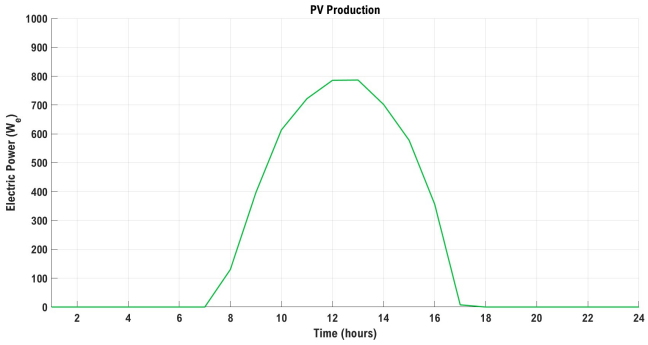

Fig. 4.18 Electricity production of 1 kW_p PV panel.

Figure 4.19 shows the temperature and thermal profiles modification in case of Strategy #2 application on a SFH and an office reference building. The financial implications of this mechanism are analysed more in detail in Section 4.3.

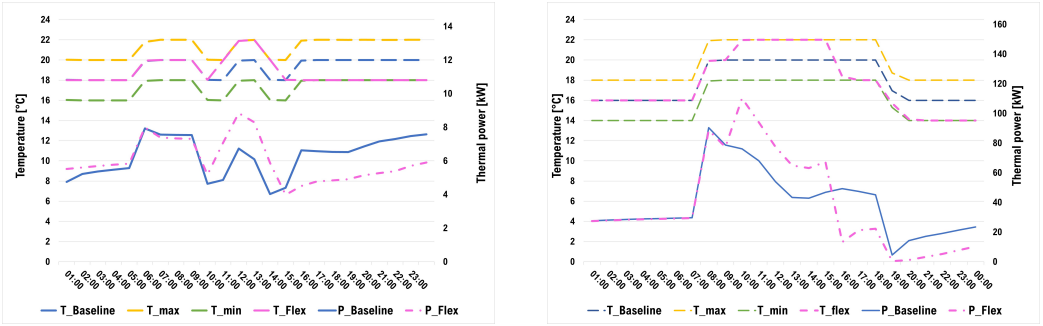

(a) Residential buildings.

(b) Offices during working days.

Fig. 4.19 Thermal power and temperature profiles in *Baseline* and *Flexible* scenarios for Strategy #2.

As can be observed in Figure 4.19, with this strategy, in contrast to the previous approach, the peak thermal demand and the subsequent electrical absorption are not reduced in absolute terms; instead, they are temporally shifted to align with the peak production of the photovoltaic system. This ensures the optimization of operation, maximizing the utilization of electricity from renewable sources. In addition, to ensure similar daily energies for both *Baseline* and *Flexible* cases, after the flexibility

action the internal temperature of the building was set to the lower edge of the comfort band. If there is a demand for downward flexibility, the operator can take advantage of absorption by the heat pumps to bring the internal temperature back to the set-point.

In line with Eqs. 2.1-2.8, also in the case of flexible demand, with E_{Flex} as the new scheduled profile, the flexibility KPIs can be calculated as follows:

$$\begin{aligned}
&\text{if } E_{Base} > E_{Flex} \\
&\textit{DOWN-flex}(h) = E_{Flex}(h) - E_{Base}(h) \\
&\text{else} \\
&\textit{UP-flex}(h) = E_{Base}(h) - E_{Flex}(h) \\
&\text{end}
\end{aligned} \tag{4.13}$$

UP-flex represents the availability for upward flexibility, meaning that the electric grid has a grater amount of power available with respect to the forecasted quantity, because the heat pumps are absorbing less energy. On the other hand, DOWN-flex answers to the downward flexibility demand of the network, by absorbing from the electric grid more energy than in the *Baseline*.

4.3 Explore multi-domain flexibility implications

The flexibility measures, such as modifying the profiles of thermal load and electrical absorption, have consequences not only in the energy sector, with different exchanges of flows between the system and the electrical and thermal networks, but also have financial implications. In fact, altering the absorption profile of heat pumps results in a different hourly amount of energy purchased on the electrical market. Generally, with knowledge of the energy profile required for the delivery day (D), energy is negotiated on the Day-Ahead Market. If on the delivery day there is the necessity to purchase more energy than expected or there is surplus energy to resell, participation in the Intraday market becomes necessary. In detail, reporting some definition, the Intraday market, referred to as "Mercato Infragiornaliero" (IDM), has the objective of compensating for the differences between the schedule set the day before and the

actual requirements during operation. Indeed, it gives the opportunity to operators to modify their buy/sell programs established in the DAM. IDM is an auction market organized into sessions in which it is possible to trade electricity using continuous trading, allowing to exchange energy fluxes up to one hour before delivery.

Moving to the financial implications of the two Case Studies, fist of all, the daily expenditure for the *Baseline* was calculated. It is valorized considering the participation to the DAM, therefore the hourly values of zonal price in €/kWh for a winter day were defined through the "Gestore dei Mercati Energetici" (GME) site [99]. The selected area was the North and the values refer to 31/01/2023. The zonal price ($Pr_{s,DAM}$) is the price at which energy is sold on the electricity market, while, considering the charges and taxes to be paid when buying energy, the purchase cost for consumption ($C_{p,DAM}$) is 2.5 times the selling price (as in Eq. 4.14), since excise duties, taxes and charges are 40% of the total expenditure on electricity.

$$C_{p,DAM}(h) = Pr_{s,DAM}(h) * 2.5 \tag{4.14}$$

To facilitate reading, from now on, the term "price" will refer to the selling price, and the term "cost" will refer to the purchase cost, including additional charges, taxes, and excise duties.

The Baseline electricity cost (C_{Base}) for the typical winter day is then defined as in Eq. 4.15 as the sum of the hourly product between the amount of energy consumption (E_{Base}) and the purchased cost ($C_{p,DAM}$).

$$C_{Base} = \sum_{h=1}^{24} C_{p,DAM}(h) * E_{Base}(h) \tag{4.15}$$

Then, the UP- and DOWN-flex energy quantities, calculated in Eq. 4.13, were associated to cost values. DOWN-flex means the quantity to be purchased, while UP-flex is the energy to be resell on the IDM. To quantify the potential economic benefit of the flexibility interventions, hourly prices were defined for a hypothetical IDM ($Pr_{s,IDM}$). As for the DAM, also the IDM purchasing cost is 2.5 times the selling value. Depending on the flexibility strategy considered, different ad-hoc hourly values were assumed. Specifically, the purchasing cost $A_{flex}(h)$ was associated to

the DOWN-flex energy. It is calculated as the hourly product between DOWN-flex and teh IDM cost ($C_{p,IDM}$). The Eq. 4.16 calculates the daily value of A_{flex}.

$$A_{flex} = \sum_{h=1}^{24} DOWN_{-flex}(h) * C_{p,IDM}(h) \tag{4.16}$$

The modification of profiles does not just incur additional costs; when surplus energy is sold, it can generate a revenue. Thus, the daily remuneration cost R_{flex} is defined as the cumulative product of the hourly amount of energy for sale *UP-flex* and the corresponding hourly energy price $PR_{s,IDM}$ on the Intraday Market. The reference equation is Eq. 4.17.

$$R_{flex} = \sum_{h=1}^{24} Pr_{s,IDM}(h) * UP_{-flex}(h) \tag{4.17}$$

Finally, the daily total cost for the operator is calculated through Eq. 4.18, by summing up the originally anticipated cost for the *Baseline*, along with the two cost components related to flexibility interventions, plus the potential cost for inconvenience related to demand side management C_{DSM}. In the formula *Sx* stands for the x-th flexibility strategy.

$$C_{total,Sx} = C_{Base} + A_{flex} - R_{flex} + C_{DSM} \tag{4.18}$$

The expense associated with DSM could be a factor in the $C_{total,Sx}$ but in our specific applications, it remains at zero. This is due to the nature of both flexibility strategies, which do not inconvenience the user as they are designed to stay within comfort thresholds. Hence, there is no requirement to financially compensate for any service disruption.
Figure 4.20 illustrates the logic diagram to be followed hourly to define the $C_{total,Sx}(h)$ for each flexibility strategy.

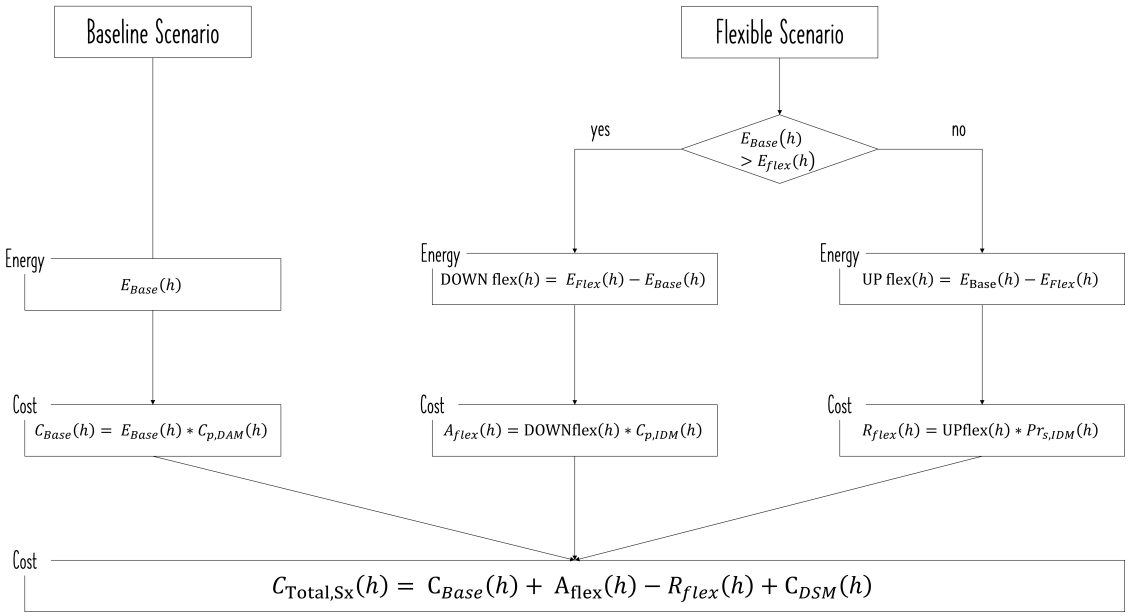

Fig. 4.20 Hourly total cost composition according to the operation profiles.

Then, to compare the *Flexible* scenarios with the *Baseline* one, the $\Delta Cost_{Sx}$ indicator was created, to evaluate if the flexibility strategies result in some financial savings. In Eq. 4.19 the value is expressed in [%].

$$\Delta Cost_{Sx} = \frac{C_{Base} - C_{Total,Sx}}{C_{Base}} * 100 \tag{4.19}$$

As a final consideration, an indicator was defined that, exclusively in the context of flexibility intervention, assesses the difference between the additional costs incurred compared to the base case and the revenues that would not have been obtained otherwise. This indicator is also expressed as a percentage value by the formula 4.20.

$$profit_{Sx} = \frac{R_{flex} - A_{flex}}{R_{flex}} * 100 \tag{4.20}$$

4.4 Analysis and discussion of final outcomes

This section is dedicated to the analysis of the outcomes of Application #2, mostly in terms of flexibility. Starting from the *Baseline* definition, the discussion will then proceed to the Sections 4.4.2 and 4.4.3 focused on the two flexibility strategies, where diverse outputs are presented and juxtaposed in both energy and financial terms.
To avoid overburdening the reader, in this section only the results of three representative districts are shown and discussed, while the remaining graphs are reported in Appendix B.

4.4.1 Flexibility assessment - *Baseline*

Starting from the characterization of the *Baseline*, Figure 4.21 illustrates the thermal load profiles required by each district, obtained as the sum of the profiles of the individual RBs, aggregated as in Table 4.1.

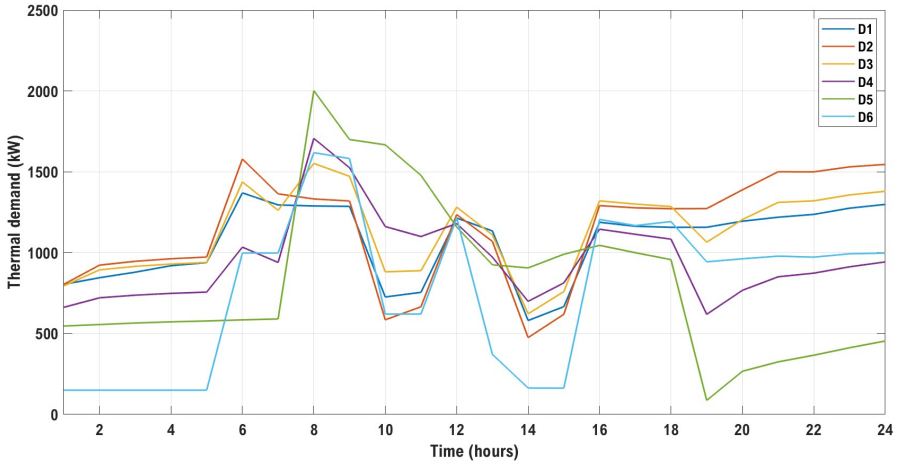

Fig. 4.21 *Baseline* - Hourly thermal profiles for the winter typical day.

First of all, it is possible to observe that the districts never reach the zero demand for thermal energy, this is due both to the fact that within the district the values of the individual RBs compensate for each other, and to the fact that it is required to maintain a set-back temperature inside the buildings, therefore on many winter days, this does not allow the heating system to turn off.

Looking at the shape of the curve, for the districts composed only of residential buildings, D1 and D2 in blue and orange respectively, there is a global peak around 06:00, the time at which the heating system is supposed to be activated, in line with the activities of households. Then there is a local peak around 12:00, the time when the occupants are expected to be at home for lunch. Finally, the curve presents an increase in demand towards the final hours of the day.
The global peak is postponed at 08:00 in the fully commercial district (D5, in green), the time at which workers start arriving in offices and mall. D5 presents a minimum in correspondence of the closing time of the offices at 19:00. For the mixed-use districts (D3 and D4, represented by yellow and violet curves) the shape is the combination of the two trends described above; there is a local maximum when the HVAC systems of the residential RBs starts and the global maximum value when the conditioning systems of the office and mall RBs come into operation. A final consideration must be reserved for the innovative district, D6 in light blue. The district is made up of recently built buildings that use radiant panels as a heat emission system (i.e., radiant floors for residential buildings and radiant ceilings for offices). This emission system, together with the best performance of the opaque and transparent envelope, allows to reduce the demand for thermal energy in the central hours of the day.
Table 4.5 shows the peak values of thermal demand ($P_{Base,peak}$) and electrical absorption $P_{el,Base,peak}$ for each district and the main thermal station in the *Baseline* scenario.

	D1	**D2**	**D3**	**D4**	**D5**	**D6**	**Main Station**	**Total DH**
$P_{Base,peak}$ $[kW_{th}]$	1370	1579	1552	1707	2002	1618	9177	18676
$P_{el,Base,peak}$ $[kW_{el}]$	354.8	403.4	402.5	436.9	506.7	-	1603.5	3636.7

Table 4.5 Peak power of district thermal and electrical demand in *Baseline* conditions.

The heat consumption values of the districts derive from the aggregation of the profiles generated by E+, while the electricity consumption is the result of the dynamic simulation of the system on Simscape, as well as is the overall thermal demand required by the district heating in the thermal power plant. The electricity consumption box for District 6 is equal to zero because, as previously explained, D6 does not have a heating substation with heat pumps, and the heat is directly

transferred from the thermal power plant at a sufficient temperature to be compatible with the radiant systems of buildings.

4.4.2 Flexibility assessment - Strategy #1

Figure 4.22 displays the modification of the thermal profiles of the six districts following the intervention of demand-side management of Strategy #1.

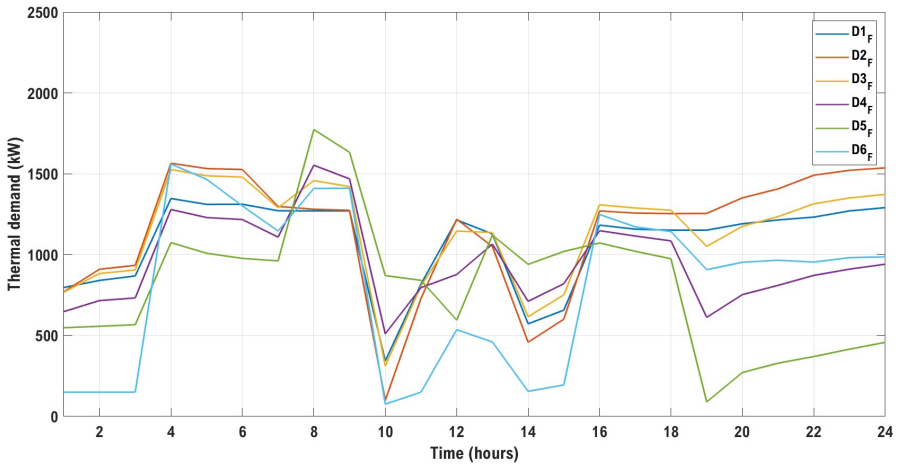

Fig. 4.22 *Strategy #1* - Hourly thermal profiles for the winter typical day.

As can be seen from the graph, the heat supply by district heating is brought forward, creating a new local peak around 04:00 in the morning, the time at which it was supposed to start heating the buildings according to Strategy #1. It has been hypothesized that the overall flexibility intervention would last for 7 hours overall (from 04:00 to 11:00) to have an energy balance between the extra energy supplied in the early hours of the morning and the energy not supplied later. The effects on the modification of the supply of thermal power, however, continue for longer, exploiting the thermal inertia of the buildings and the network. The demand management system, by anticipating the start of heating time and producing both thermal and electrical flexibility, also led to a decrease in the peak of thermal demand between the *Baseline* and *Flexible* scenarios. The percentage reduction has been calculated with Eq. 4.21 and is reported in Table 4.6.

$$PeakReduction = \frac{P_{Base,peak} - P_{Flex,peak}}{P_{Base,peak}} * 100 \tag{4.21}$$

Where $P_{Base,peak}$ and $P_{Flex,peak}$ are the maximum thermal demand required in the *Baseline* and *Flexible* scenarios, respectively. The maximum decrease in the peak occurs for district 5 which is the purely commercial district and is also the one showing the greatest peak in the *Baseline* scenario.

	D1	**D2**	**D3**	**D4**	**D5**	**D6**	**Main Station**
$P_{Base,peak}$ $[kW_{th}]$	1370	1579	1552	1707	2002	1618	9177
S1 - $P_{Flex,peak}$ $[kW_{th}]$	1347	1565	1527	1553	1774	1561	8650
Peak Reduction [%]	2%	1%	2%	9%	11%	4%	6%

Table 4.6 Peak power of district thermal demand in *Baseline* and *S1-Flexible* profile conditions.

Shifting the focus to the electrical carrier, the results for some significant districts (D2 – entirely residential and D5 – entirely commercial) and the main thermal plant are presented below. The remaining districts are addressed in the Appendix B. In the case under consideration, given the all-electric system and the use of the heat pump as the sole conversion technology, operational flexibility aligns with the cross-carrier flexibility of the system for the electric vector; therefore, below it is commonly referred to as electrical operational flexibility.

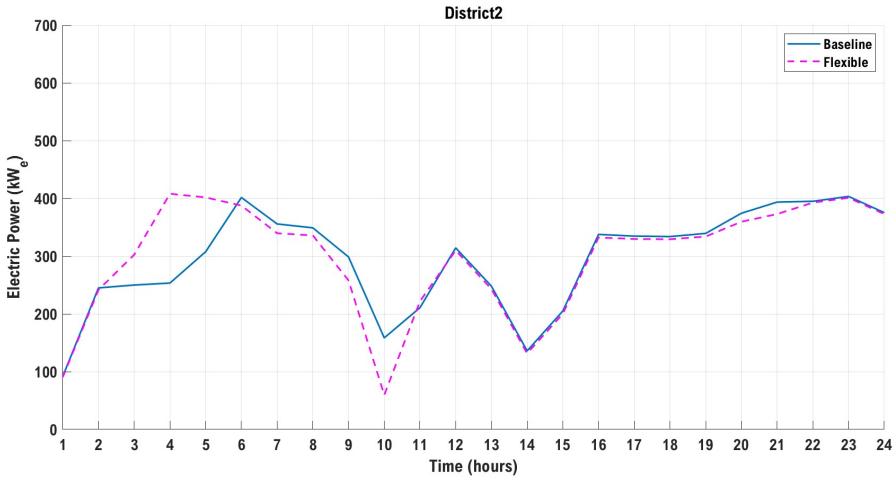

Fig. 4.23 *Strategy #1* - Electrical power absorbed by heat pumps in District 2 substation.

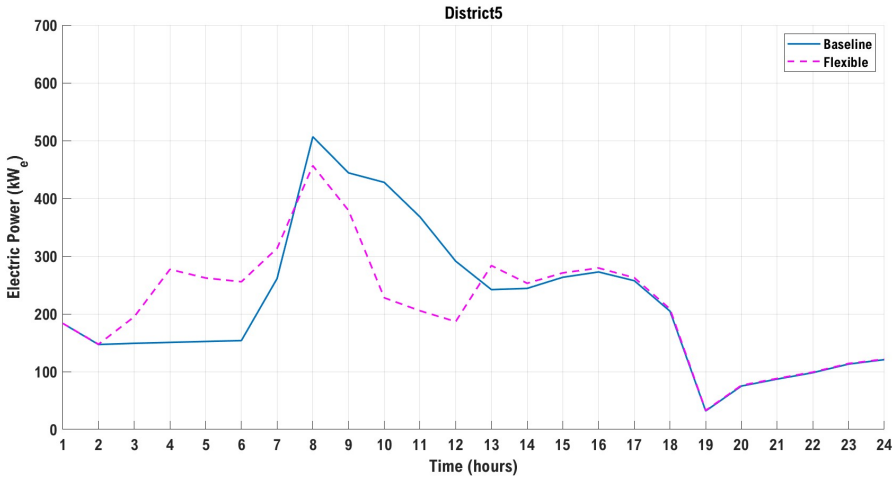

Fig. 4.24 *Strategy #1* - Electrical power absorbed by heat pumps in District 5 substation.

Figure 4.23 and 4.24 show the electrical absorption profiles of the heat pumps in the substations of Districts 2 and 5. They are the result of load tracking by the heat pumps. In fact, the dashed pink curve represents the electrical power absorbed by the heat pumps to cover the *Flexible* load of the district, while the blue line shows the absorption of the heat pumps for the *Baseline* load, similarly to what is shown in Figure 4.17 for thermal considerations. The curves are the result of the sum of the electricity withdrawals of the two machines installed in each substation.
Comparing the Figures, since the districts are made up of buildings with different destinations of use and functions, the curves, and consequently the flexibility made available, are very different both in terms of profile shape and absolute power value. Looking at Figure 4.23, electrical consumption for the *Flexible* profile has the same shape as the thermal one, with a new peak around 04:00 and a subsequent decrease in absorption that deviates from the *Baseline* profile from 08:00 to 11:00. Moving to District 5, similar comments can be made. The *Flexible* electrical profile presents a new local peak at 04:00, the early heat supply decreases the maximum peak of 08:00 but is still not sufficient to eliminate it. The advance in the heat supply leads to a period, between 09:00 and 12:00, in which the district heat pumps can draw less energy from the grid while ensuring comfort for the occupants as imposed by the boundary conditions. Considering both Figures, from 12:00 onward, the *Flexible* and *Baseline* profiles return to match almost perfectly, presenting only small variations. This is a consequence of the fact that the electrical output is the result of the dynamic simulation of the system and therefore depending on the simulated scenario, the

input conditions to the substation can change hour by hour, i.e., the temperature of the water on the evaporator side of the HP1. This leads to a different performance of the machine which was modeled as sensitive to variations in the conditions of the inlet water. This aspect is valid for all districts.
Figure 4.25 and Figure 4.26 show the flexibility made available to the electricity grid by the two districts. In detail, the UP- and DOWN-flex KPIs were calculated hourly by comparing the *Baseline* and *Flexible* profiles (according to Eq. 4.13), and were then graphically represented as area graphs.

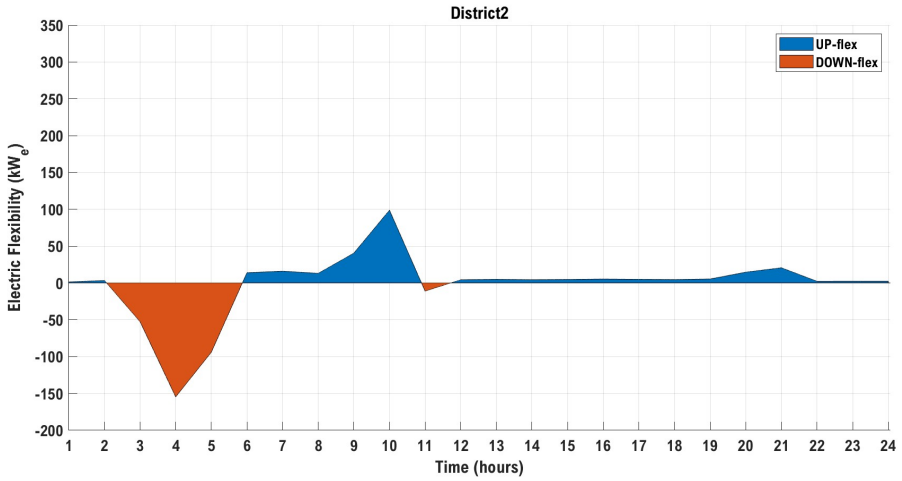

Fig. 4.25 *Strategy #1* - Operational electrical flexibility made available by District 2.

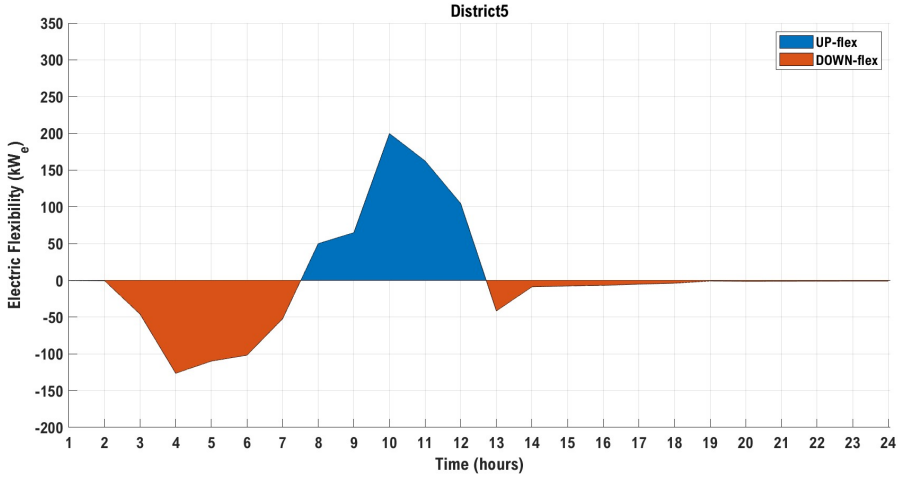

Fig. 4.26 *Strategy #1* - Operational electrical flexibility made available by District 5.

DOWN-flex (red area) is detected in the hours in which the absorption of the heat pumps is greater than the expected profile, it is represented with negative values because, looking at the situation from the power grid, the network has less power available than expected. On the contrary, in the hours in which the heat pumps absorb less than the *Baseline*, UP-flex (blue area) is available for the network which has a greater amount of power available than the forecasts.
Consistent with the electrical profiles presented earlier, the operational flexibility provided by the two districts differs, especially in terms of magnitude. District 5 offers a total of 577.60 kWh for upward and 607.05 kWh for downward on the reference day, whereas District 2 provides 282.93 kWh and 311.54 kWh, respectively.

Since District 6, the so-called "innovative" district, in the substation does not have heat pumps but only the district heat exchanger, the effect of the modification of the thermal profile (see Figure 4.27) on the electricity carrier cannot be observed at the substation level, but it is seen directly at the level of the main thermal power plant.

Fig. 4.27 *Strategy #1* - Thermal demand modification for District 6.

This aspect is shown in Figure 4.28 and Figure 4.29. While the electrical flexibility provided by the substations is the result of the modification of the load profiles of the buildings, the flexibility of the heat pump located in the main plant is affected both by the different functioning of the heat pumps of the traditional substations (i.e., Districts from 1 to 5), the dynamics and losses along the thermal

network, and in addition also the modification of the load profiles of the buildings that compose the "innovative" district.

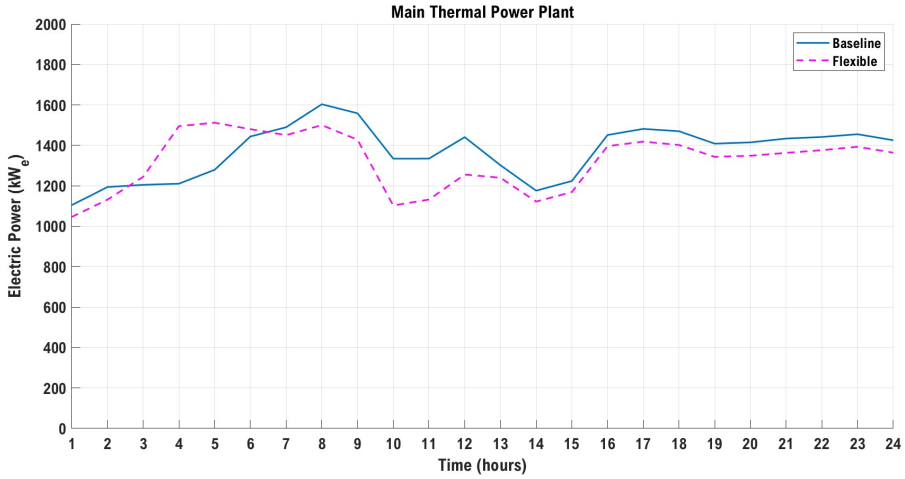

Fig. 4.28 *Strategy #1* - Electrical power absorbed by heat pumps in in the main thermal plant.

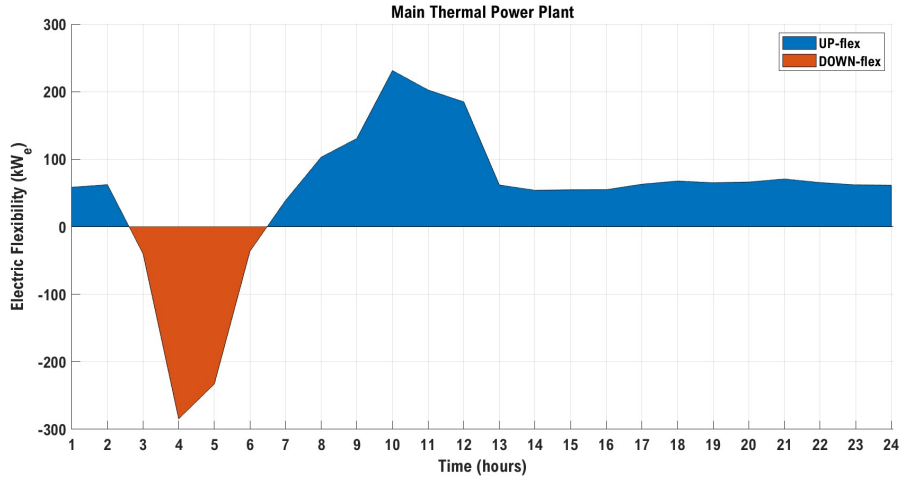

Fig. 4.29 *Strategy #1* - Operational electrical flexibility made available by the main thermal plant.

Finally, when considering the district heating system comprehensively and envisioning its interaction with the electrical grid at a singular point, by summing all the contributions along the entire energy chain it is possible to obtain the operational flexibility globally made available by the system and represented in Figure 4.30. The areas in Figure are the combined result of:

- the thermal flexibility deriving from the variation of the load profiles compared to those foreseen by the *Baseline*, respecting the limits imposed via boundary conditions and comfort bands;
- the electrical flexibility of the districts, obtained thanks to the heat pumps installed in the substations, which transform electrical energy absorbed by the network into the required thermal energy, with the related constraints on delivery and return temperatures;
- the effect of the "innovative" district directly on the electrical absorption profile of the geothermal heat pump located in the main thermal plant;
- the dynamics of the thermal network with the relative losses along it.

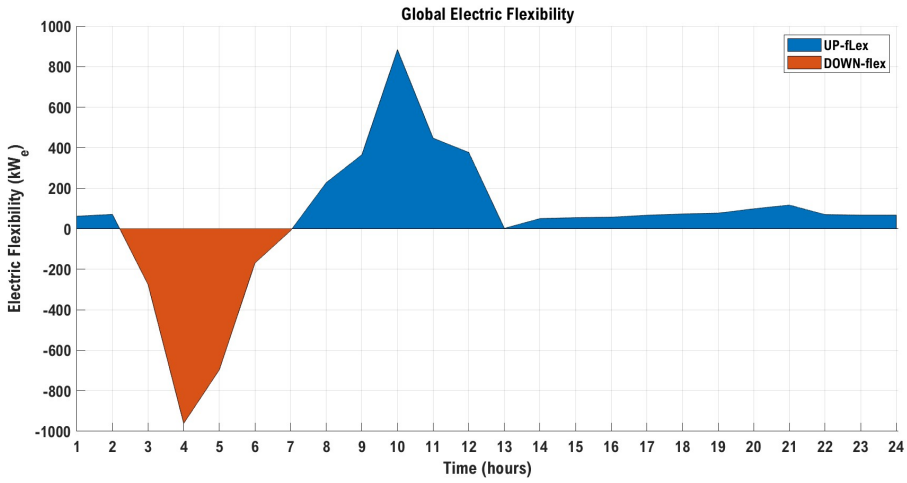

Fig. 4.30 *Strategy #1* - Total operational electric flexibility of the fifth-generation district heating system.

Therefore, as the overall flexibility is the combination of all these factors, the global operational flexibility profile, in 4.30, is also the combination of the graphs shown before. As expected, the system is able of providing DOWN-flex only during hours when the supply of heat is anticipated, and heat pumps absorb more power from the electric grid (2212 kWh of daily DOWN-flex). Then, there is a significant amount of UP-flex in the midday hours to offset the imbalance experienced earlier. Finally, there is a reduced quota of UP-flex from 13:00 onward, mainly attributable to the dynamics of the network (3167 kWh of daily UP-flex). This can be asserted

because, as observed, the thermal and electrical profiles of the districts in the hours following 12:00 are almost perfectly coincident. This result shows the importance of the proposed simulation-based methodology, as without the dynamic simulation of the network it would not have been possible to capture all these aspects.

Financial implications of flexibility

Focusing on the non-energy implications of the possibility of providing flexibility by the fifth-generation district heating system, the economic aspect is certainly relevant. Starting from the *Baseline* analysis, through participation in the day-ahead market (DAM), it is possible to obtain the energy expenditure for purchasing electricity. The graph in Figure 4.31 shows in blue the hourly trend of the zonal price of electricity on the DAM. It was obtained via GME [99], extrapolating the values for the North zone for a winter day (i.e., 31/01/2023).

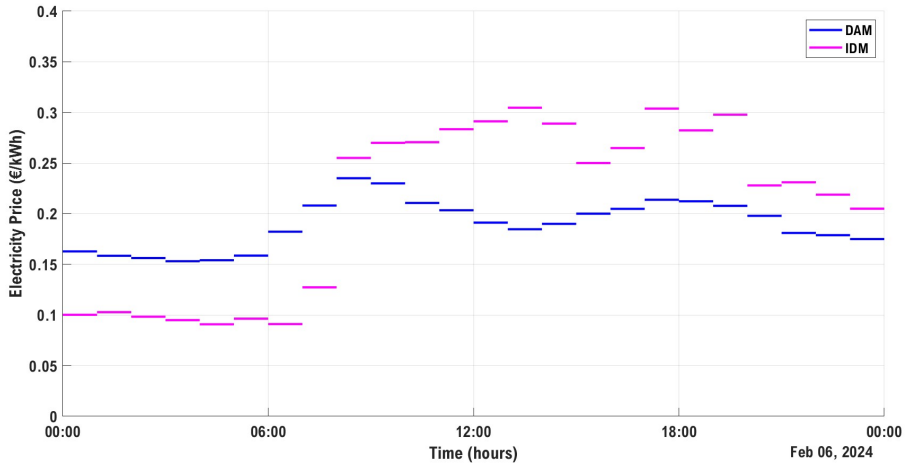

Fig. 4.31 *Strategy #1* - Day-ahead and Intraday zonal prices for the North area.

The lines in the figure represent the value at which the electricity is sold on the DAM. To obtain the purchase cost, taxes, excise duties and charges must also be taken into consideration, using the formula 4.14. By multiplying the purchase cost by the amount of energy expected to be absorbed for the *Baseline*, using the Eq. 4.15, C_{Base} is obtained, which is a fixed cost to be paid even for flexibility scenarios. Indeed, the operator committed to buying that quantity of energy at that price; thus, it is an expense incurred in any case. For Strategy #1, it is assumed to do peak

shaving in the early morning, so to anticipate the heating provision with respect to the *Baseline* both to avoid morning peak and to follow convenient energy prices on the intra-day market (IDM). Therefore, for the purpose of the application, more advantageous offers on the IDM market have been hypothesized, in line with a trend that could actually lead to the intervention of flexibility.
IDM prices are represented in pink in Figure 4.31 and values are lower than the DAM ones for the hours in which more energy must be purchased compared to the *Baseline* and higher in the hours in which the energy already purchased and which will not be used can be sold. The participation in the IDM market and the application of Eqs. 4.16, 4.17 and 4.18 lead to the results in the Table 4.7.

Financial KPIs	**Values [€/day]**
C_{Base}	31196.82
$C_{total,S1}$	30885.57
A_{flex}	497.34
R_{flex}	810.98

Table 4.7 Electricity costs for *Strategy #1*.

As can be seen from the results, the cost arising from the flexibility intervention ($C_{total,S1}$) is lower than that estimated for the *Baseline*, in line with the objective of the Strategy #1 application. This happens because the remuneration (R_{flex}) due to the sale of energy no longer needed exceeds the cost to be paid (A_{flex}) for purchasing the extra energy in the morning. In detail, to compare the *Baseline* and *Flexible* scenarios, the KPIs in the Table 4.8 were calculated.

Financial KPIs	**Values**
$\Delta Cost_{S1}$	1.01%
$Profit_{S1}$	38.68%

Table 4.8 Costs comparison for *Strategy #1*.

The overall $\Delta Cost_{S1}$ between the two scenarios is 1%. This is because the difference in energy between the *Flexible* and *Baseline* configuration is small compared to the electrical energy that is purchased for the *Baseline* in any case. However, by limiting to the flexibility action, it leads to a profit of 38.68%, given the fact that, in

exchange for an additional expense to purchase electricity in the early hours of the morning, there is a greater revenue due to the sale of the electricity in the central hours of the day.

4.4.3 Flexibility assessment - Strategy #2

Figure 4.32 displays the modification of the thermal profiles of the six districts following the intervention of demand-side management of Strategy #2.

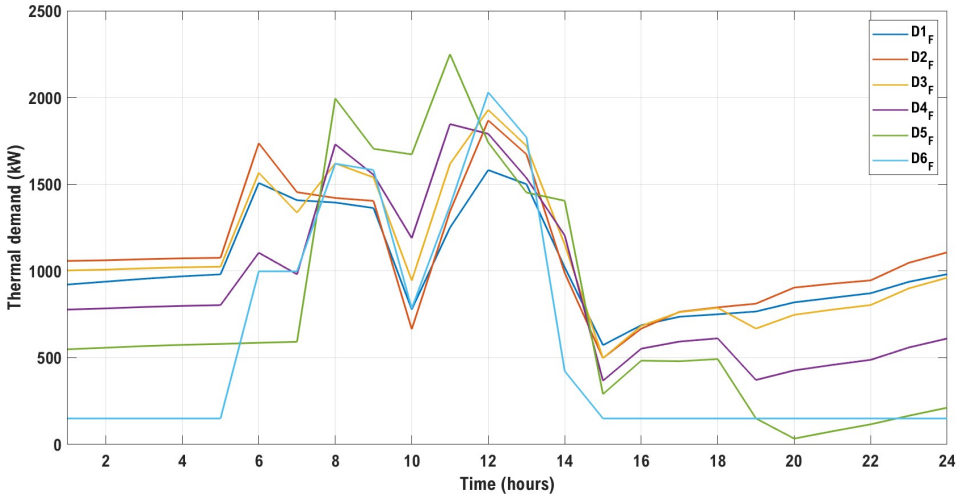

Fig. 4.32 *Strategy #2* - Hourly thermal profiles for the winter typical day.

Compared to the *Baseline* chart (in Figure 4.21), the profiles are coincident until 10:00, while they change in the day's remaining hours. The S2 provides a greater absorption of HPs between 10:00 and 14:00, the hourly interval in which there is the maximum production of electricity from photovoltaic. Instead, there is a reduction in electricity consumption compared to the *Baseline* from 15:00 to 24:00. The change of the electrical absorption in input to the HPs translates in the variation of the thermal production in the output shown in figure. This modification, however, allows the occupants to be guaranteed an internal air temperature inside the indoor environment that falls within comfort category B. This is possible thanks to the characteristics of the building envelope. The building behaves as a thermal storage that stores heat during the hours when it is supplied more energy than necessary and releases it when the plant operates at reduced load, from 15:00 onward.

Strategy #2, in contrast to the previous one, has not the objective of reducing thermal peaks in district heating. Consequently, electrical absorption does not decrease in absolute terms but is temporally shifted to coincide with the peak production of the photovoltaic system. This strategy ensures optimal usage, maximizing the utilization of electricity from renewable sources. For this reason, looking at Table 4.9 concerning the thermal peak values of *Baseline* and Strategy #2 scenarios, it is observed that the S2 leads to an increase in the peak, instead of a reduction. Therefore, the percentage deviation calculated by Eq. 4.21 has negative values.

	D1	**D2**	**D3**	**D4**	**D5**	**D6**	**Main Station**
$P_{Base,peak}$ $[kW_{th}]$	1370	1579	1552	1707	2002	1618	9177
S2 - $P_{Flex,peak}$ $[kW_{th}]$	1518	1868	1929	1847	2250	2030	10829
Peak Reduction [%]	-11%	-18%	-24%	-8%	-12%	-25%	-18%

Table 4.9 Peak power of district thermal demand in *Baseline* and *S2-Flexible* profile conditions.

Moving to the electric vector, as for Strategy #1, only the outcomes regarding Districts 2 and 5 are presented in this section, while the graphical outputs of the remaining districts are shown in Appendix B.

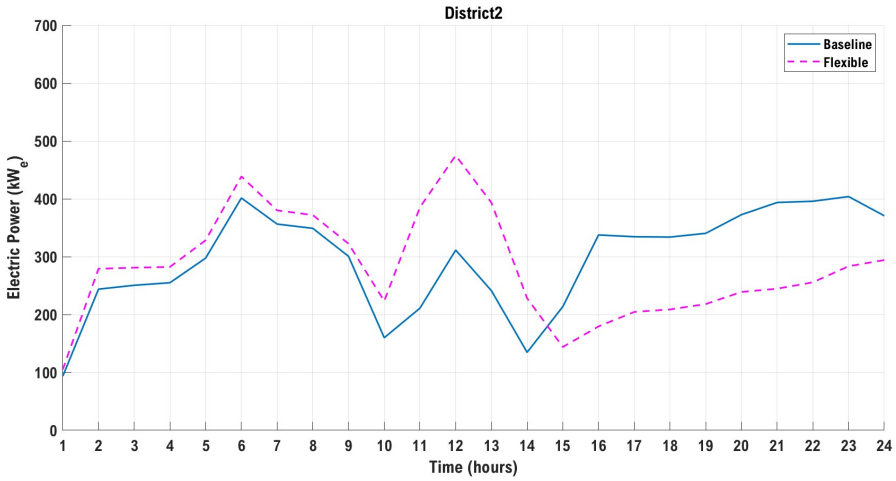

Fig. 4.33 *Strategy #2* - Electrical power absorbed by heat pumps in District 2 substation.

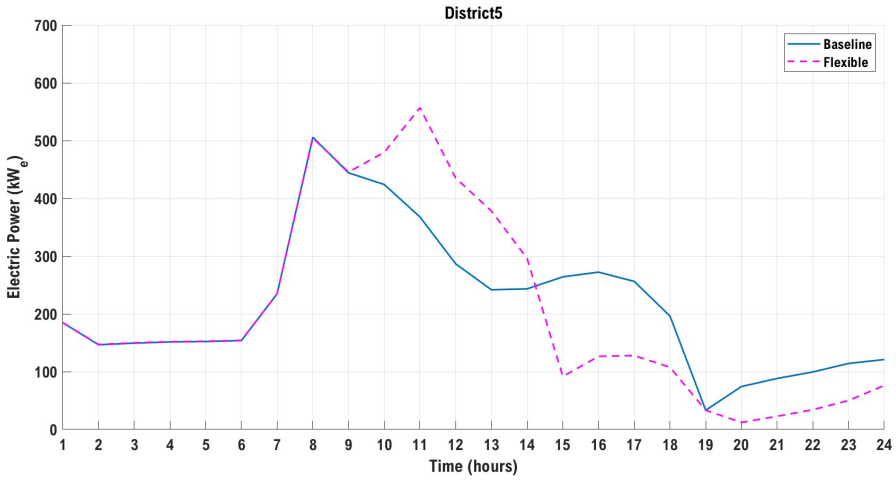

Fig. 4.34 *Strategy #2* - Electrical power absorbed by heat pumps in District 5 substation.

Figures 4.33 and 4.34 show the hourly pattern of absorption of D2 and D5 substations in the *Baseline* (blue) and Strategy #2 (pink) scenarios. These profiles are obtained by summing the contributions of the two heat pumps that make up the substations. The profile of the *Baseline* is the same as the one presented for *Strategy #1*, since it was supposed to propose two flexibility interventions for the same day. While the pink curve represents the electrical absorption in the flexible scenario. According to the thermal profiles, there is a significant increase in electricity consumption in the middle of the day, consumption that has been assumed to be covered with renewable energy. From 15:00 onward, however, a lower electrical absorption is observed, to balance the energy supplied to the buildings as a whole. It is noteworthy that the morning peak, coinciding with the start of occupants' activities in the buildings, persists, and a new consumption peak emerges between 11:00 and 12:00, depending on whether the district is commercial or residential. In the case of the commercial district (D5), the deviation from the *Baseline* is more moderate than for the previous strategy. This can be attributed to the office envelope and its internal gains. Specifically, the RB, as depicted in Figure 4.6, has a relevant fenestration surface in comparison to the opaque casing. Consequently, during the central hours of the day when the solar gains are maximum and are added to the gains due to the presence of people, lights, and equipment, the internal temperature of thermal zones is already close to the set-point. As a result, minimal intervention by the heating system is required. Thus, in the hypothesis of providing more heat

in this time interval, while staying within the maximum comfort band (+2°C of the set-point), the increment is limited enough not to cause discomfort to occupants.

Moving to flexibility considerations, Figure 4.35 and Figure 4.36 depict the value of operational flexibility indicators for D2 and D5. Looking at the electricity flux from the power grid, Figures show red areas for DOWN-flex in the time interval corresponding to a greater HPs absorption with respect to the base case, meaning the grid has less electricity than predicted. On the other hours of the day, indeed, the grid has at disposal more electricity than the estimated value because the HPs require less.

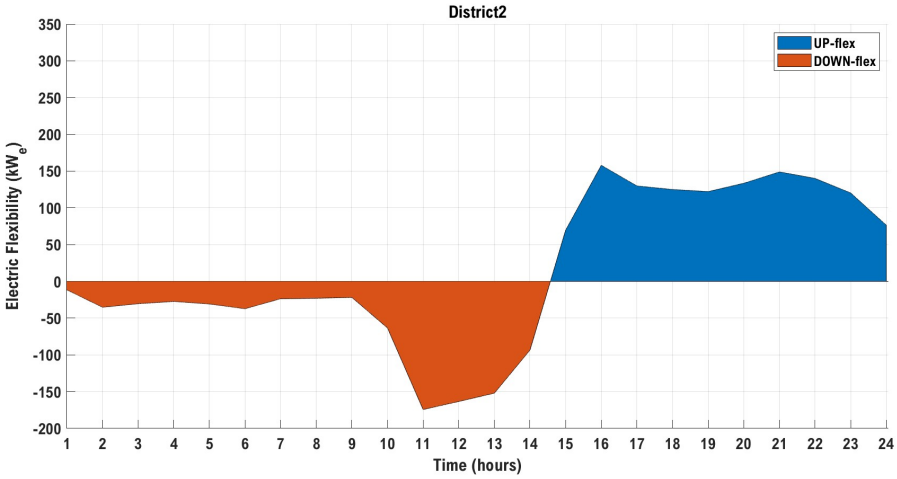

Fig. 4.35 *Strategy #2* - Operational electrical flexibility made available by District 2.

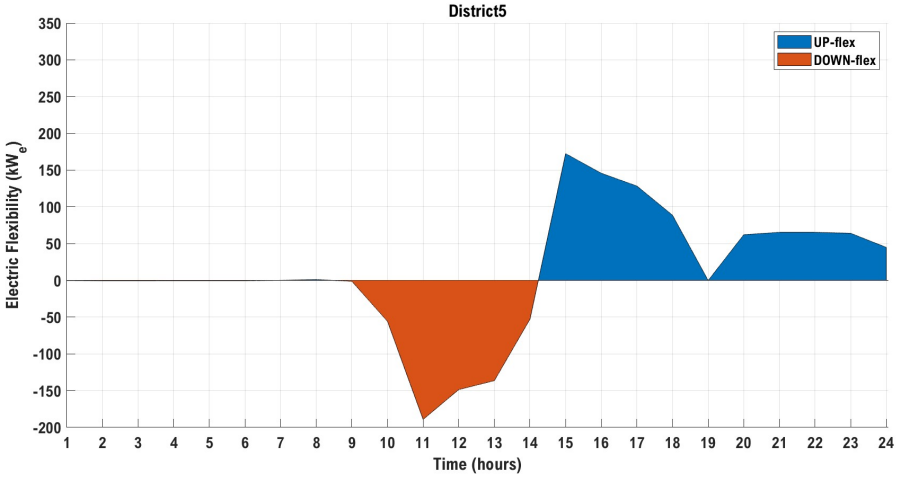

Fig. 4.36 *Strategy #2* - Operational electrical flexibility made available by District 5.

The operational flexibility provided by the two districts differs significantly, especially in terms of magnitude, coherently with the previously presented electrical profiles. Indeed, District 5 offers a total of 816.37 kWh in UP-flex and 586.26 kWh in DOWN-flex in the reference day, whereas District 2 provides 1186.20 kWh and 882 kWh, respectively. Considering the overall district heating system, with this strategy residential districts are the ones unlocking greater flexibility resources, presenting higher values of available energy despite the lower installed power.

Concerning District 6, comments similar to those of Strategy #1 can be made. In fact, the system configuration mirrors that of the *Baseline*, so there is no need to re-heat the water to serve the district's users. Consequently, quantifying the magnitude of electric flexibility indicators at district level becomes unfeasible. However, the alteration in thermal profiles (depicted in Figure 4.37) is reflected, along with other components (i.e., other districts modifications and network effects), in the electrical flexibility available at the thermal power plant level.

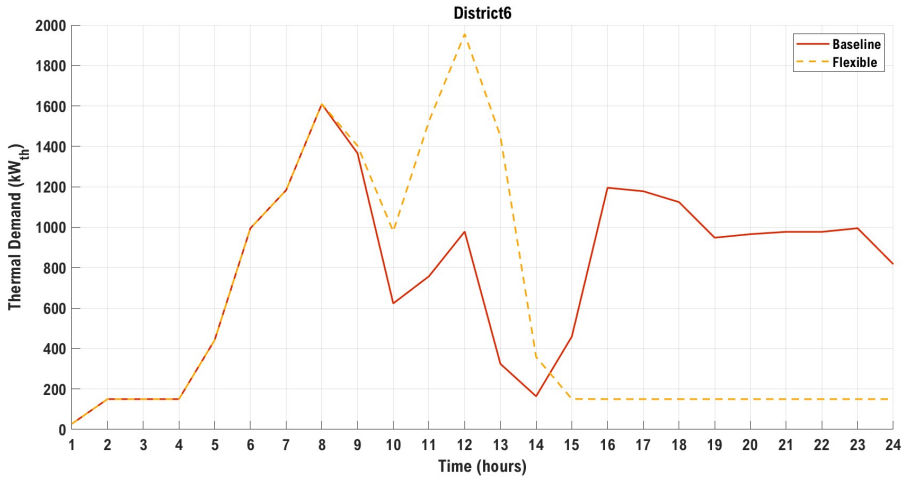

Fig. 4.37 *Strategy #2* - Thermal demand modification for District 6.

Figure 4.38 illustrates the electric consumption trend for the main thermal power plant for *Baseline* and Strategy #2 scenarios, while Figure 4.39 represents the flexibility indicators.

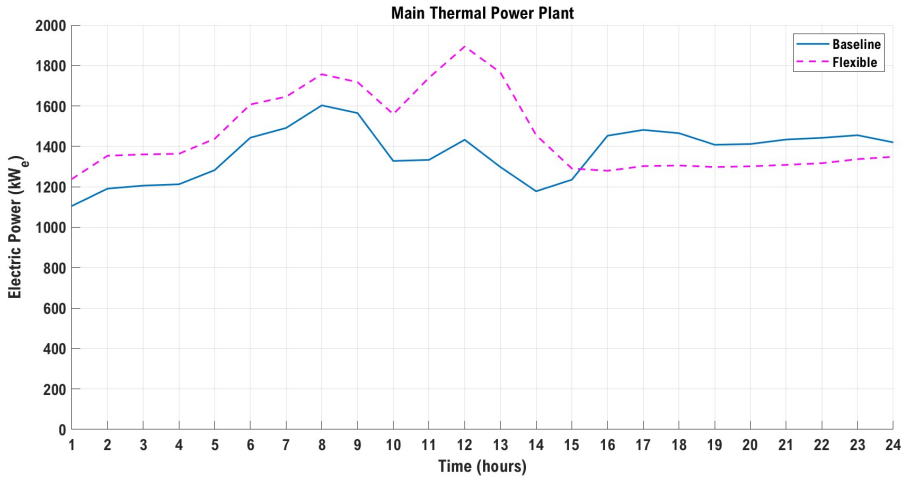

Fig. 4.38 *Strategy #2* - Electrical power absorbed by heat pumps in in the main thermal plant.

The increased electrical energy absorption by the heat pump in the central thermal unit in the time slot before 10:00 is due to the variation in return temperature compared to the *Baseline*. Indeed, as explained earlier, the heat pump's performance varies depending on the temperature at the condenser inlet and the evaporator outlet. This variance in return temperature is not solely attributed to a slight fluctuation in the thermal load of District 6 during the early hours but also encompasses variations induced by district substations across Districts 1 to 5. Furthermore, thermal losses along the subterranean pipes exacerbate the overall temperature shifts. The different electrical absorption results in the availability of flexibility represented in Figure 4.39.

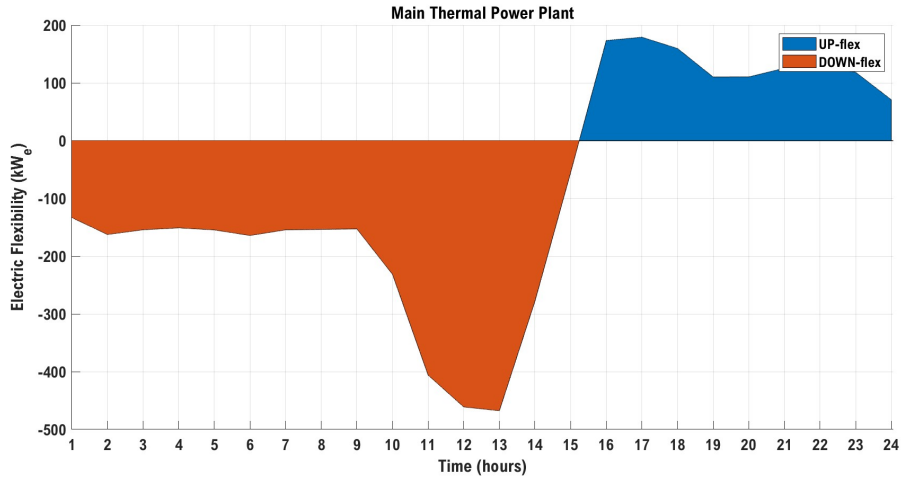

Fig. 4.39 *Strategy #2* - Operational electrical flexibility made available by the main thermal plant.

In conclusion, when looking at the district heating system as a whole, global operational flexibility can be achieved by summing all contributions along the blocks of the system (i.e., main station, Districts form 1 to 5, innovative district D6, thermal network), as depicted in the Figure 4.40.

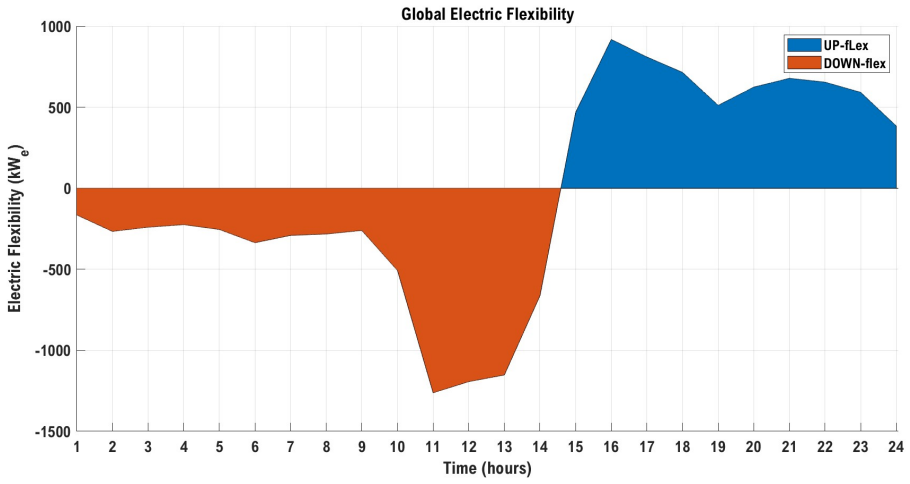

Fig. 4.40 *Strategy #2* - Total operational electric flexibility of the fifth-generation district heating system.

Globally, Strategy #2 allows to offer in the reference day 6169 kWh for upward flexibility and 6868 kWh for downward flexibility.

Financial implications of flexibility

Even if it was not the main external forcing, a study was also conducted for Strategy #2 to assess the potential financial implications of the flexibility intervention. Following the approach applied for Strategy #1, the zonal price for the day-ahead market, relative to 31/01/2023 for the North zone, was taken from the the GME (Figure 4.41). Then the cost of purchasing the electricity necessary to allow the operation of the fifth-generation district heating system in the *Baseline* scenario was calculated C_{Base}.

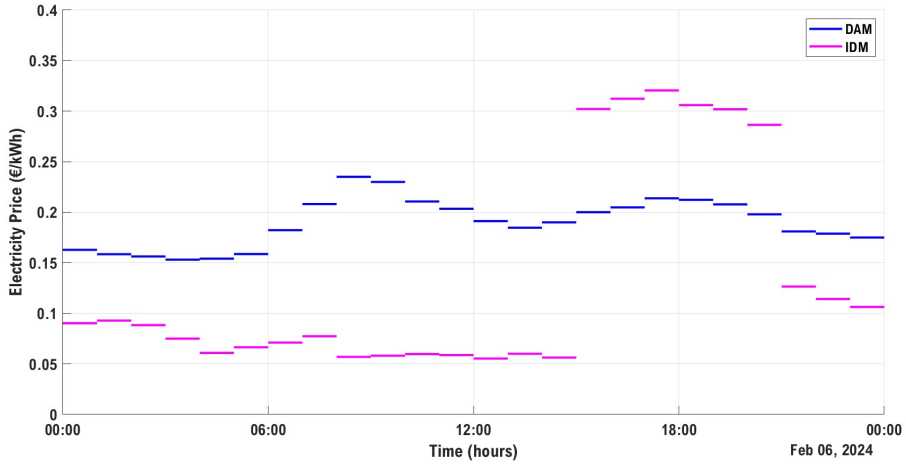

Fig. 4.41 *Strategy #2* - Day-ahead and Intraday zonal prices for the North area.

Subsequently, a daily trend of the zonal price was proposed on the intra-day market (in pink) and the total cost for the flexibility intervention ($C_{total,S2}$) was calculated, represented by the sum of the cost of the Baseline, the cost of purchasing the extra energy during the hours when the PV production is maximum (A_{flex}) and the revenues (R_{flex}) due to the sale of the energy that is no longer used in the remaining part of the day.

Also with this strategy and with the hypothesis of prices of Figure 4.41, the revenues are higher than the purchasing cost, resulting in a lower total cost with respect to the *Baseline* case. The numerical values of financial KPIs are listed in 4.10.

Financial KPIs	Values [€/day]
C_{Base}	31196.82
$C_{total,S2}$	30660.00
A_{flex}	1101.00
R_{flex}	1517.10

Table 4.10 Electricity costs for *Strategy #2*.

Analyzing the comparative KPIs presented in Table 4.11, the $\Delta Cost_{S2}$ stands at 1.72%. While this indicates a saving compared to the base case, it remains relatively small. A significant constraint also for this strategy is the need to adhere to boundary conditions related to internal temperature of buildings, limiting the potential for altering thermal profiles and subsequent electrical absorption.

Financial KPIs	Values
$\Delta Cost_{S2}$	1.72%
$Profit_{S2}$	27.42%

Table 4.11 Costs comparison for *Strategy #2*.

However, focusing solely on flexible interventions, despite an additional expenditure of 1101 €, it provokes a remuneration of 1517 € that would not have otherwise materialized, yielding a profit indicator of 27.42%.

4.5 Conclusions

To answer research question RQ 4: "*How can flexibility be introduced into an all-electric district heating system incorporating heat pumps?*", Application #2 was developed. It is composed of a low-temperature fifth-generation district heating system (T_{supply} = 40°C) with a decentralized layout and heat pumps in thermal power station and district substations. It is an all-electric solution which allows, if coupled with electricity produced from renewable sources, to follow the direction imposed by the European Union with the Energy Efficiency Directive (EED of 2023) [46], which requires efficient district heating by 2050 with 100% of the heat produced by

renewable sources or waste heat.
From Kleinschmidt's classification of the sources of flexibility they can be divided into three categories: conversion, storage and demand-side management [55]. Application #1 was responsible for investigating the flexibility available thanks to the conversion technologies installed in the thermal power plant of the case study. As regards the all-electric system composed only of heat pumps, this was not possible, since without any other backup technology, the generation system results non-flexible. However, it is possible to make it flexible by taking advantage of the great potential of buildings, capable of acting as thermal storage for a short interval of time, allowing the necessary variation in the demand for thermal energy compared to a *Baseline* case. By employing the heat pump technology it is possible to transform the thermal flexibility made available by flexible buildings into electrical flexibility. Therefore, the answer to RQ 4 is that, by exploiting the availability of buildings to modify their thermal load profiles, through demand-side management programs, it is possible to make flexible even all-electric networks with only heat pump systems.
To study the flexibility of buildings it was not sufficient to use the monitored load profiles of Application #1 but, to be able to diversify the types of users and directly control the parameters of interest for the analysis, models of residential buildings, offices and malls for different construction periods were created, following the Reference Buildings approach. Energy Plus software was used for the energy modeling and simulation of the buildings and the results were then aggregated to form six user districts.
To constrain on the possibility of modulating the load profiles, it was chosen to control the set-point temperature of the buildings, imposing a maximum deviation of $\pm$ 2°C compared to the *Baseline* set-point, guaranteeing users a class of comfort B, according to [98]. Energy simulations of the buildings were carried out with these boundary conditions, and were then used as input to the overall simulation of the system performed on Simscape. The district heating model and simulator developed in Application #1 was modified to make it compatible with a different district heating generation and this was possible thanks to the versatility and customization of the developed tool.

Finally, two flexibility strategies were tested, not with the aim of proposing new strategies or metrics, but to bring realistic examples of the use of the proposed methodology and show the potentiality of the tool. Strategy #1 proposed the example of a change in user thermal profiles driven by an external economic forcing, i.e. the

greatest convenience of electricity on the intra-day market in a given time interval. Thanks to this example it was possible to extend the considerations relating to flexibility also to the economic field. Assuming a favorable trend in the cost of energy on IDM, it was also possible to estimate, using indicators, a financial convenience given by the flexibility event. Strategy #2 was suggested for assessing the system's response to another external signal, specifically the presence of electricity generated by a photovoltaic plant in the middle of the day. The heat pumps were therefore allowed to absorb more electricity from the grid during the hours of greatest photovoltaic production, to maximize consumption from renewable sources. Also in this case, a financial analysis was conducted in parallel to verify the potential economic convenience of the proposed strategy.

As for Application #1, the created simulator gave the the possibility of identifying thermal and electrical profiles and, through integration with a data processing code, it was possible to calculate and show the flexibility of the system. In this case, the developed tool has been used both as a forecasting tool for the purchase of energy on DAM, and in operation for the participation in the IDM.

Moving on to financial indicators, of particular interest is the $\Delta Cost_{Sx}$. In both proposed strategies, it is always positive, this implies an economic advantage of the flexible strategy compared to the baseline, but of the order of 1-2%. This aspect is closely related to the Case Study and the boundary conditions associated with the comfort bands in buildings that have to be respected. Indeed, they represent a constraint on the ability to modify load profiles. If there were more flexibility, for example, by turning off the system when users are not at home or not having to maintain a set-back, the energy difference between the two scenarios would become higher, and consequently, the $\Delta Cost_{Sx}$ could be greater. It is noteworthy that, similar to the aforementioned constraint, compliance with internal temperature conditions has posed a substantial limitation in maximizing the potential for modifying thermal profiles and electrical absorption in this strategy as well.

4.5.1 Potential expansions of the work

An interesting challenge from a simulation point of view could be to implement a co-simulation between the building simulation tool and the network/production one, therefore EnergyPlus and Simscape. There is a Simscape tool that allows

co-simulation, but it was not used in the Thesis. The problem should be better investigated, especially in terms of simulation time, linked to the fact of having to simultaneously simulate at least twenty reference buildings and then to aggregate them at district level before they can be used by Simscape. However, it represents an exciting challenge in the perspective of varying the buildings' temperature set-points dynamically based on how the entire system behaves.

Another possible expansion of the Application #2 is to extend the considerations to other services such as district cooling and domestic hot water provision. Concerning the first one, with the increasing average global temperature, there will be a growing demand for cooling environments, both in offices (where systems are generally already in place) and in residential homes. The fifth-generation system proposed in this application is already equipped for the production and delivery of district cooling in terms of technologies at the central and substation levels. However, the focus of the Thesis was on district heating, so the operational and control mechanisms for district cooling services within the network and substations were not thoroughly explored.

Moving to domestic hot water, the topic opens the way to several areas of interest and future explorations. Indeed, from the generation side, considering the DHW service could unlock the spread of solar thermal panels on the building rooftops, and it would be interesting to analyze how the demand and flexibility profiles change in function of the solar resource availability. This topic brings additional challenges, such as investment costs, available space, and resource availability. The same considerations can be applied to thermal storage. It is not guaranteed that the user has the necessary space in the substation for installing the technology and/or the financial capacity to sustain the investment. Both topics will be interesting to evaluate in the continuing of this study. Similarly, the possibility of running simulations for other typical days (e.g. one for month) could provide insight into what happens during the mid-seasons, when heating demand is lower, or during the summer, when there might only be a need for DHW or cooling.

All these considerations will be interesting for future applications to add another pieces to the puzzle and look at the problem from a broader perspective.

Chapter 5

Conclusions

The ongoing energy transition is impacting all sectors of society in response to the effects of climate change. Energy has emerged as a critical issue at both European and global levels, driven by the shared goal of mitigating the rise in Earth's average temperature. Central to this transition is the energy sector itself, encompassing the production, transportation, distribution, and consumption of energy resources. The shift from the traditional model, characterized by centralized systems heavily reliant on fossil fuels, to decentralized configurations featuring robust integration of renewable energy sources is imperative and urgent. This evolution not only signifies a departure from carbon-intensive practices but also heralds a fundamental transformation in the role of energy end-users, from mere passive consumers into active participants. Additionally, the increasing and essential use of RES to achieve decarbonization underscores the importance of flexibility as a prerequisite for every energy system.

The research carried out during my Ph.D. pathway was conducted in this context, focusing on one of the sectors considered as a possible driver to reach the post-carbon society: the district heating. Indeed, heating buildings represents one of the primary sectors contributing to greenhouse gas emissions. District heating systems can be defined as multi-vector energy integrated networks as they use different energy carriers to provide heat to end users. In line with this, the Thesis tackled these themes, with the final objective of evaluating and quantifying flexibility in a multi-vector energy network.

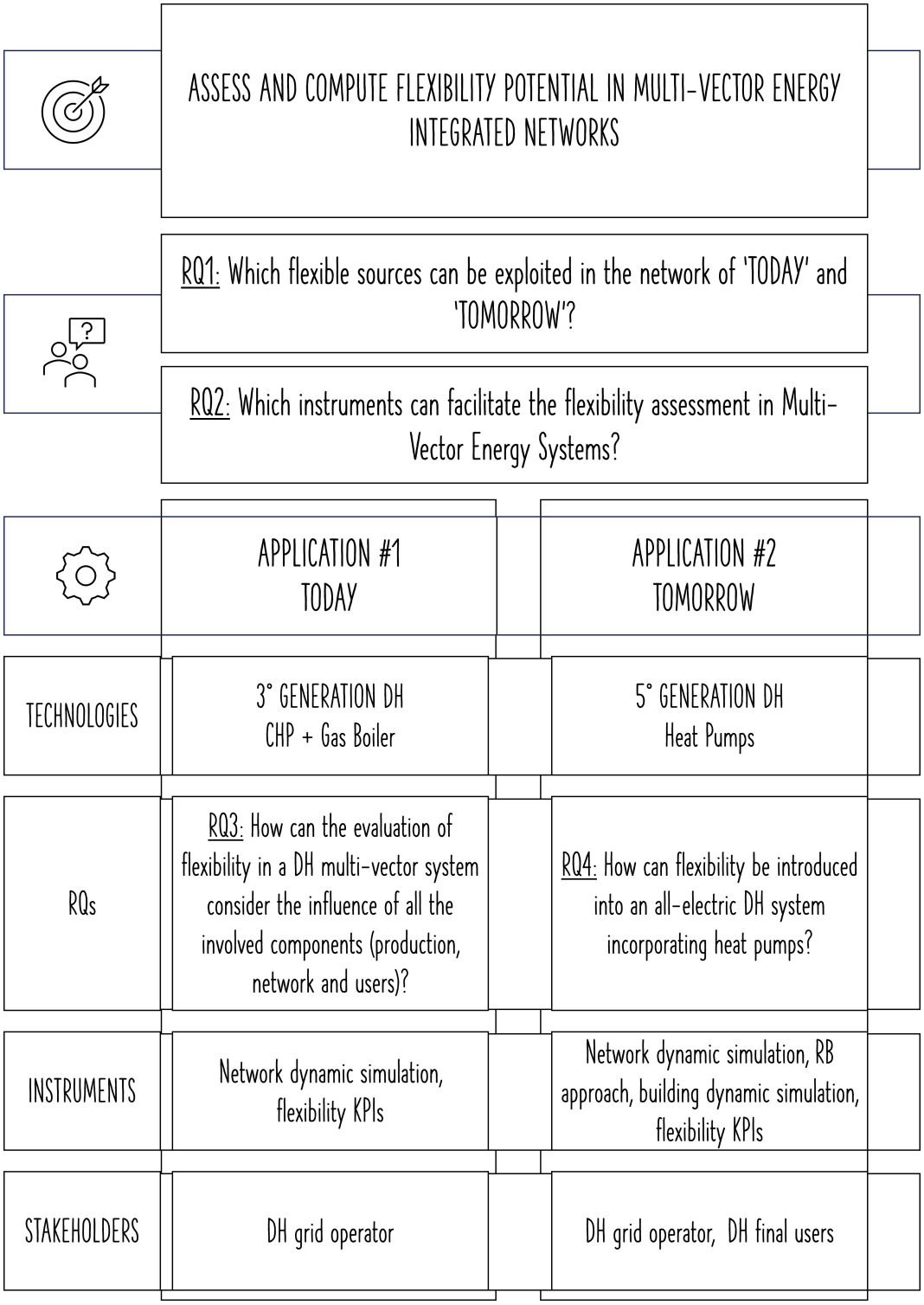

Fig. 5.1 Graphical summary of the research.

To summarize the journey undertaken in these three years of Ph.D. studies, it may be helpful to examine Figure 5.1. The image recalls the one found in Chapter 1, adding to the previously described aspects, also new information. It encapsulates the motivations and questions that propelled and sustained the research, along with the analyzed applications (as shown in Figure 1.2), while the tools used, and the stakeholders potentially interested in the work done are added. This image thus provides an overall and comprehensive framework of the research. Referring back to the initial puzzle metaphor, everything originated from the first puzzle piece, which encompassed the need to quantify flexibility in a multi-vector system as district heating is. This led to the formulation of two overarching research questions, indicated in the figure as RQ 1 and RQ 2. To answer these general questions, a methodology was initially developed and elaborated in Chapter 2. The methodology aimed to facilitate the calculation of flexibility and the evaluation not only by means of energy metrics but also through economic indicators. Secondly, two applications were created. The first one relates to a third-generation fossil fuel district heating, to explore an example of a "DH of today", the second one deals with a fifth-generation system with heat pumps as an example of a "DH of the future". The implementation of these two case studies raised additional research questions (RQ 3 and RQ 4) which were answered in Chapters 3 and 4, then, piece by piece, answers were achieved even to the two cross-sectoral questions.

Starting from the punctual research questions, RQ 3 concerns "*How can the evaluation of flexibility in a district heating integrated system consider the influence of all the involved components, including the network?*".
Briefly reviewing the outputs of the Application #1, it was demonstrated how the dynamic simulation of the district heating network is a fundamental instrument not only for calculating flexibility, but also for verifying the functioning of the network through the sub-hourly visualization of some reference quantities (e.g., temperature, pressure and flow rate along the pipes). The use of energy simulation, unlike other approaches such as energy hubs that mainly deal with conversion technologies, allows also the dynamics of the water flowing along the pipes to be taken into consideration, enabling the identification of more accurate physical constraints that can limit the supply of flexibility, identifying the flexibility margins with greater precision.

Then, moving to RQ 4, it states: "*How can flexibility be introduced into an all-electric district heating system incorporating heat pumps?*". This question arises

from the fact that the heat pump is increasingly used as a technology for individual HVAC systems in buildings, especially thanks to its reversibility which allows its use even in the summer season. Thanks to these characteristics, the application of these electrical technologies is being studied for installation in networks of the future, both at centralized level and at district substation. However, heat pumps have the particularity of being demand-oriented technologies which therefore produce heat only in the presence of thermal demand. Thus, it is not possible to provide flexibility in a system composed only of these conversion technologies. In Application #2, it was studied, in a fifth-generation DH with heat pumps, how Demand-Side Management can also be exploited on users' thermal loads. By varying the consumption according to external forcing (i.e., advantageous prices on intra-day market or presence of renewables at certain hours of the day) it was possible to modify the electrical absorption of the heat pumps to follow the load, providing upward or downward flexibility to the electric grid. Thanks to the simulation model developed in Application #1, it was possible to quantify and graphically visualize the available flexibility.

Building on this response, it is appropriate to expand the discussion to address RQ 1: "*Which flexible sources can be exploited in the network of 'TODAY' and 'TOMORROW'?*". Following Kleinshmidt's classification [55], forms of flexibility can be divided into three categories: conversion, storage and demand-side management. Nowadays, most of the existing district heating networks are third-generation and use natural gas as their main source to serve combined cycle plants. For these types of networks, electrical flexibility can be obtained mainly on the supply-side, with the same heat demand of the users, by intervening on the regulation of the conversion technologies. An example could be to operate the CHP in electric-only mode at certain times of the day, if the technological mix installed still allows the heating service to be guaranteed to users. Most of the conversion technologies currently used in district heating are suitable for "conversion" flexibility (e.g., gas or biomass CHPs and boilers). Application #1 focused on exploring the flexibility facilitated by the conversion technologies integrated into the thermal power plant of the case study. However, as previously mentioned in Application #2, not all conversion technologies are independent of users' thermal demand requirements, such as heat pumps. Given that to facilitate decarbonization and achieve the goals set at the European level, there will be a shift towards electrification of thermal uses the installation of heat pumps as heat production systems for district heating systems will be increasingly widespread. For these networks it will not be possible to provide flexibility to the electricity

network with the same thermal demand, therefore demand-side management actions will have to be carried out aimed at modifying the thermal profiles that allow the modification of the electrical absorption of the heat pumps. Much of the possibility of having flexibility in the networks of the future will depend on the ability to engage consumers who will have to accept (against adequate compensation) to make the heat supply modifiable on request. There is therefore a need to develop new and adequate business models.
Finally, the only aspect not considered during the Thesis was the potential to obtain flexibility through the use of storages. The various electrical and thermal storage technologies available on the market enable a wide range of applications. Thanks to the different sizes, they can lead to installations on several scales, from the main thermal power plant, to district substations, to individual building use. In all cases, the presence of storage allows for the temporal decoupling of energy production and consumption, for example, enabling the storage of energy produced from renewable sources when available and mitigating unexpected changes in heat requests without causing unforeseen fluctuations to the grid. Therefore, it appears clear the significant potential for flexibility provision that could be obtained by also leveraging storage. One of the future goals of the working group that accompanied me during the Ph.D. pathway could be to analyze and simulate this aspect as well, and in addition attempting to combine a simulation that takes into account all three sources of flexibility.

To conclude, RQ 2 must be answered:"*Which instruments can facilitate the flexibility assessment in Multi-Vector Energy Systems?*". As seen partially in response to RQ 3, one of the fundamental tools for the proper evaluation of the problem is dynamic simulation. Starting from the definition of the methodological framework, it emerged clearly the need for a simulation-based methodology. During the Thesis, a great modeling and simulation effort was carried out, firstly to determine the level of detail necessary for the simulations to be accurate but at the same time quick, secondly to identify or create the simulation blocks of all the elements necessary, containing the appropriate physical equations. In Application #1 the simulation effort regarded only the dynamic simulation of the heat production system and the network, using thermal, energy and hydraulic equations. The thermal demand was instead elaborated from monitoring data and considered "passive" during the calculation interval. In Application #2, however, the importance of dynamic simulation also on the demand-side was demonstrated, since it allows to obtain results with hourly

and sub-hourly intervals and ensure to manage the different variables that influence the potential flexibility that can be provided (e.g., set-point temperatures) through demand management. The choice of the appropriate tool for simulations is also of fundamental importance. In detail, for the simulation of thermal demand EnergyPlus was used which allowed the simulation of Reference Buildings whose geometric, construction, thermophysical and use characteristics were known. Instead, for the production and network sides, the Simscape software was used, being suitable because it is able to simulate different energy vectors (i.e., gas, thermal, electric) and being from the Matlab package it makes the simulation outputs easily usable in codes always developed in Matlab for flexibility calculation. In fact, the results of the simulations must then be reprocessed and compared to calculate the differences between the *Baseline* and *Flexible* scenarios, calculate the significant indicators and make a graphical display of the results available. For instance, in Application #2, the proposed simulator gave the possibility for identifying thermal and electrical consumption profiles. By integrating it with a data processing code developed in Matlab, the flexibility of the system could be calculated and shown. The developed tool was used both as a forecasting tool for the purchase of energy on DAM (*Baseline* scenario), as well as in operation for participating in the IDM (*Flexible* scenario). In line with this, other necessary instruments for flexibility assessment are the flexibility KPIs. In detail, physical, operational and cross-carrier flexibility indicators were computed, together with other significant metrics as, for example, the peak reduction. But not only energy is important in this evauations, therefore the lens was shifted towards the financial sphere, proposing also financial KPIs. Finally, it is necessary to make this information accessible to the interested stakeholders (e.g., final consumers or DH grid operators), therefore a clear representation of the data, possibly also graphic (e.g., area graphs for UP-flex and DOWN-flex indicators) were developed in the analysis.

Ultimately, to translate these discussions into action and implementation (for the puzzle to be framed), it is imperative to develop customized business models that enable and incentivize flexibility interventions. Proposing business and market models aimed at enhancing flexibility within the district heating context, aimed not only at leveraging the electrical flexibility made available to the grid but also the internally managed thermal flexibility, could serve as a starting point for future work of the research group.

Nomenclature

A: inlet port
A_{flex}: purchasing cost for the flexibility intervention [€]
B: outlet port
Base: as subscript, related to the Baseline scenario
C_{Base}: Baseline electricity cost [€]
C_{DSM}: cost associated to DSM [€]
c_p: water specific heat (assumed constant and equal to 4.186 kJ/(kgK))
C_p: purchase cost [€/kWh]
CHP: Combined Heat and Power
Cond: condenser
COP: Coefficient of Performance [-]
C_{DSM}: total daily cost for the DH operator [€]
D: pipe diameter [m]
DAM: Day-Ahead Market
DDS: Deviation from Distribution Supply newtwork
$\Delta Cost_{Sx}$: delta between Baseline and Flexible Costs [%]
DH: District Heating
d_i: i-th installed device
DHW: Domestic Hot Water
DMES: Distributed Multi-Energy System
DOWN-flex: downward flexibility
D_x: x-th district (from 1 to 6)
E: energy [kWh]
E+: EnergyPlus software
E_{Base}: Energy consumption profile of the *Baseline* scenario [kWh]
EED: Energy Efficiency Directive

EER: Energy Efficiency Ratio [-]
E_{Flex}: Energy consumption profile after flexibility action in the *Flexible* scenario [kWh]
EPBD: Energy Performance of Buildings Directive
EU: European Union
Eva: evaporator
$F_{op,U}/F_{op,DOWN}$: UP-flex and DOWN-flex indicators [kW]
$F_{ph,d}$: Physical flexibility indicator [kW]
F_{UP_CC}/F_{DOWN_CC}: cross-carrier UP- and DOWN-flex indicators [kW]
Flex: as subscript, related to the Flexibility scenarios
GB: Gas Boiler
GHG: Greenhouse Gas
GWSHP: Groundwater Source Heat Pump
HP: Heat Pump
HVAC: Heating, Ventilation and Air Conditioning
HX: Heat Exchanger
HX_{L-L}: System-Level Heat Exchanger
IDM: Intra-Day Market
IWEC: International Weather Energy Calculations
k: thermal conductivity of the fluid [W/mK]
k_{HX}: pressure loss coefficient for heat exchangers
KPI: Key Performance Indicator
$\dot{m}$: water mass flow rate [kg/s]
MDS: Main Distribution Supply network
MEN: Multi-Energy Network
MES: Multi-Energy System
MFH: Multi-Family House
MVES: Multi-Vector Energy System
p: water pressures [Pa]
$P_{base,d}$: baseline operation point [kW]
$P_{max,d}/P_{min,d}$: maximum and minimum allowed power modulation [kW]
ϕ: energy flow rates, entering the A port and exiting the B port [kW]
Pr_s: zonal selling price [€/kWh]
PS: Power Station
Q_{conv}: convective power associated to a non-zero water flow [kW]

Q_e : electric power [kW]
Q_H: power exchanged between the pipe outside layer and the environment [kW]
Q_p: isentropic compression power [kW]
Q_u : thermal power provided to the final user [kW]
R_{flex}: daily remuneration cost [€]
RB: Reference Building
RED II: Renewable Energy Directive
RES: Renewable Energy Sources
ρ: density of the fluid [kg/m^3]
RQ: Research Question
S_H: tube lateral surface [m^2]
SB: Set-Back temperature [°C]
SC: Space Cooling
SFH: Single-Family House
SH: Space Heating
$\sigma_d^{v1,v2}$: conversion factor that transform one vector in the other
SP: Set-Point temperature [°C]
T: water temperatures [K]
T_H: tube temperature [K]
TABULA: Typology Approach for Building Stock Energy Assessment
TH: terraced-house
U.S. DOE: Department of Energy of the United States
U_i: i-th user
ULTDH: Ultra-Low Temperature District Heating
UP-flex: upward flexibility
V: volume of the water in the pipe [m^3]
v_j: j-th energy vector
WH: Waste Heat

References

[1] E. Corsetti, V. Casamassima, A. La Bella, and I. Abbà. Valutazione della flessibilità di sistemi multienergetici. *Ricerca sul Sistema Energetico (RSE). RdS report n. 21010810*, 2021.

[2] F. Bianchi, E. Corsetti, and I. Abbà. Analisi preliminare del potenziale di flessibilità dei carichi elettrici e approcci per l'aggregazione. *Ricerca sul Sistema Energetico (RSE). RdS report n. 22013969*, 2022.

[3] Andreis C. Corsetti E. Lazzari R. Muro Alvarado M.A. Abbà, I. Sistemi multi-energetici: sviluppo di modelli, architetture di controllo e impianti sperimentali per la validazione per reti calore. ricerca sul sistema energetico (rse). *Ricerca sul Sistema Energetico (RSE), RdS Report n. 23013281*, 2023.

[4] B. D. Solomon and K. Krishna. The coming sustainable energy transition: History, strategies, and outlook. *Energy Policy*, 39(11):7422–7431, 2011.

[5] P. Hanlon, S. Carlisle, M. Hannah, A. Lyon, and D. Reilly. A perspective on the future public health: an integrative and ecological framework. *Perspectives in Public Health*, 132(6):313–319, 2012.

[6] A. Kläy, A. B. Zimmermann, and F. Schneider. Rethinking science for sustainable development: Reflexive interaction for a paradigm transformation. *Futures*, 65:72–85, 2015.

[7] I. Fazey, P. Moug, S. Allen, K. Beckmann, D. Blackwood, M. Bonaventura, K. Burnett, M. Danson, R. Falconer, A. S. Gagnon, et al. Transformation in a changing climate: a research agenda. *Climate and Development*, 10(3):197–217, 2018.

[8] I. Fazey, N. Schäpke, G. Caniglia, J. Patterson, J. Hultman, B. Van Mierlo, F. Säwe, A. Wiek, J. Wittmayer, P. Aldunce, et al. Ten essentials for action-oriented and second order energy transitions, transformations and climate change research. *Energy Research & Social Science*, 40:54–70, 2018.

[9] United Nations Framework Convention on Climate Change (UNFCCC). Cop24. the paris agreement, 2018. https://unfccc.int/process-and-meetings/the-paris-agreement.

[10] United Nations Framework Convention on Climate Change (UNFCCC). Cop24. conference of the parties in katowice, 2018. https://unfccc.int/event/cop-24.

[11] United Nations Framework Convention on Climate Change (UNFCCC). Cop24. conference of the parties in glasgow, 2021. https://unfccc.int/event/cop-27.

[12] United Nations Framework Convention on Climate Change (UNFCCC). Cop24. conference of the parties in dubai, 2023. https://unfccc.int/event/cop-28.

[13] TERNA. La transizione energetica. https://lightbox.terna.it/it/transizione/transizione-energetica/.

[14] I. Abbá, A. La Bella, S. P. Corgnati, and E. Corsetti. Assessing flexibility in networked multi-energy systems: A modelling and simulation-based approach. *Energy Reports*, 11:384–393, 2024.

[15] S. Long, O. Marjanovic, and A. Parisio. Generalised control-oriented modelling framework for multi-energy systems. *Applied Energy*, 235:320–331, 2 2019.

[16] M. Yuan, J. Zinck Thellufsen, H. Lund, and Y. Liang. The electrification of transportation in energy transition. *Energy*, 236:121564, 12 2021.

[17] F. Neirotti, M. Noussan, and M. Simonetti. Towards the electrification of buildings heating - real heat pumps electricity mixes based on high resolution operational profiles. *Energy*, 195:116974, 3 2020.

[18] A. La Bella, A. Falsone, D. Ioli, M. Prandini, and R. Scattolini. A mixed-integer distributed approach to prosumers aggregation for providing balancing services. *International Journal of Electrical Power and Energy Systems*, 133:107228, 12 2021.

[19] A. Turk, Q. Wu, M. Zhang, and J. Østergaard. Day-ahead stochastic scheduling of integrated multi-energy system for flexibility synergy and uncertainty balancing. *Energy*, 196, 2020.

[20] H. Kondziella and T. Bruckner. Flexibility requirements of renewable energy based electricity systems – a review of research results and methodologies. *Renewable and Sustainable Energy Reviews*, 53:10–22, 1 2016.

[21] P. Mancarella. Mes (multi-energy systems): An overview of concepts and evaluation models. *Energy*, 65:1–17, 2 2014.

[22] L. Bartolucci, S. Cordiner, V. Mulone, S. Pasquale, and A. Sbarra. Design and management strategies for low emission building-scale multi energy systems. *Energy*, 239:122160, 1 2022.

[23] I. Abbá and A. La Bella. Overview of multi-energy systems. *REHVA Journal*, pages 10–14, 2022.

[24] D. Balakrishnan, A. B. Haney, and J. Meuer. What a mes(s)! a bibliometric analysis of the evolution of research on multi-energy systems. *Electrical Engineering*, 98:369–374, 12 2016.

[25] G. Onen, P. S.and Mokryani and R.H.A. Zubo. Planning of multi-vector energy systems with high penetration of renewable energy source: A comprehensive review. *Energies*, 15(15):5717, 2022.

[26] E. Guelpa, A. Bischi, V. Verda, M. Chertkov, and H. Lund. Towards future infrastructures for sustainable multi-energy systems: A review. *Energy*, 184:2–21, 10 2019.

[27] O. Kraan, E. Chappin, G. J. Kramer, and I. Nikolic. The influence of the energy transition on the significance of key energy metrics. *Renewable and sustainable energy reviews*, 111:215–223, 2019.

[28] G. Crespi, I. Abba, and S.P. Corgnati. Innovative metrics to evaluate hvac systems performances for meeting contemporary loads in buildings. *Energy Reports*, 8:9221–9231, 2022.

[29] K. Witkowski, P. Haering, S. Seidelt, and N. Pini. Role of thermal technologies for enhancing flexibility in multi-energy systems through sector coupling: technical suitability and expected developments. *IET Energy Systems Integration*, 2(2):69–79, 2020.

[30] A. La Bella, A. Del Corno, and A. Scaburri. Data-driven modelling and optimal management of district heating networks. Institute of Electrical and Electronics Engineers Inc., 2021.

[31] A. Arteconi. An overview about criticalities in the modelling of multi-sector and multi-energy systems. *Environments - MDPI*, 5:1–10, 2018.

[32] P. Mancarella, G. Andersson, J. A. Peças-Lopes, and K. R.W. Bell. Modelling of integrated multi-energy systems: Drivers, requirements, and opportunities. Institute of Electrical and Electronics Engineers Inc., 8 2016.

[33] European Union's Horizon 2020 research and innovation programme. Magnitude european project. https://www.magnitude-project.eu/.

[34] European Union. Senergy nets european project. https://senergynets.eu/.

[35] European Parliament and Council. Fit for 55. 2022.

[36] European Parliament and Council. European green deal. 2022.

[37] Y. Zhang, P. Johansson, and A. S. Kalagasidis. Assessment of district heating and cooling systems transition with respect to future changes in demand profiles and renewable energy supplies. *Energy Conversion and Management*, 268:116038, 2022.

[38] F. Calise, F. L. Cappiello, L. Cimmino, M. Dentice d'Accadia, and M. Vicidomini. A comparative thermoeconomic analysis of fourth generation and fifth generation district heating and cooling networks. *Energy*, 284:128561, 2023.

[39] H. Lund, S. Werner, R. Wiltshire, S. Svendsen, J. E. Thorsen, F. Hvelplund, and B. V. Mathiesen. 4^{th} generation district heating (4gdh): Integrating smart thermal grids into future sustainable energy systems. *Energy*, 68:1–11, 2014.

[40] K. Askeland, K. N. Bozhkova, and P. Sorknaes. Balancing europe: Can district heating affect the flexibility potential of norwegian hydropower resources? *Renewable energy*, 141:646–656, 2019.

[41] A. Arabkoohsar and A. S. Alsagri. A new generation of district heating system with neighborhood-scale heat pumps and advanced pipes, a solution for future renewable-based energy systems. *Energy*, 193:116781, 2020.

[42] M. Bilardo, F. Sandrone, G. Zanzottera, and E. Fabrizio. Modelling a fifth-generation bidirectional low temperature district heating and cooling (5gdhc) network for nearly zero energy district (nzed). *Energy Reports*, 7:8390–8405, 2021.

[43] H. Golmohamadi and K. G. Larsen. Economic heat control of mixing loop for residential buildings supplied by low-temperature district heating. *Journal of Building Engineering*, 46:103286, 2022.

[44] H. Lund, P. A. Østergaard, M. Chang, S. Werner, S. Svendsen, P. Sorknæs, J. E. Thorsen, F. Hvelplund, B. O. G. Mortensen, B. V. Mathiesen, et al. The status of 4th generation district heating: Research and results. *Energy*, 164:147–159, 2018.

[45] European Parliament and Council. Directive (eu) 2018/2001 of the european parliament and of the council of 11 december 2018 on the promotion of the use of energy from renewable sources (recast). 2018.

[46] European Parliament and Council. Directive (eu) 2023/1791 of the european parliament and of the council of 13 september 2023 on energy efficiency and amending regulation (eu) 2023/955 (recast). 2023.

[47] K. Lygnerud, T. Popovic, S. Schultze, and H. K. Støchkel. District heating in the future-thoughts on the business model. *Energy*, 278:127714, 2023.

[48] International Energy Agency. International energy agency, district heating needs flexibility to navigate the energy transition, iea, paris. https://www.iea.org/commentaries/district-heating-needs-flexibility-to-navigate-the-energy-transition. 2019.

[49] O. M. Babatunde, J. L. Munda, and Y. Hamam. Power system flexibility: A review. *Energy Reports*, 6:101–106, 2020.

[50] M. Lechl, T. Fürmann, H. de Meer, and A. Weidlich. A review of models for energy system flexibility requirements and potentials using the new flexblox taxonomy. *Renewable and Sustainable Energy Reviews*, 184:113570, 2023.

[51] A. Ulbig and G. Andersson. Analyzing operational flexibility of electric power systems. *International Journal of Electrical Power and Energy Systems*, 72:155–164, 11 2015.

[52] G. Mavromatidis, K. Orehounig, L. A. Bollinger, M. Hohmann, J. F. Marquant, S. Miglani, B. Morvaj, P. Murray, C. Waibel, D. Wang, and J. Carmeliet. Ten questions concerning modeling of distributed multi-energy systems. *Building and Environment*, 165:106372, 11 2019.

[53] G. Chicco, S.q Riaz, A. Mazza, and P. Mancarella. Flexibility from distributed multienergy systems. *Proceedings of the IEEE*, 108:1496–1517, 9 2020.

[54] E. Corsetti, S.q Riaz, M. Riello, and P. Mancarella. Modelling and deploying multi-energy flexibility: The energy lattice framework. *Advances in Applied Energy*, 2:100030, 5 2021.

[55] V. Kleinschmidt, T. Hamacher, V. Perić, and M. Reza Hesamzadeh. Unlocking flexibility in multi-energy systems: A literature review. 2020.

[56] P. D. Lund, J. Lindgren, J. Mikkola, and J. Salpakari. Review of energy system flexibility measures to enable high levels of variable renewable electricity. *Renewable and Sustainable Energy Reviews*, 45:785–807, 5 2015.

[57] Y. V. Makarov, C. Loutan, J. Ma, and P. de Mello. Operational impacts of wind generation on california power systems. *IEEE Transactions on Power Systems*, 24:1039–1050, 2009.

[58] A. Amadeh, Z.y E Lee, and K. M. Zhang. Quantifying demand flexibility of building energy systems under uncertainty. *Energy*, 246:123291, 2022.

[59] G. M. Tina, S. Aneli, and A. Gagliano. Technical and economic analysis of the provision of ancillary services through the flexibility of hvac system in shopping centers. *Energy*, 258:124860, 2022.

[60] I. Vigna, R. Pernetti, W. Pasut, and R. Lollini. New domain for promoting energy efficiency: Energy flexible building cluster. *Sustainable cities and society*, 38:526–533, 2018.

[61] Q. Wang, Y. Ding, X.i Kong, Z. Tian, L. Xu, and Q. He. Load pattern recognition based optimization method for energy flexibility in office buildings. *Energy*, 254:124475, 2022.

[62] I. Vigna, R. Lollini, and R. Pernetti. Assessing the energy flexibility of building clusters under different forcing factors. *Journal of Building Engineering*, 44:102888, 2021.

[63] A. Arteconi, A. Mugnini, and F. Polonara. Energy flexible buildings: A methodology for rating the flexibility performance of buildings with electric heating and cooling systems. *Applied Energy*, 251:113387, 2019.

[64] L.A. Hurtado, J.D. Rhodes, P.H. Nguyen, I.G. Kamphuis, and M.E. Webber. Quantifying demand flexibility based on structural thermal storage and comfort management of non-residential buildings: A comparison between hot and cold climate zones. *Applied energy*, 195:1047–1054, 2017.

[65] R. Yan, J. Wang, S. Huo, J. Zhang, S. Tang, and M. Yang. Comparative study for four technologies on flexibility improvement and renewable energy accommodation of combined heat and power system. *Energy*, 263:126056, 2023.

[66] A. La Bella, F. Bonassi, C. Sandroni, L. Fagiano, and R. Scattolini. A hierarchical approach for balancing service provision by microgrids aggregators. *IFAC-PapersOnLine*, 53:12930–12935, 1 2020.

[67] N. Good and P. Mancarella. Flexibility in multi-energy communities with electrical and thermal storage: A stochastic, robust approach for multi-service demand response. *IEEE Transactions on Smart Grid*, 10(1):503–513, 2017.

[68] Simscape webpage, https://it.mathworks.com/products/simscape.html.

[69] R. Krug, V. Mehrmann, and M. Schmidt. Nonlinear optimization of district heating networks. *Optimization and Engineering*, 22:783–819, 2021.

[70] Z. Li, W. Wu, M. Shahidehpour, J. Wang, and B. Zhang. Combined heat and power dispatch considering pipeline energy storage of district heating network. 7(1):12–22, 2015.

[71] A. La Bella and A. Del Corno. Optimal management and data-based predictive control of district heating systems: The novate milanese experimental case-study. *Control Engineering Practice*, 132:105429, 2023.

[72] I. Abbà, G. Crespi, G. Vergerio, C. Becchio, and S. P. Corgnati. Key performance indicators for decision support in building retrofit planning: An italian case study. *Energies*, 17(3):559, 2024.

[73] CEF TELECOM 2018. Dynamic data analytics services (dydas). project number: 2018-it-ia-0101.

[74] European Parliament and Council. Directive 2010/31/eu of the european parliament and of the council of 19 may 2010 on the energy performance of buildings (epbd recast).

[75] S. P. Corgnati, E. Fabrizio, M. Filippi, and V. Monetti. Livelli di prestazione energetica ottimali per edifici a energia quasi zero: creazione degli edifici di riferimento. *Contributo in Atti di Convegno*, 67, 2012.

[76] V. Corrado, I. Ballarini, and S. P. Corgnati. Building typology brochure–italy. fascicolo sulla tipologia edilizia italiana. nuova edizione. 2014.

[77] Iee project episcope - 2016, https://episcope.eu.

[78] Department of Energy of the United States. Commercial reference building models of the national. Report, NREL; PNNL; LBNL; Energy, United States Department of Energy (DOE).

[79] Istituto nazionale di statistica. Censimento permanente popolazione e abitazioni, https://www.istat.it/it/censimenti-permanenti/popolazione-e-abitazioni.

[80] G. Crespi and E. Bompard. Drivers for energy transition of italian residential sector. *REHVA Journal*, 57(1):6–11, 2020.

[81] E. Bompard, A. Botterud, S. P. Corgnati, P. Leone, S. Mauro, G. Montesano, C. Papa, F. Profumo, D. Grosso, T. Huang, et al. Electrify italy. 2020.

[82] Presidente della Repubblica. Decreto del presidente della repubblica 26 agosto 1993. regolamento recante norme per la progettazione, l'installazione, l'esercizio e la manutenzione degli impianti termici degli edifici ai fini del contenimento dei consumi di energia, in attuazione dell'art. 4, comma 4, della legge 9 gennaio 1991, n. 10.

[83] European Committee for Standardization. Energy performance of buildings – ventilation for buildings. part 1: Indoor environmental input parameters for design and assessment of energy performance of buildings addressing indoor air quality, thermal environment, lighting and acoustics (en16798).

[84] Department of Energy of the United States. Energyplus software.

[85] Ente Nazionale Italiano di Unificazione. Illuminazione di interni residenziali domestici con luce artificiale. (uni/ts 11826).

[86] International Organization for Standardization. Energy performance of buildings — schedule and condition of building, zone and space usage for energy calculation (iso18523).

[87] ENEA. Caratterizzazione del parco edilizio nazionale. determinazione dell'edificio tipo per uso ufficio.

[88] Ministero dello Sviluppo Economico. Aggiornamento del decreto 11 marzo 2008 in materia di riqualificazione energetica degli edifici. 2010.

[89] Ministero dello Sviluppo Economico. Decreto 26 giugno 2015, applicazione delle metodologie di calcolo delle prestazioni energetiche e definizione delle prescrizioni e dei requisiti minimi degli edifici - appendice a. 2015.

[90] Ente Nazionale Italiano di Unificazione. Impianti aeraulici al fine di benessere. generalità, classificazione e requisiti. regole per la richiesta d'offerta, l'offerta, l'ordine e la fornitura (uni 10339). 1995.

[91] European Commitee for Standardisation. Energy performance of buildings - impact of building automation, control and building management. (en1532). 2012.

[92] Cittá di Torino. Geoportale e governo del territorio. http://geoportale.comune.torino.it/web/.

[93] Pederiva G. Thesis on: Sustainable urban district: an assessment process supported by cosima analysis. san salvario district's case. politecnico di torino, 2019.

[94] F. Dell'Anna, G. Pederiva, G. Vergerio, C. Becchio, and M. Bottero. Supporting sustainability projects at neighbourhood scale: Green visions for the san salvario district in turin guided by a combined assessment framework. *Journal of Cleaner Production*, 384:135460, 2023.

[95] N. Rossi. *Manuale del termotecnico. Fondamenti. Riscaldamento. Condizionamento. Refrigerazione*. Hoepli Editore, 2019.

[96] Ministero dello Sviluppo Economico. Decreto unico 13 novembre 2015, strategia per la riqualificazione energetica del parco immobiliare nazionale (strepin).

[97] H. Edtmayer, P. Nageler, R. Heimrath, T. Mach, and C. Hochenauer. Investigation on sector coupling potentials of a 5th generation district heating and cooling network. *Energy*, 230:120836, 2021.

[98] Ente nazionale italiano di unificazione. ergonomia degli ambienti termici - determinazione analitica e interpretazione del benessere termico mediante il calcolo degli indici pmv e ppd e dei criteri di benessere termico locale. (uni 7730:2006). 2006.

[99] Gestore dei Mercati Energetici. Mercato elettrico. https://www.mercatoelettrico.org/it/default.aspx.

Appendix A

In this Appendix, the geometric and stratigraphic data of the reference buildings presented in Section 4.2.1 are reported.

A.0.1 Residential buildings

Geometrical features

Type of building	**Era of construction**	**Number of floors**	**Conditioned area [m^2]**	**Conditioned volume [m^3]**	**Total window surface [m^2]**
MFH	pre-1980	5	912.5	3002.1	121.7
	1981-2000	3	1122.6	3839.3	150.1
	post-2001	3	1122.6	3839.3	150.1
TH	pre-1980	2	115	396.8	25.5
	1981-2000	2	199	724.4	33.2
	post-2001	2	172	602	30.6
SFH	pre-1980	2	115	396.8	30.6
	1981-2000	2	199	724.4	51
	post-2001	2	172	602	45.9

Table A.1 Geometrical features for residential buildings [73].

Stratigraphy of the opaque envelope - MFHs

Construction	**Materials**	**U** $[W/m^2K]$
External wall (in contact with outside)	Lime and cement plaster (15 mm) – hollow bricks (300 mm) – air gap not ventilated (0.18 $m^2 * K/W$) – hollow bricks (300 mm) – gypsum plaster (15 mm)	1.16
Wall to stairs	Lime and cement plaster (20 mm) – hollow bricks (250 mm) – gypsum plaster (20 mm)	1.53
Basement (in contact with the cellar)	Concrete screed (90 mm) – brick slab (250 mm) – gypsum plaster (10 mm)	1.29
Attic (in contact with the roof)	Concrete screed (70 mm) – brick slab (250 mm) – gypsum plaster (10 mm)	1.63
Roof (in contact with outside)	Flat tile (20 mm) – Air gap strongly ventilated (0.09 $m^2 * K/W$) – brick slab (250 mm)	2.22

Table A.2 Stratigraphies for MFHs before 1980 [73].

Construction	**Materials**	**U** $[W/m^2K]$
External wall (in contact with outside)	Lime and cement plaster (15 mm) – expanded polyethylene (40 mm) – hollow bricks (250 mm) – gypsum plaster (15 mm)	0.80
Wall to stairs	Lime and cement plaster (15 mm) – expanded polyethylene (40 mm) – hollow bricks (250 mm) – gypsum plaster (15 mm)	0.80
Basement (in contact with the pilotis)	Concrete screed (90 mm) – expanded polyethylene (10 mm) – brick slab (250 mm)	1.13
Attic (in contact with the roof)	Concrete screed (70 mm) – expanded polyethylene (10 mm) – brick slab (250 mm) – gypsum plaster (10 mm)	0.99
Roof (in contact with outside)	Flat tile (20 mm) – Air gap strongly ventilated (0.09 $m^2 * K/W$) – brick slab (250 mm)	2.22

Table A.3 Stratigraphies for MFHs from 1981 to 2000 [73].

Construction	**Materials**	**U** $[W/m^2K]$
External wall (in contact with outside)	Lime and cement plaster (15 mm) – hollow bricks (300 mm) – expanded polyethylene (40 mm) – air gap not ventilated (0.156 $m^2 * K/W$) – hollow bricks (150 mm) – gypsum plaster (15 mm)	0.59
Wall to stairs	Lime and cement plaster (15 mm) – expanded polyethylene (40 mm) – concrete masonry (300 mm) – gypsum plaster (15 mm)	0.57
Basement (in contact with the pilotis)	Concrete screed (90 mm) – expanded polystyrene (30 mm) – brick slab (250 mm)	0.82
Attic (in contact with the roof)	Concrete screed (70 mm) – expanded polystyrene (40 mm) – brick slab (250 mm) – gypsum plaster (10 mm)	0.70
Roof (in contact with outside)	Flat tile (20 mm) – Air gap strongly ventilated (0.09 $m^2 * K/W$) – brick slab (250 mm)	2.22

Table A.4 Stratigraphies for MFHs after 2001 [73].

Stratigraphy of the transparent envelope - MFHs

Construction period	Type of window	U [W/m^2K]
Before 1980	Single glazing, wooden frame	4.90
1981-2000	Low-emissivity double glazing with air gap and wooden frame	3.70
After 2001	Low-emissivity double glazing with air gap and wooden frame	2.20

Table A.5 Stratigraphies for windows in MFHs [73].

Stratigraphy of the opaque envelope - SFHs and THs

Construction	Materials	U [W/m^2K]
External wall (in contact with outside)	Lime and cement plaster (15 mm) – stone masonry lined with bricks (400 mm) – gypsum plaster (15 mm)	1.64
Basement (in contact with ground)	Concrete base (200 mm)	1.97
Roof (in contact with outside)	Flat tile (20 mm) – Air gap (0.09 $m^2 * K/W$) – wooden plank (150 mm)	1.84

Table A.6 Stratigraphies for SFHs and THs before 1980 [73].

Construction	**Materials**	**U** $[W/m^2K]$
External wall (in contact with outside)	Lime and cement plaster (15 mm) – hollow bricks (400 mm) – expanded polyethylene (10 mm) – hollow bricks (400 mm) – gypsum plaster (15 mm)	0.78
Basement (in contact with the cellar)	Concrete screed (70 mm) – expanded polystyrene (10 mm) – brick slab (250 mm)	0.99
Roof (in contact with outside)	Flat tile (130 mm) – air gap strongly ventilated (0.11 $m^2 * K/W$) – brick slab (240 mm)	1.12

Table A.7 Stratigraphies for SFHs and THs from 1981 to 2000 [73].

Construction	Materials	U $[W/m^2K]$
External wall (in contact with outside)	Lime and cement plaster (15 mm) – expanded polyethylene (40 mm) – hollow bricks (300 mm) – hollow bricks (100 mm) – gypsum plaster (15 mm)	0.60
Basement (in contact with the cellar)	Concrete screed (90 mm) – expanded polystyrene (30 mm) – brick slab (250 mm)	0.78
Attic (in contact with teh roof)	Concrete screed (70 mm) – expanded polystyrene (40 mm) – brick slab (250 mm) – gypsum plaster (10 mm)	0.70
Roof (in contact with outside)	Flat tile (20 mm) – air gap strongly ventilated (0.09 $m^2 * K/W$) – brick slab (250 mm)	2.22

Table A.8 Stratigraphies for SFHs and THs after 2001 [73].

Stratigraphy of the transparent envelope - SFHs and THs

Construction period	Type of window	U $[W/m^2K]$
Before 1980	Single glass (metal frame, no thermal break)	5.70
1981-2000	Double glazing with air gap and wooden frame	2.80
After 2001	Low-emissivity double glazing with air gap and wooden frame	2.20

Table A.9 Stratigraphies for windows in in SFHs and THs [73].

A.0.2 Office buildings

Geometrical features

For office buildings the geometry for the medium-size building was the same for all the construction periods. It is made of a basis of 15 m X 30 m, for a total conditioned area of 2254.8 m^2. The building presents 5 floors with an inter-floor height of 3 m for the construction period pre-1991 and 2.9 m for the other four construction eras. This difference in the height of floors lead to a difference in the conditioned volume, that is 6764.4 m^3 for the first period and 6538.9 m^3 for the others. Data are listed in Table A.10.

Era of construction	**Number of floors**	**Length [m]**	**Depth [m]**	**Height [m]**	**Conditioned area [m^2]**	**Conditioned volume [m^3]**	**Total window surface [m^2]**
pre-1991	5	15	30	3	2254.8	6764.4	595.5
post-1991	5	15	30	2.9	2254.8	6538.9	600.8

Table A.10 Geometrical features for office buildings [73].

Stratigraphy of the opaque envelope

Construction	**Materials**	**U** $[W/m^2K]$
External wall (in contact with outside)	Plaster (25 mm) – hollow bricks (120 mm) – polystyrene (80 mm) – air gap (120 mm) – hollow bricks (80 mm) – plaster (25 mm)	0.97
Basement (in contact with ground)	Floor tiles (20 mm) – mat (30 mm) – semirigid panel (50 mm) – slab (300 mm) – pebbles (180 mm)	0.51
Roof (in contact with outside)	Concrete cladding (30 mm) – mat (30 mm) – semirigid panels (30 mm) – slab (180 mm) – plaster (30 mm)	0.82

Table A.11 Stratigraphies for office buildings from 1972 to 2005 [73].

Construction	Materials	U [W/m^2K]
External wall (in contact with outside)	Plaster (25 mm) – hollow bricks (120 mm) – expanded polystyrene (63 mm) – air gap (120 mm) – hollow bricks (80 mm) – plaster (25 mm)	0.47
Basement (in contact with ground)	Floor tiles (20mm) – mat (30 mm) – semirigid panels (65 mm) – slab (300 mm) – pebbles (180 mm)	0.44
Roof (in contact with outside)	Concrete coating (30 mm) – mat (30 mm) – semirigid panels (81 mm) – slab (180 mm) – plaster (30 mm)	0.43

Table A.12 Stratigraphies for office buildings from 2006 to 2010 [73].

Construction	Materials	U [W/m^2K]
External wall (in contact with outside)	Plaster (25 mm) – hollow bricks (120 mm) – expanded polystyrene (93 mm) – air gap (120 mm) – hollow bricks (80 mm) – plaster (25 mm)	0.35
Basement (in contact with ground)	Floor tiles (20 mm) – mat (30 mm) – semirigid panels (97 mm) – slab (300 mm) – pebbles (180 mm)	0.33
Roof (in contact with outside)	Concrete cladding (30 mm) – mat (30 mm) – semirigid panels (128 mm) – slab (180 mm) – plaster (30 mm)	0.30

Table A.13 Stratigraphies for office buildings from 2011 to 2015 [73].

Construction	Materials	U [W/m^2K]
External wall (in contact with outside)	Plaster (25 mm) – hollow bricks (120 mm) – expanded polystyrene (110 mm) – air gap (120 mm) – hollow bricks (80 mm) – plaster (25 mm)	0.03
Basement (in contact with ground)	Floor tiles (20 mm) – mat (30 mm) – semirigid panels (110 mm) – slab (300 mm) – pebbles (180 mm)	0.31
Roof (in contact with outside)	Concrete coating (30 mm) – mat (30 mm) – semirigid panels (158 mm) – slab (180 mm) – plaster (30 mm)	0.25

Table A.14 Stratigraphies for office buildings after 2016 [73].

Stratigraphy of the transparent envelope

Construction period	Type of window	U [W/m^2K]
1972-2005	Double glazing with aluminum frame	3.94
2006-2010	Double glazing with thermal break	2.80
2011-2015	Double glazing with thermal break	2.20
After 2016	Double glazing with thermal break	1.80

Table A.15 Stratigraphies for windows in office buildings [73].

Appendix B

This Appendix presents the results and graphs of the districts' outcomes that were not shown in Chapter 4.4 to avoid overburdening the reader. In detail, Districts 1, 3 and 4, in terms of electrical absorption profiles and operational flexibility made available are reported for Strategy #1 and Strategy #2.

B.0.1 Strategy #1

District 1

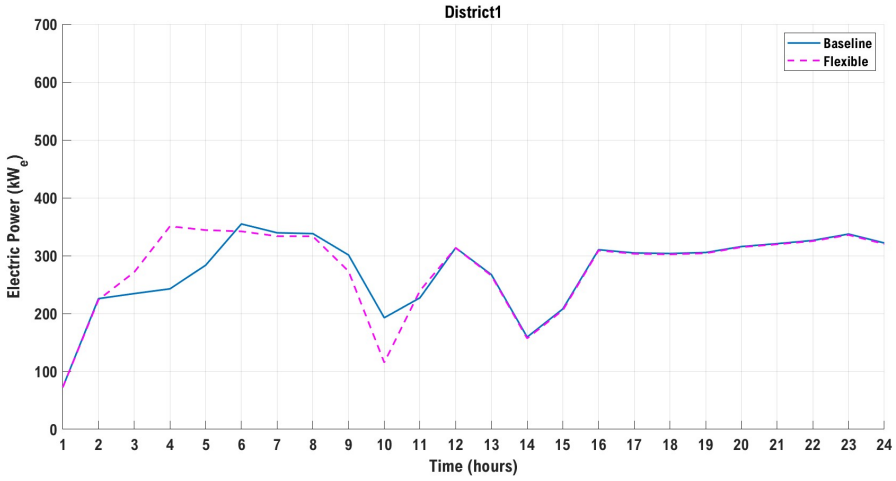

Fig. B.1 *Strategy #1* - Electrical power absorbed by heat pumps in District 1 substation.

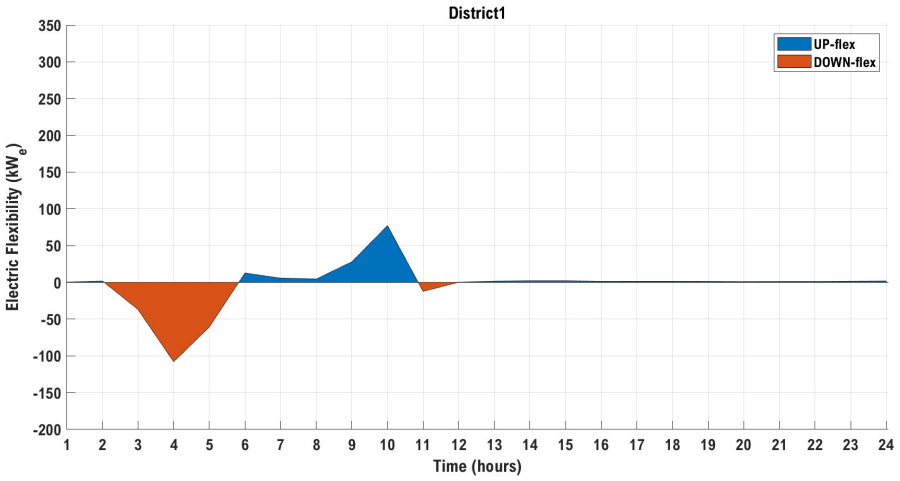

Fig. B.2 *Strategy #1* - Operational electrical flexibility made available by District 1.

District 3

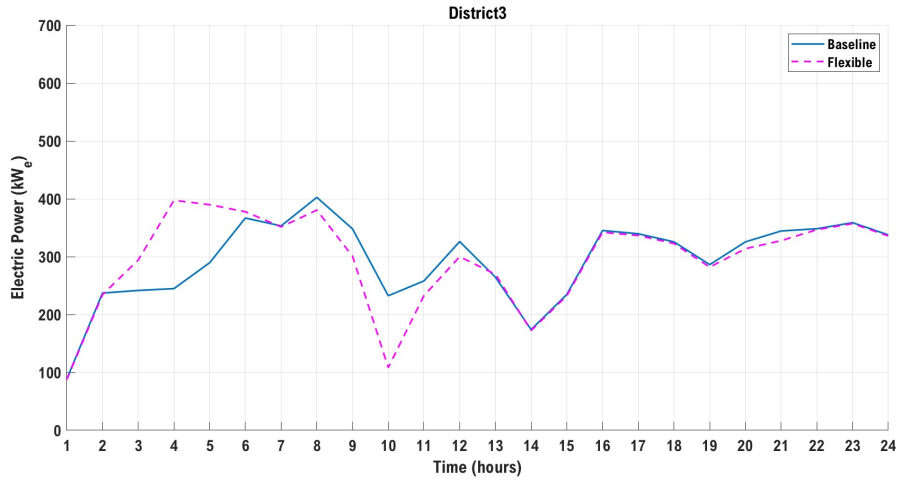

Fig. B.3 *Strategy #1* - Electrical power absorbed by heat pumps in District 3 substation.

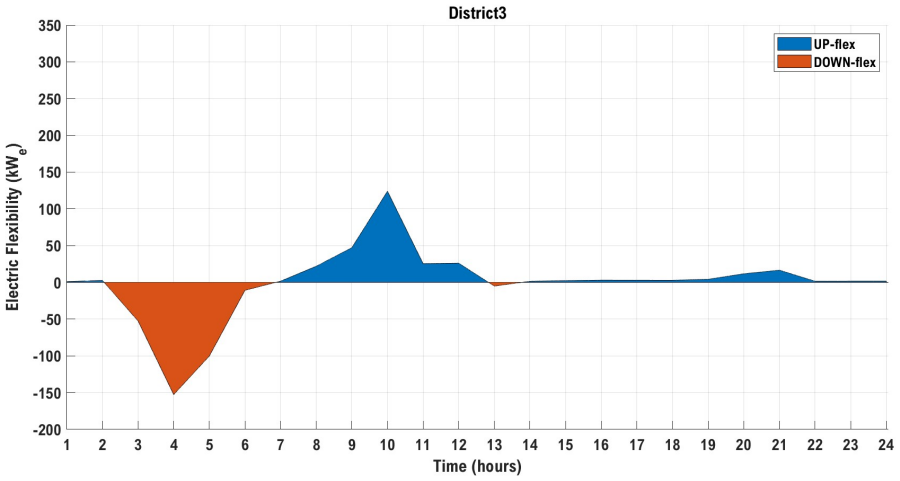

Fig. B.4 *Strategy #1* - Operational electrical flexibility made available by District 3.

District 4

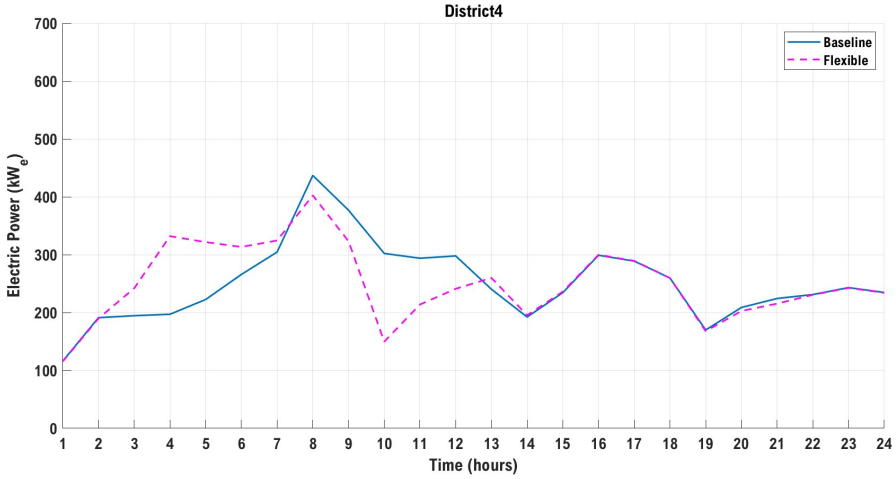

Fig. B.5 *Strategy #1* - Electrical power absorbed by heat pump in District 4 substation.

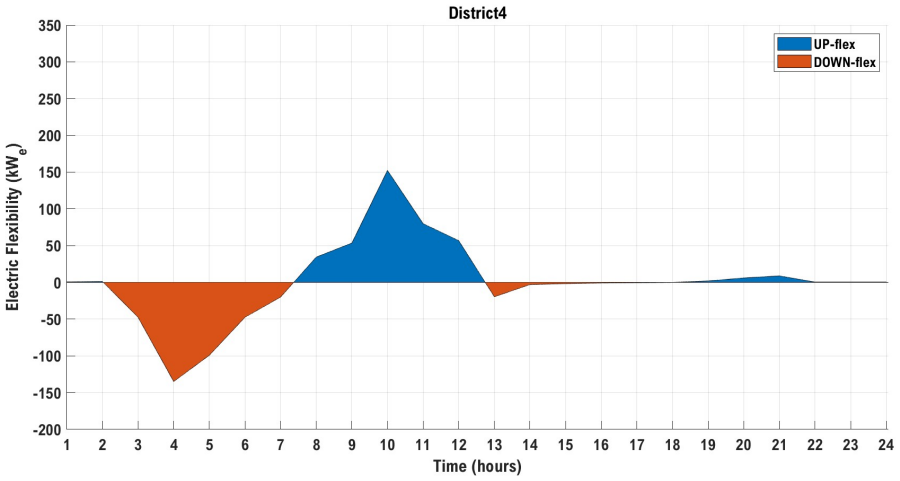

Fig. B.6 *Strategy #1* - Operational electrical flexibility made available by District 4.

B.0.2 Strategy #2

District 1

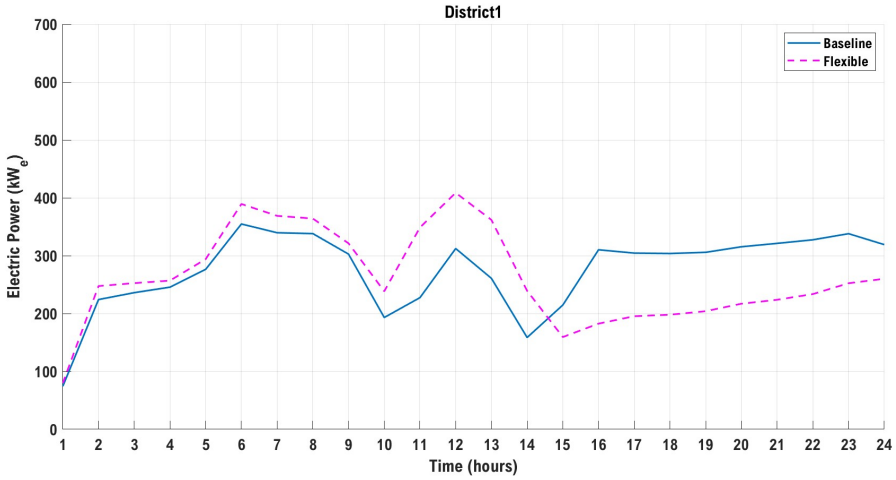

Fig. B.7 *Strategy #2* - Electrical power absorbed by heat pumps in District 1 substation.

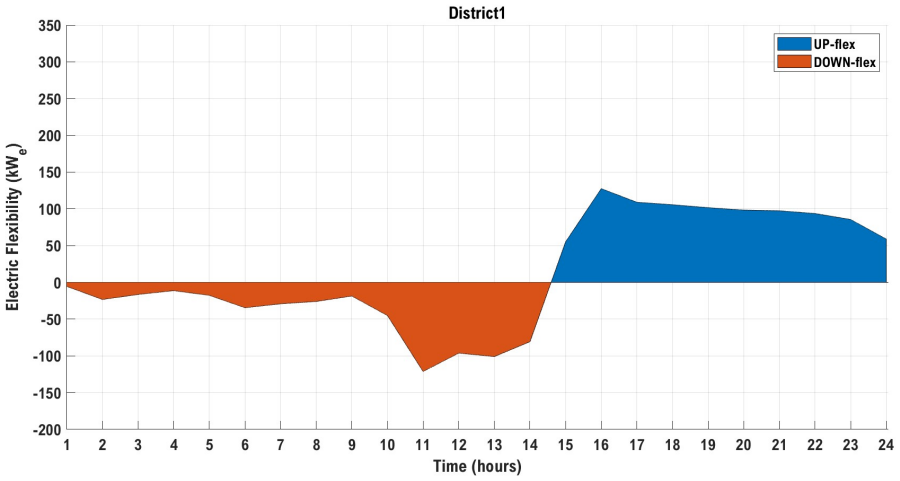

Fig. B.8 *Strategy #2* - Operational electrical flexibility made available by District 1.

District 3

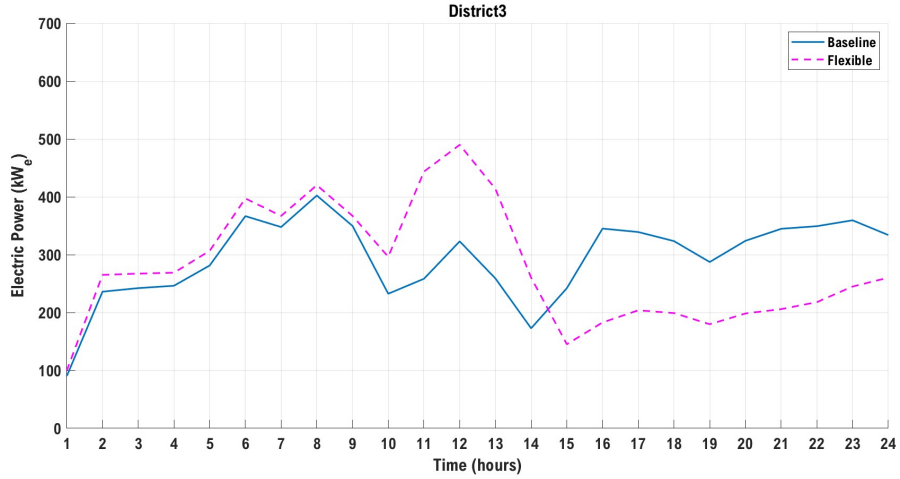

Fig. B.9 *Strategy #2* - Electrical power absorbed by heat pumps in District 3 substation.

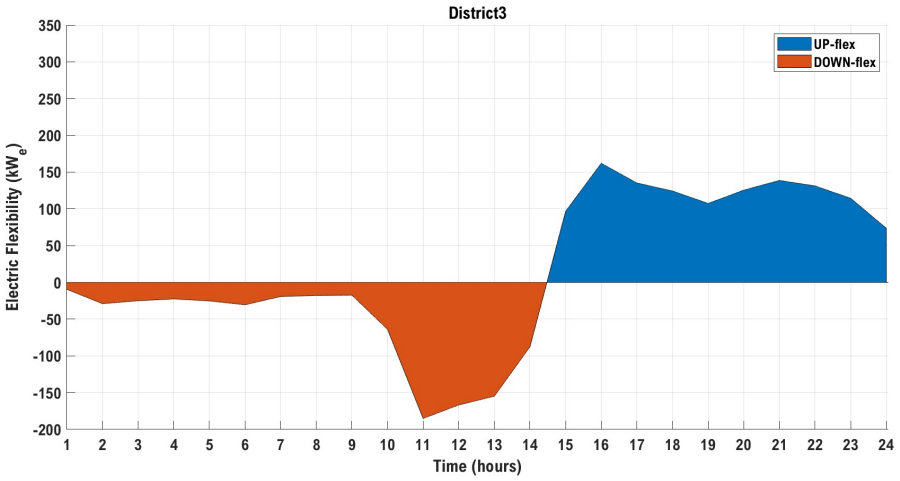

Fig. B.10 *Strategy #2* - Operational electrical flexibility made available by District 3.

District 4

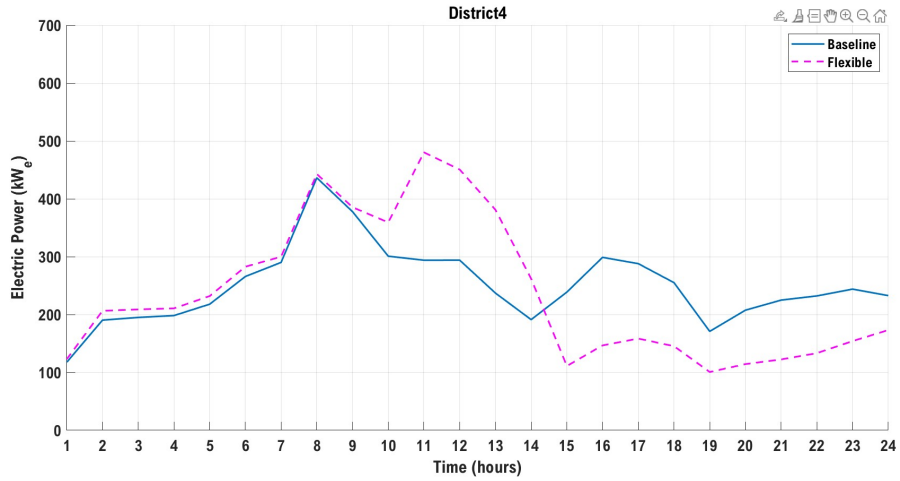

Fig. B.11 *Strategy #2* - Electrical power absorbed by heat pump in District 4 substation.

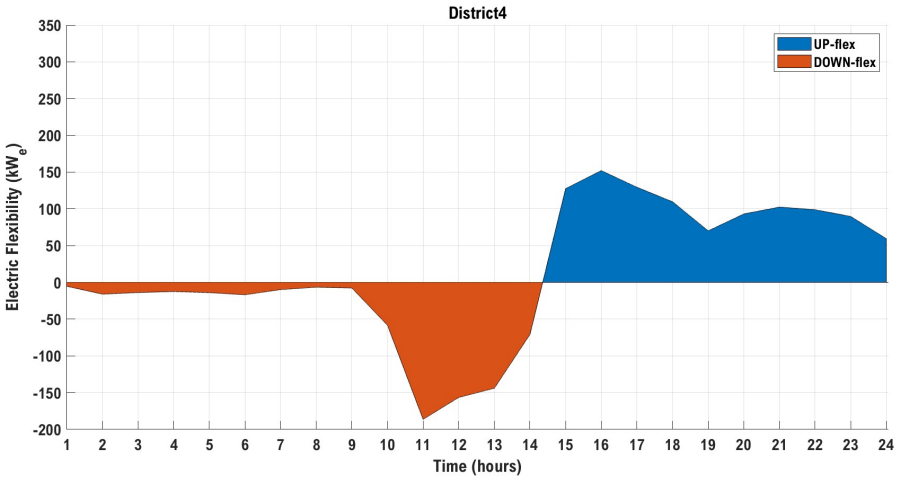

Fig. B.12 *Strategy #2* - Operational electrical flexibility made available by District 4.

Appendix C

In this Appendix C more information on the heat pumps used in the model are provided. In detail, technical data from commercial data sheet are reported through tabular and graphical representation. The heat pumps selected for the district application are two reversible unit, so they provide both heated and chilled water according to users' needs. They are high efficiency machines that use R-134a as refrigerant fluid and each of them can provide up to almost 2.3 MW in cooling mode and up to 2.5 MW for heating provision. As explained before, in the district substation they are arranged in a cascade configuration in order to provide a double step increase of temperature, while maintaining an high efficiency. For the water source heat pump, since no commercial data sheet were available, the heat pump performances described above has been scaled proportionally for a maximum thermal power of 11 MW.

Despite the fact that the application presented in this dissertation focused on the heating mode, the performances of the heat pump unit in relation with water temperature are reported below also for the cooling mode.

C.0.1 Heating mode

Nominal Heating Power [kW]		Tev,i_N			
		8°C	10°C	15°C	18°C
Tcond,o	30°C	2010	2127	2442	2481
	35°C	1905	2007	2297	2443
	40°C	1882	1962	2191	2371
	45°C	1912	1984	2204	2347
	50°C	1910	2016	2249	2321
	55°C	1880	1983	2251	2279
	60°C	1852	1952	2212	2238
	65°C	1828	1922	2155	2214

Table C.1 Nominal heating power dependency on water temperature. Tev,i_N: Nominal T evaporator water inlet; Tcond,o: T condenser water outlet.

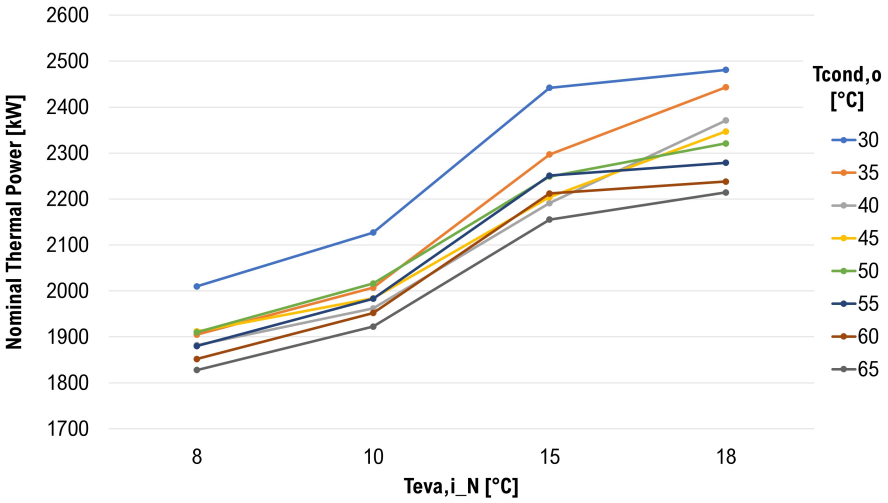

Fig. C.1 Nominal heating power dependency on water temperature.

Nominal COP		Tev,i_N			
		8°C	10°C	15°C	18°C
Tcond,o	30°C	6.31	6.43	6.67	6.71
	35°C	5.74	5.86	6.13	6.23
	40°C	5.24	5.34	5.58	5.72
	45°C	4.82	4.90	5.12	5.24
	50°C	4.38	4.49	4.71	4.77
	55°C	4.01	4.13	4.39	4.42
	60°C	3.62	3.74	4.00	4.03
	65°C	3.01	3.14	3.43	3.52

Table C.2 Nominal Coefficient of performance (COP) dependency on water temperature. Tev,i_N: Nominal T evaporator water inlet; Tcond,o: T condenser water outlet.

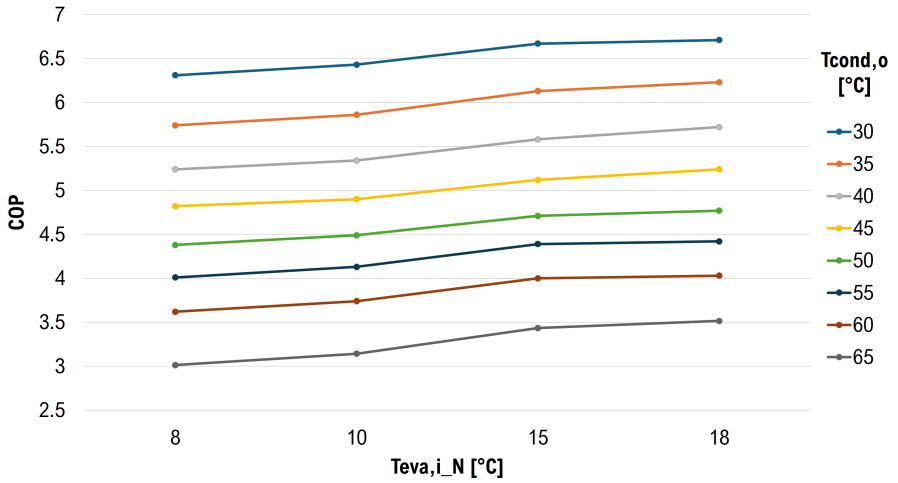

Fig. C.2 Coefficient of performance (COP) dependency on water temperature.

C.0.2 Cooling mode

Nominal Cooling Power [kW]		Tcond,i_N					
		20°C	30°C	35°C	40°C	45°C	50°C
Tev,o	5°C	1740	1611	1563	1566	1527	1459
	7°C	1849	1702	1630	1628	1623	1552
	10°C	2021	1855	1743	1737	1758	1694
	15°C	2170	2110	1999	1951	1896	1813
	18°C	2321	2259	2118	2060	2022	1938

Table C.3 Cooling load dependency on water temperature. Tev,o: T evaporator water outlet; Tcond,i_N: Nominal T condenser water inlet.

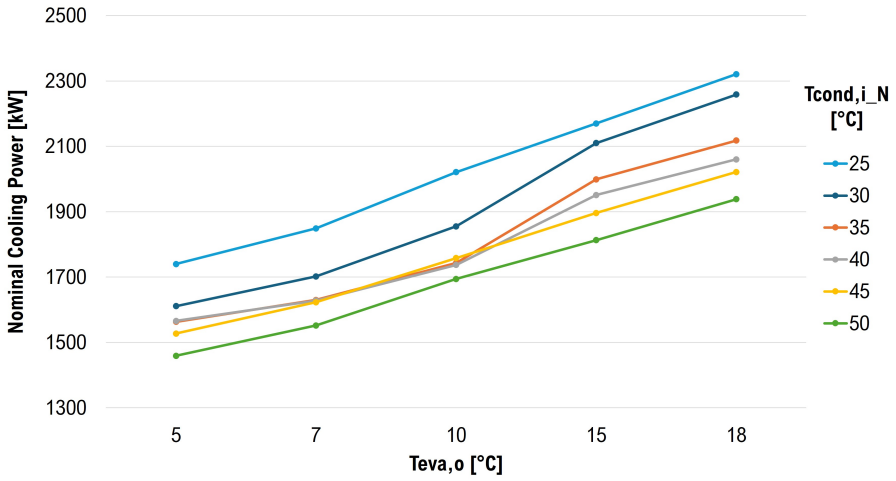

Fig. C.3 Nominal cooling power dependency on water temperature.

Nominal EER		Tcond,i_N					
		20°C	30°C	35°C	40°C	45°C	50°C
Tev,o	5°C	5.78	5.08	4.53	4.08	3.6	3.13
	7°C	5.96	5.24	4.64	4.18	3.74	3.25
	10°C	6.21	5.48	4.82	4.33	3.91	3.43
	15°C	6.41	5.81	5.16	4.6	4.08	3.57
	18°C	6.64	6.04	5.34	4.75	4.25	3.73

Table C.4 Energy efficiency ratio (EER) dependency on water temperature. Tev,o: T evaporator water outlet; Tcond,i_N: Nominal T condenser water inlet.

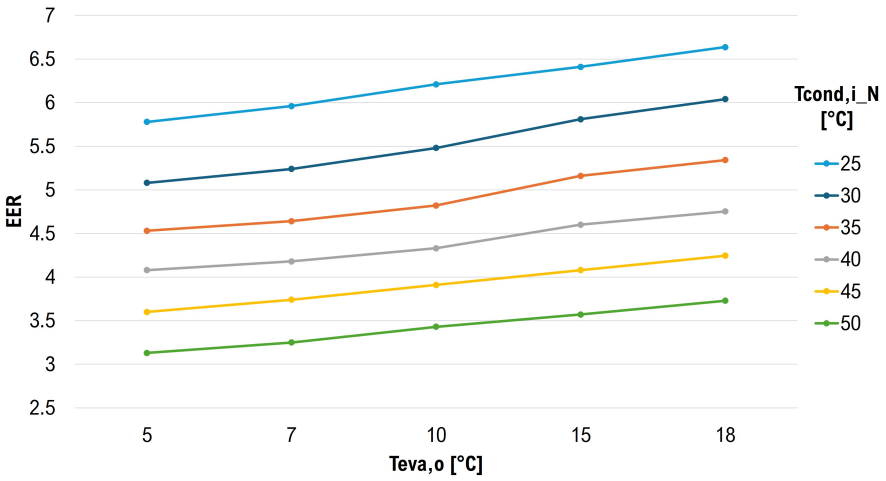

Fig. C.4 Energy efficiency ratio (EER) dependency on water temperature.

Appendix D

This Appendix collects the papers published during the Ph.D. Some of these publications were previously referenced within the dissertation, serving as supporting material for the conducted research activities.

D.0.1 Publications on Journals

- **Abbà, I.**; Crespi, G.; Vergerio, G.; Becchio, C.; Corgnati, S.P. Key Performance Indicators for Decision Support in Building Retrofit Planning: An Italian Case Study. *Energies*, vol. 17(3), n. 559. 2024.
- **Abbà, I.**; La Bella, A.; Corgnati, S.P.; Corsetti, E. Assessing flexibility in networked multi-energy systems: a modelling and simulation-based approach. *Energy Reports*, 11:384-393. 2024.
- Crespi, G.; **Abbà, I.**; Corgnati, S.P. Innovative metrics to evaluate HVAC systems performances for meeting contemporary loads in buildings. *Energy Reports*, 8, 9221-9231. 2022.
- **Abbà, I.**; La Bella, A. Multi-energy systems as enablers of the flexible energy transition. *REHVA JOURNAL*, vol. 59, pp. 10-14. 2022.
- Crespi, G.; **Abbà, I.**; Corgnati, S.P.; Prendin, L.; Babuin, M. Contemporary and unbalanced loads in buildings: new performance indicators. *REHVA JOURNAL*, vol. 59, pp. 16-20. 2022.
- **Abbà, I.**; Cellura, S.; Corgnati, S.P.; Morassutti, S.; Prendin, L. Overall energy performance of polyvalent heat pump systems. *REHVA JOURNAL*, vol. 57, n.1, pp. 26-31. 2020.

- Bompard, E.; Botterud, A.; Corgnati, S.P.; Leone, P.; Mauro, S.; Montesano, G.; Papa, C.; Profumo, F.; Grosso, D.; Huang, T.; Delmastro, C.; Jafari, M.; Crespi, G.; **Abbà, I.**; Becchio, C.; Vergerio, G.; Viazzo, S.; Rosciarelli, L.; Battocchio, T.; Gaidano, M.; Fragno, M. S.; Armiento, M.; Napoli, C.; Di Rosa, D. Electrify Italy, pp.1-238. 2020.
- **Abbà, I.**; Crespi, G.; Lingua, C.; Becchio, C.; Corgnati, S.P. Theoretical and actual energy behavior of a cost-optimal based Nearly-Zero Energy Building. *AICARR Journal*, vol. 62, n. 3., pp. 36-39. 2020.

D.0.2 Publications for International conferences

- **Abbà, I.**; La Bella, A.; Corgnati, S.P.; Corsetti, E. Achieving Flexibility in the Energy Transition: Opportunities and Challenges of Multi-Energy Systems. In *SDEWES 2022 Conference*.
- **Abbà, I.**; Becchio, C.; Corgnati, S.P.; Pasquali, P.; Pinto; M.C.; Roglia, E.; Viazzo, S. Insights of the DYDAS Project: The Use Case Energy. *In CLIMA 2022 conference.*
- **Abbà, I.**; Crespi, G. A Multi-criteria Assessment of HVAC Configurations for Contemporary Heating and Cooling Needs. *In New Metropolitan Perspectives 2022*, LNNS 482, pp. 1711-1720.
- Crespi, G; **Abbà, I.**; Corgnati, S.P.; Morassutti, S.; Prendin, L. HVAC polyvalent technologies to balance contemporary loads in buildings. In *SDEWES 2021 Conference.*
- Lingua, C.;**Abbà, I.**; Becchio, C.; Corgnati, S.P. Legislation and standards for the implementation of reversible heat pump technologies in Mediterranean climate. In *10th HVAC Mediterranean Congress ClimaMed 2021.*
- **Abbà, I.**; Minuto, F. D.; Lanzini, A. Feasibility Analysis of a Multi-family House Energy Community in Italy. In: *New Metropolitan Perspectives. NMP 2020. Smart Innovation, Systems and Technologies*, pp.1165-1175.
- **Abbà, I.**; Crespi, G.; Corgnati, S. P.; Morassutti, S.; Prendin, L. Sperimentazione numerica delle dinamiche di funzionamento di sistemi polivalenti. In *37° Convegno Nazionale AiCARR*, pp.23-37.